UNIVERSITY OF ROMA TRE
Faculty of Engineering

Doctoral School of Engineering
Civil Engineering Section
PhD in Civil Engineering

XXVI Cycle

Doctoral Thesis

Subsurface Flow and Transport Modelling at the Hillslope scale

Candidate: Melkamu Alebachew Ali

Supervisor : Prof. Aldo Fiori

PhD Coordinator: Prof. Aldo Fiori

Roma,

April 2014

Doctoral School of Engineering/**PhD in Civil Engineering**

SCUOLA DOTTORALE / DOTTORATO DI RICERCA IN

XXVI

CICLO DEL CORSO DI DOTTORATO

Subsurface Flow and Transport Modelling at the Hillslope scale

Titolo della tesi

Melkamu Ali _____

Nome e Cognome del dottorando firma

Prof. Aldo Fiori _____

Docente Guida/Tutor: Prof. firma

Prof. Aldo Fiori _____

Coordinatore: Prof. firma

Collana delle tesi di Dottorato di Ricerca
In Scienze dell'Ingegneria Civile
Università degli Studi Roma Tre
Tesi n° xx

Dedicated to: To the memory of my father, Alebachew Ali who passed away at the end of the completion of this thesis. I miss him every day, but I am glad to know he saw this process through its completion, offering the support to make it possible, as well as lots of encouragement. Thank you father for your friendly advice, your prayer always help me in all the time of my successes.

Subsurface Flow and Transport Modelling at the Hillslope scale

Abstract

In hilly and humid forest areas with highly conductive soils, subsurface flow consider as the main mechanism of stream flow generation and responsible for the transport of solutes into the surface water bodies which is transported through the subsurface soil. However, the contribution of the subsurface flow is poorly represented in current generation of land surface hydrological models (LSMs). The lack of physical basis of their common parameterizations precludes a priori estimation, which is a major drawback for prediction in ungauged basins. This thesis is organized in to three sections which analyze the subsurface flow and transport through numerical modeling starting from a simple analysis of homogenous system to complex hillslope with variable soil and topographic properties.

First, the relation $Q(S)$ (where Q is the discharge and S is the saturated storage in the hillslope), as a function of some simple structural parameters is evaluated through two-dimensional numerical simulations and makes use of dimensionless quantities. The method lies in between simple analytical approaches, like those based on the Boussinesq formulation, and more complex distributed models. The results confirm the validity of the widely used power law assumption for $Q(S)$. Similar relations can be obtained by performing a standard recession curve analysis.

Second, physically based parameterization of the storage-discharge relationship

relating to subsurface flow is developed using the Richards' equation. These parameterizations are derived through a two-step up-scaling procedure: firstly, through simulations with a physically based subsurface flow model for idealized three dimensional rectangular hillslopes, accounting for within-hillslope random heterogeneity of soil hydraulic properties, and then through subsequent up-scaling to the catchment scale by accounting for between-hillslope and within-catchment heterogeneity of topographic features. These theoretical simulation results produced parameterizations of the storage-discharge relationship in terms of soil hydraulic properties, topographic slope and their heterogeneities that were consistent with results of previous studies. The resulted parameterization is regionalized across 50 actual catchments in eastern United States, and compared with the equivalent empirical results obtained on the basis of analysis of observed streamflow recession curves, revealed a systematic inconsistency. It was found that the difference between the theoretical and empirically derived results could be explained, to first order, by climate in the form of climatic aridity index.

Third, the performances of four different models of solute transport in catchments were analysed. The models employ the concept of travel time distribution. A recapitulation and critical analysis of the models and their basic assumptions is performed first, emphasizing their limitations and potential problems arising in their application. Then, detailed numerical experiments are used as a benchmark for the calibration and the assessment of the models' capabilities to simulate transport. The scope of the exercise is to test the performance of the models and their limitations in the ideal case in which the catchment system and all the hydrological variables (flow, concentration, storage, etc.) are perfectly known at any level of detail. The performance of the models and their limitations is presented and discussed. The results suggest that a time invariant formulation of the travel time distribution is usually inappropriate and not much effective in predicting transport.

Acknowledgements

First and above all, I praise the Almighty God for providing me this opportunity and granting me the capability to proceed successfully. This PhD work appears in its current form with the assistance and guidance of several people. I would therefore like to forward my sincere thanks to all of them.

Foremost, I would like to express my sincere gratitude to my advisor Prof. Aldo Fiori for his continuous support of my PhD study and research, for his patience, motivation, enthusiasm, and immense knowledge. His guidance helped me in all the time of research and writing of this thesis. I could not have imagined having a better advisor and mentor for my PhD study.

Besides my advisor, I would like to thank Prof. Murugesu Sivapalan for the opportunity he has offered me to stay at the University of Illinois Urbana Champaign for one year as exchange scholar and allowing me to be part of his research project. His encouragement, insightful comments, and hard questions help me to improve my understanding in the subject matter.

My sincere thanks also goes to the co-authors of my papers Dr. Giorgio, Dr. Sheng Ye, Dr. Hong-yi Li, Dr.Maoyi Huang and Dr. L. Ruby Leung for their hard-work, willingness to help, and knowledge. Special thanks for Dr. Sheng Ye for her assistance and providing me the necessary data. I should also mention Northwest Pacific Lab for allowing me to visit the laboratory and their assistant and hospitality during my stay.

Thanks also to all professors and the members of the Hydraulic and Hydrology lab at the Civil Engineering Department, University of RomaTre providing me good friendship and support. My friends in Italy and other parts of the World were also sources of laughter, joy, and support. Special thanks goes to Fish, Ephi, Ademe, Tsehaye, Eleni, Feke, Sol and Siraj. I had great time with you and

am very happy that, in many cases, my friendships with you have extended well beyond our shared time in Rome.

Most importantly, none of this would have been possible without the love and patience of my family. I would like to express my heart-felt gratitude to my family. Thank you for your love, support, and strong belief in me. Without you, I would not be the person I am today. I love them so much.

Above all I would like to thank my lovely wife Rosi, whose love and encouragement allowed me to finish this journey. She is keeping me healthy in all the late nights and early mornings. She already has my heart so my heartfelt thanks go to her and thank you for being my best friend. I owe you everything.

Melkamu Alebachew

2004

Subsurface Flow and Transport Modeling at the Hillslope scale

Melkamu Alebachew Ali

Dissertation for the degree of Doctor of Science in Civil Engineering to be presented with due permission of the Department of Engineering, for public examination and debate at the University of RomaTre

Table of Contents

List of Figures

List of Tables

Acronyms and Abbreviations

DEM	*Digital elevation model*
SSURGO	*Soil survey geographic dataset*
MOPEX	*Model parameter estimation experiment*
NHD	*National hydrograph dataset*
STATSGO	*United state general soil map*
NRCS	*National resource conservation service*
USGS	*United states Geological survey*
TTD	*Transit time distribution*
3-D/2-D/1-D	*Three/two/one dimensional*
HSB	*Hillslope storage Boussinesq model*
CPU	*Central processing unit*
LSM	*Land surface model*
VIC	*Variable infiltration capacity*
AIC	*Akaike information criterion*
LPM	*Lumped parameter model*

1 Introduction

1.1 Background

In hilly and humid forest areas with highly conductive soils, subsurface flow consider as the main mechanism of stream flow generation and responsible for solute transport (eg. agricultural fertilizers and nutrients) into the surface water bodies which is transported through the subsurface soil (*Anderson and Burt, 1990; McGlynn et al., 2003; Sidle et al., 2000; Weiler and McDonnell, 2006; Zuber, 1986*). Several studies in the past two decades at different part of the world (eq. Maimai experiment in New Zealand, Panola mountain research, USA, and other studies) indicated that the pre-event water (which is stored in the subsurface soil before a rainfall occurs) is the dominate contributor of stream flow (*Botter et al., 2010; Buttle, 1994; Fiori, 2012; McDonnell, 1990; Neal and Rosier, 1990; Sklash, 1990; Wenninger et al., 2004*) with percentages more than 70% of the total flow. In those field experiments, hillslopes are fundamental landscape units that control the flow processes where rainfall is transported to streams. Indeed, it is highly important to predict flow, solute transport and land stability at hillslope scale in order to understand the dynamic of hydrological processes and possible governing mechanisms within the subsurface.

Much of the process understanding in hillslope hydrology at steep landscape has studied from field experiments, for example, several studies at the

Panola mountain research watershed, USA (*Clark et al., 2009; Freer et al., 2002; Lehmann et al., 2006; McGlynn et al., 2001; Tromp-van Meerveld et al., 2008; Tromp-van Meerveld and McDonnell, 2006a*, *b; Uchida et al., 2005; Wang, 2011*); Maimai, New Zealand (*McDonnell, 1990; Pearce et al., 1986; Sklash, 1990; Woods and Rowe, 1996*; *McGlynn et al., 2002*) and , Hitachi Ohta experimental watershed, Japan (*Noguchi et al., 2001; Pearce et al., 1986; Sidle et al., 2011; Sidle et al., 1995; Sidle et al., 2000; Tani, 1997; Tsukamoto and Ohta, 1988*), characterize the enormous heterogeneity and complexity of surface and subsurface flow processes. However, the ability to employ these findings to ungauged regions still remains largely out of reach (McDonnell et al., 2007). Parallel to the field experiments, numerical models are increasingly used for studying flow and solute transport at hillslope scale (*Bogaart and Troch, 2006; Fiori and Russo, 2007; Harman and Sivapalan, 2009a*, *b; Lee, 2007; Rocha et al., 2007; Szilagyi et al., 1998; Troch et al., 2003*)

Though flow and transport modelling at hillslope scale is receiving much attention in the recent years and different numerical modelling and field experiments have been developed to increase our understanding of flow and transport, a few studies have been done to bring those physical based models to the ground since there is absence of strong techniques of upscaling point based flow and transport equation to hillslope scale and then catchment where mostly water resource development has been carried out. Several issues are also still raised on current generation of subsurface models and remain

unsolved such as i) the spatial variability of hydraulic parameters, which is not well captured in most analytical models; ii) there is also a fundamental problem in upscaling processes from point to hillslope and catchment scales since Darcy's based flow equation are initially developed for point scale and could not physically evident to study large scales with average catchment characteristics which exhibit tremendous spatial variability of soil and landscape properties within the catchment (e.g. soil properties such as hydraulic conductivity); iii) factors controlling the connectivity of hillslope flow (surface and subsurface topography, slope angle, hydraulic conductivity, rainfall intensity etc.); and how these variables affect the connectivity. So far several research works have been carried out to address these issues (e.g. *Lehmann et al., 2006; Viney and Sivapalan, 2004*; *Hopp and McDonnell, 2009*) and in present work similar issues are also undertaken addressing some of the components of hillslope hydrology (such as storage – discharge relationship and solute transport) with an appropriate numerical model.

1.2 General objectives and Scopes

The objective of the present work is to study flow and transport at hillslope scale, and particularly the effect of landscape and soil properties on the subsurface flow generation by examining the storage-discharge curve which is necessary to analyse the contribution of the subsurface flow to the stream. It is also extended to develop a global formulation of a lumped storage-

discharge relationship using nonlinear reservoir approach (power-law). This has been started with a simple 2D flow modelling to illustrate the power-law storage discharge curve and the flow recession curve assuming a homogenous system with a quasi - steady flow modelling approach. Then, it is further relaxed with a complex flow modelling of a 3D aquifer with heterogeneous soil properties and variable slope to develop a global closure equation that can be used for ungauged catchments regardless of their characteristics.

In general, each piece of work has their specific objective and has been carried out independently. **Chapter 3** aims at the determination of the nonlinear storage-discharge relationship by means of numerical computations using a 2D model. The proposed approach tries to develop simple solutions, with a minimal set of physical parameters, which are as parsimonious and simple as the analytical approaches available in the literature, but relaxing some of the assumptions, like e.g. the boundary conditions and the hydrostatic, Dupuit hypothesis. In **Chapter 4**, some of the assumptions in the 2D modeling which are physically far from the reality were dropped and certain form of reality was considered (i.e. 3D flow system with heterogeneous soil and landscape characteristics), and extended work has been done to analyze the subsurface flow mechanism. It aims to derive physically based storage-discharge relations as parameterizations of subsurface stormflow, which can be embedded in global land surface models without the need to resolve the flows at smaller scales explicitly. **Chapter 5**

evaluates the performance of some categories of solute transport models (both lumped parameter and complex analytical models which requires detail knowledge of the flow velocity and subsurface storage) to reproduce the observed transit time distribution obtained from a coupled flow and transport numerical model at hillslope scale. In this part of the work, all the cases are tested based on the results from numerical experiments (Richards equation) employing three dimensional (3-D) synthetic hillslope dynamic model with real hydrological input (i.e. rainfall) so as the numerical models offer the freedom in full control of all quantities and more realistic subsurface setup.

1.3 Organization of the thesis

The thesis is structured in six chapters which are categorized into three sections. The first section consists of two chapters describe the overall background and literature review. Two sections consists of three chapters describe the flow and transport modelling, respectively and finally conclusion and recommendation closes the thesis. The organization of the thesis with chapters is as follow:

In **Chapter 1** the overall background of the research is presented. The overall objectives of the research work and the general flow of the research is also presented in this chapter.

In **Chapter 2**, the detailed literature review on Hillslope hydrological modeling with past research works on the area. The flow and transport equation were used in the thesis also presented in this chapter.

In **Chapter 3**, Numerical modeling of Storage–discharge curves at homogenous hillslope is presented with the perspective of the model parameters to develop the relation $Q(S)$ (where Q is the discharge and S is the saturated storage in the hillslope), as a function of some simple structural parameters.

In **Chapter 4**, 3-D numerical modelling of the storage discharge curve is analysed and physically based parameterizations of the storage-discharge relationship relating to subsurface flow are developed. These parameterizations are derived through a two-step up-scaling procedure; point to hillslope scale and then to catchment scale employing simple and robust upscaling approach. This parameterization is also applied for 50 catchments in the United State and compared with the same parameters found empirically from observed data.

In **Chapter 5**, performance of solute transport models using traditional lumped parameter based TTD and a comparable analytical model routes the inflow concentration into outflow to reproduce the observed transit time distribution obtained from tracer study using a numerical experiment at hillslope scale with and without the presence of evapotranspiration is evaluated and the preference of each modeling approach is presented.

In **Chapter 6**, the overall summary of the research with some concluding remarks are given. The limitations and some assumptions made during the research are presented in this chapter.

2 Subsurface Flow and Transport at Hillslope scale: Theoretical overview

2.1 General overview of Hillslope Hydrology

"*One of the aims of hillslope hydrology is to explore the process complexity underlying watershed responses through carefully constructed field experiments in selected hillslopes, and through detailed numerical models that are able to capture key or dominant processes and which, in turn, are validated by the field observations*." (*Sivapalan, 2003*).

In most hydrological models at catchment scale, flow and transport are generally modelled in a lumped or distributed mode. The distributed models are often divide large catchment into small homogenous units that are supposed to have uniform characteristics (*Sivapalan, 2003*) whereas lumped models consider an entire catchment as one unit, characterized by a small number of parameters and variables which are uniform and spatially averaged over the catchment (e.g. mean areal rainfall). However, due to the large multi-scale heterogeneities that nature exhibits, it is uncertain to study processes using such lumped at a scale in which the spatial heterogeneity is fairly represented (*Watson et al.,2001*) and conversely, the fully explicit distributed models represent sufficiently but are data demanding. Thus, this spatial scale within the models which is more appropriate with our

understanding of the hydrological processes and the dominant controlling factors can be modelled at the hillslope scale (*Fan and Bras, 1995*).

Hillslope scale hydrological models based on the flow equation are the most essential approach to quantify hydrological responses for both gauged and ungauged catchments. It can also easily handle the dynamic characteristics of the flow and transport processes which results inexpensive respect to both conceptual and computational complexity. In fact, it is clear that physical equation explains flow through homogenous media at the point scale, but does not explain processes at large scale such as effect of variable soil properties and bed rock properties on subsurface flow through soil macropores (*Beven and Clarke, 1986; Freer et al., 2002; Tromp-van Meerveld and McDonnell, 2006a*) . As such, applying hydrological models at the large scale requires estimating equivalent soil and landscape parameter values that can represent the overall properties. Although such approach has been used to study hydrological processes at catchment, there are several factors that limit the application of the homogenous equivalent physical-based models over large areas (*Beven, 2002*). First, an increase in modelling scale is usually accompanied by an increase in the variability of physical properties (such as soil and topography) at different ranges of space (Figure 2.1). Averaging these catchment properties is not commensurate with the reality and may provide inappropriate modelling responses when applying for a complex spatially variable catchment. Second, some models evolve very complex approach to capture flow processes at the hillslope scale (e.g.

macropore flow), but an incomplete description of processes at the watershed scale (e.g. subsurface flow interaction with streams) (*Clark et al., 2009*). Finally, detail large scale (catchment scale) process-based models often have large computational requirements even though there are advanced computer hardware technologies to make detailed simulations at large scale. It is therefore, hillslope scale models are recently being developed and scientifically recognized to overcome such limitations (*Ali et al., 2013; Anderson and Burt, 1990; Brooks et al., 2004; Burns et al., 1998; Fiori and Russo, 2008; Graham and McDonnell, 2010; Harman and Sivapalan, 2009b; Harman et al., 2010; Hopp and McDonnell, 2009; Uchida et al., 2005; Wenninger et al., 2004*)

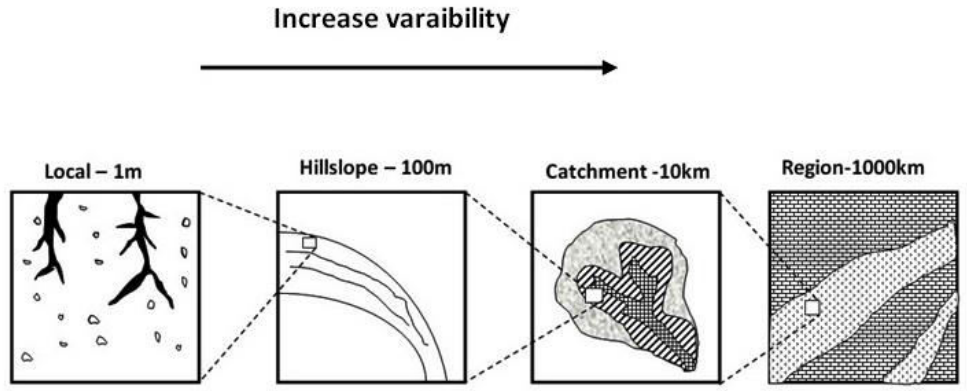

Figure 2.1: Variability of catchment and hydrological processes at a range of space scale (*Blöschl and Sivapalan, 1995*)

Different hillslopes in a catchment generate runoff at different timing and amount during a storm even since they have different topographic and landscape properties. These hillslopes are integrated by the river channel where they are contributed and which make a catchment with a single outlet so that areas outside of the river channel in a catchment are considered as hillslope (Figure 2.2), even they are completely flat (hillslope with zero slope). Therefore, in several hydrological models hillslopes are taken as a computational unit for both surface and subsurface flow modelling in order to capture all the hydrological processes with fair representation of the soil heterogeneity and topographic slope. It is clear that insight into the hydrological processes at hillslope scale and the effect of the variability of hydraulic characteristics of landscape elements is required to further our understanding and ability to model catchment hydrological processes.

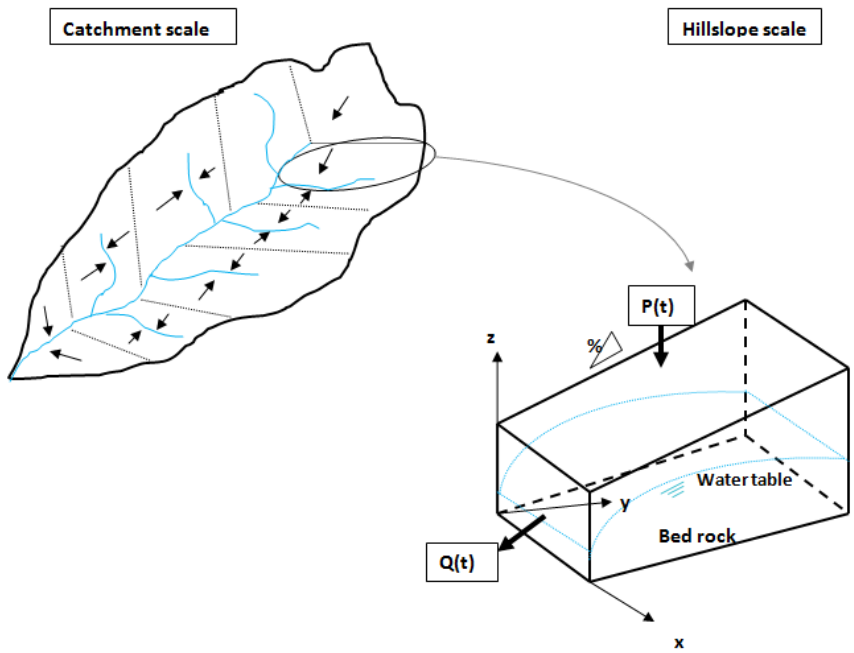

Figure 2.2: Schematic view of catchment with its hillslope units and hillslope discretization scheme (the arrow indicates the flow direction to the streams)

Several models have been developed over the past decades to quantifying the flow processes employing different flow equations and modelling approaches. Among these modelling approach, the most widely used models involve numerically solving are based on Richard's equation *(Paniconi and Wood, 1993)*. However, these models are very complex and demand high computational effort. Indeed, there are other models recently used which avoid such model complexity by adopting some basic assumptions in which the three-dimensional soil mantle of complex hillslopes with variable width

are collapsed into a one-dimensional drainage pore space (*Fan and Bras, 1998; Troch et al., 2002; Troch et al., 2003*). For example, *Troch et al. (2004*) presented an analytical solution of the linearized HSB equation for exponential hillslope width functions. Analytical solutions like these provide essential insights in the functioning of hillslopes and may form the basis of hillslope similarity analysis (*Brutsaert, 1994*). Though, such models are practically easy to simulate subsurface flow and storage with less cost, they are based on analytical solutions to the Boussinesq equation assuming equivalent representative values of catchment properties (e.g., *Brutsaert and Nieber, 1977;Brutsaert and Lopez, 1998; Rupp and Selker, 2005, 2006)* and the effects of heterogeneity of topographic gradient and soil hydraulic properties within hillslopes and catchments are not well captured. It is therefore essential to employ three dimensional model of Richards' equation so that the actual effect of soil and landscape variability can be embedded implicitly in the numerical models. Details of the Richard's equation and methods used to solve Richard's equation are discussed in the next sections.

2.2 Governing Flow and Transport Equations

In this section, the fundamental flow and transport equations used in the present work are summarized. Mathematical equations that describe the subsurface flow and transport processes may be developed from the fundamental principle of continuity equation and conservation of mass of fluid or of solute. Accordingly, the mathematical background and basic

assumptions employed in the Richards' equation (flow equation) and the convection-dispersion equation (solute transport equation) are discussed in this section.

2.2.1 Subsurface flow equation: The Richard's equation

The recognized physical model for the subsurface flow of water is the three dimensional (3D) Richards' Equation (*Richards, 1931*). It is very useful to analyse soil water fluxes in variable saturated soils and able to solve the strong nonlinearity of soil hydraulic functions.

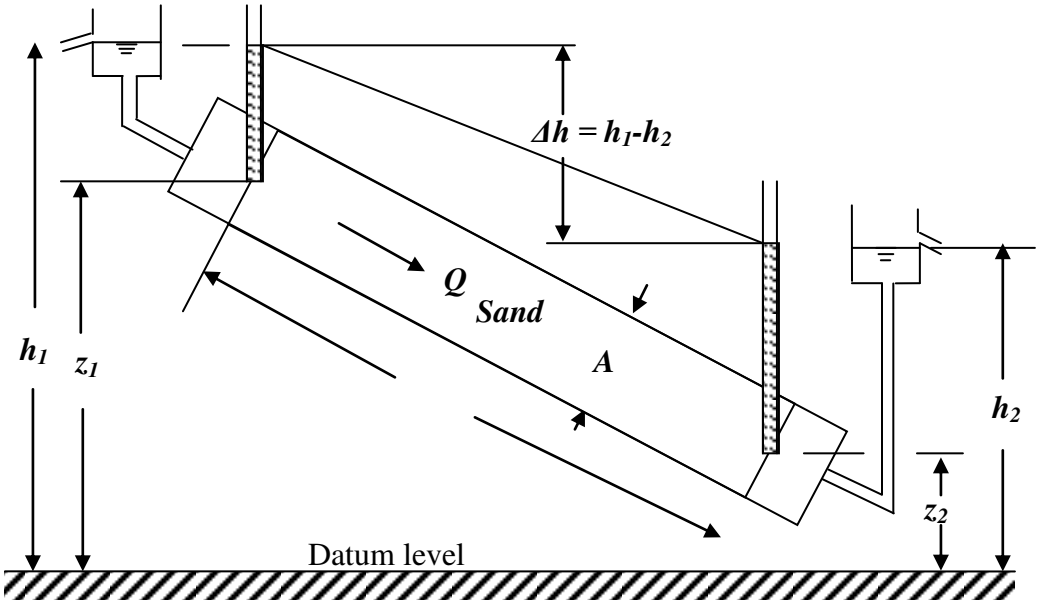

Figure 2.3: Darcy's law experiment

Starting from the Darcy's law experiment shown in Figure 2.3 which relates the flow velocity q to the hydraulic conductivity K and the pressure head inside the flow system h

$$q = -K\nabla(h+z) \tag{2.1}$$

with z denotes the vertical coordinate in the medium. The continuity equation in unsaturated soils

$$\frac{\partial\theta}{\partial t} - \nabla q = 0 \tag{2.2}$$

combined with Darcy law in equation (2.1) leads to Richards' equation

$$\frac{\partial\theta}{\partial t} - \nabla.(K\nabla(h+z)) = 0 \tag{2.3}$$

Different mathematical models used the Richards equation in equation (2.3) that made used to describe variable saturated flow and derived by combing the Darcy's law with the continuity equation in porous media so that the hydraulic conductivity depends on water content and pressure head. There are generally three main form of Richards' equation presented in the literature namely the pressure head (h) based formulation, water content (θ) – based formulation and mixed formulation (*Celia et al., 1990; Azizi et al., 2011*).

Pressure based

$$C(h)\frac{\partial h}{\partial t} - \nabla \cdot K(h)\nabla h - \frac{\partial K(h)}{\partial z} = 0 \tag{2.4}$$

Water content based

$$\frac{\partial \theta}{\partial t} - \nabla \cdot D(\theta) \nabla \theta - \frac{\partial K(\theta)}{\partial z} = 0 \qquad (2.5)$$

Mixed form

$$\frac{\partial \theta}{\partial t} - \nabla \cdot K(h) \nabla h - \frac{\partial K(h)}{\partial z} = 0 \qquad (2.6)$$

where h is the pressure head (L), z is the vertical coordinate (L), θ is the volumetric water content, $C(h) = \partial\theta / \partial h$ is the specific moisture capacity (1/L), K(θ or h) is the hydraulic conductivity (L/T), $D(\theta) = K(\theta) / C(\theta)$ is the diffusivity (L^2/T) and t is time (T).

The θ-based form cannot be used for the simulation of unsaturated-saturated flow and might generate significant local numerical errors for a coarse grid near interfaces with abrupt permeability changes, where heterogeneous porous media are concerned (*Zaidel and Russo, 1992*). The h-based form is not conservative and, as a result, cannot be used with reasonable time steps, especially for modelling infiltration into relatively dry soils. The mixed form of Richards' equation (*Celia et al., 1990*) has been provided attractive representation of the unsaturated- saturated flow and so, we will focus on this form of the flow equation.

The water content and the soil water potential may be related together through the use of an empirical function called water retention curve, which states that for a specific moisture level there is a defined value for suction.

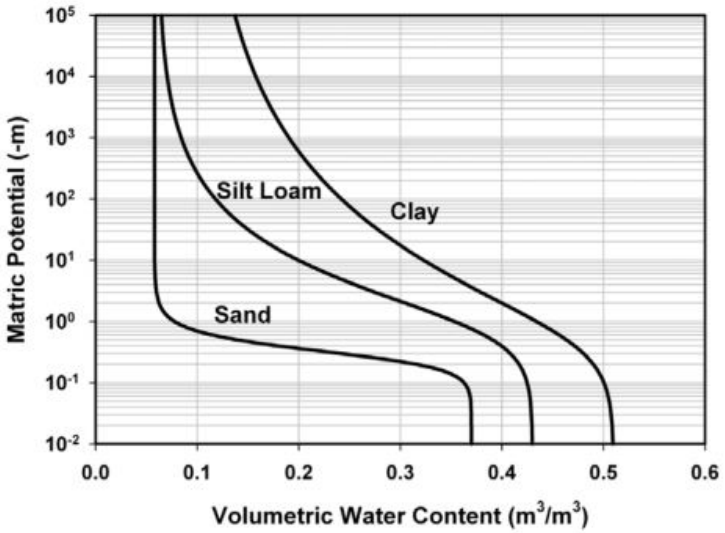

Figure 2.4: Soil water characteristic curves for selected soils ranges from sand to clay (*Tuller and Or, 2004*)

The shape of the water retention curves depends on the pore size distribution of the soil and exhibit different suction ranges for different soil since capillary forces are getting larger for finer textured soils (see Figure 2.4). Several models have been developed in order to describe the water retention curve and the Richards' equation can be solved. Brooks and Corey's model (*Brooks and Corey, 1964*) and Van Genuchten model (*van Genuchten, 1980*) are among the widely used models. The Van Genuchten model uses mathematical relations to relate soil water pressure head with water content

and unsaturated hydraulic conductivity. This model matches experimental data but its functional form is rather complicated and it is therefore difficult to implement it in most analytical solution schemes whereas Brooks and Corey's model has a more precise formulation. Table 2.1 indicates water retention and conductivity function for Van Genuchten and Brooks and Corey models.

Table 2-1: Water retention and conductivity functions for Brooks and Corey model (*Brooks and Corey, 1964*), and Van Genuchten model (*van Genuchten, 1980*)

	Brooks and Corey's model	**Van Genuchten model**
Capillary Pressure function	$S_e = \left(\frac{h_d}{h}\right)^{\lambda} \quad for\, h > h_d$ $S_e = 1 \quad for\, h \le h_d$	$S_e = \left[1 + (\alpha h)^n\right]^m \quad for\, h > 0$ $S_e = 1 \quad for\, h \le 0$
Hydraulic conductivity function	$K = K_s S_e^{1/2}\left[1 - \left(1 - S_e^{1/m}\right)^m\right]^2$	$K = K_s S_e^{(2+3\lambda)/\lambda}$

Notations: h is capillary pressure head; h_d is the air entry pressure head; λ is pore size distribution index; S_e is effective saturation; K is the hydraulic conductivity at specific water saturation; K_s is the saturated hydraulic conductivity; α and n are the Van Genuchten model parameters.

Several research works have been done to provide numerical and analytical solution of Richards' equation in order to simplify and easily implemented for field soils with some sort of assumptions. In recent years, semi-analytical methods have been developed for Richards' equation (*Srivastava and Yeh, 1991*; *Elnawawy and Azmy 1992*; *Marinelli and Durnford, 1998*; *Hogarth and Parlange, 2000*; *Lu and Zhang, 2004*; *Menziani et al., 2007*). These analytical solutions of the Richards' equations are an excellent tool to solve simple subsurface flow problems such that the nonlinear Richards' equation should be converted to a linear form even though it is highly non-linear and unlikely valid for complex conditions. *Tracy (2006)* obtained multidimensional solutions to the Richards equation in which the quasi-linear approximation combined with relative hydraulic conductivity varying exponentially with pressure head. This combined result with Kirchoff's transformation and the moisture content which is also varying linearly with relative conductivity allows the linearization of Richards' equation for both steady and unsteady flow simulation. *Basha (2000)* has also produced multidimensional analytical solutions for unsteady infiltration towards a shallow water table using the same approximation. There are methods to transform and separate variables. For example, *Basha (2000)* uses Green's functions to obtain the multi-dimensional solutions. Boltzmann similarity transformation is also used for 1D Richards' equation that converts the partial differential equation (PDF) to an ordinary differential equation (ODE) (*Logan, 1987*). Other methods are Laplace and Fourier transformation (*Fityus and Smith, 2001*), and inverse approach (*Broadbridge et al., 1996*).

Since the subsurface flow condition is highly nonlinear due to the extent of the non-linearity in hydraulic properties, multidimensional nature of water flow and pressure relationships of media; numerical methods combined with some iteration schemes are typically used to solve the Richards' equation (*Celia et al., 1990*; *Paniconi et al., 1994*; *Fiori and Russo, 2007*). However, they are usually computationally expensive and cannot be used to model large catchments. Thus as we discuss earlier, it can be minimized the computational cost using small scale problems necessarily to study detail hydrological processes followed by upscaling.

Once the form of the flow equation has been chosen one must select the solution procedure. Since analytical solutions for the Richards' equation are known for simplified situations only, thus for more involved situations, numerical methods which are preferable in view of the reliability of the computed solutions. The numerical methods which are employed to solve Richards' equation are a finite difference, a finite element and a finite volume method. Even though there are several research works have been carried out on the convergence properties of these methods to improve the physical discretization of these standard solutions, comprehensive analyses on the accuracy and efficiency of such methods in heterogeneous formations have not been performed so far. This aspect is particularly important in highly heterogeneous formations, such as those encountered when considering flow along hillslopes. The numerical discretization of the Richards' equation in

this study has been discussed in the later section. Table 2.2 indicates some previous research works that have been developed using Richards' equation based on different formulation and numerical discretization

Table 2-2: Summary of numerical models of Richards' equation for unsaturated- saturated flow (adopted and then modified from *Clement et al., 1994*

Model	**Subsurface Flow Equations**	**Solution procedures**
FEMWATER (*Yeh, 1981*)	h-based 2D variable saturated flow	Finite element; with Gauss elimination
3D FEMWATER (*Yeh, 1992*)	h- based 3D Richards equation	Finite element; with Gauss elimination
Cooley (1983)	h–based 2-D variable saturated flow	Finite element; combination of Newton-Raphson and strong implicit
Allen and Murphy (1986)	Mixed form of Richards' equation	Collocation finite element; Gauss elimination
VS2DT (*Healy, 1990*)	h-based form of general variable saturated flow (2D)	Finite difference; strong implicit procedure
Hydrus Model (*Simunek et al., 1996)*	Mixed form of Richards' equation	Galerkin-type finite element
MODHMS (*Panday and Huyakorn, 2004*)	Mixed form of 3D Richards' equation	Block centred Finite difference scheme
GSSHA model (*Downer and Ogden, 2004*)	h- based Richards' equation	Implicit finite difference
WASH123D(*Yeh et al., 2004; Yeh et al., 2006*)	3D Richards equation	Finite element method
Fiori and Russo (2007)	Mixed form of 3D Richards' equation	Finite difference, implicit procedure based on nodes distribution
AquiFlow (*Wang et al., 2010*)	h-based 3D Richards' equation	Finite difference method

2.2.2 Governing Transport Equation

Solute transport occurs in the subsurface system through the combination of diffusion and advection. The convection-dispersion equation (CDE) considers the solute flux to be the result of the average bulk motion of the solute in the direction of subsurface flow (advection) and a Fickian-type mixing between the original and displacing fluid (dispersion) (*Gillham et al., 1984*). For unsaturated - saturated flow in isotropic heterogeneous porous media, the governing equation is written as,

$$\frac{\partial(\theta c)}{\partial t} = \nabla \cdot (\theta D \nabla c) - \nabla(u \theta c) \qquad (2.7)$$

where c is the solute concentration expressed as mass per unit volume; u is the flow velocity and D is the hydrodynamic dispersion tensor.

The dispersion tensor for isotropic media is given as (*Bear, 1972*)

$$D_{ij} = \alpha_T \bar{u} \delta_{ij} + (\alpha_L - \alpha_T) u_i u_j / \bar{u} + \hat{D} \delta_{ij} \qquad (2.8)$$

where α_T and α_L are transversal and longitudinal pore scale dispersivities ; δ_{ij} is the Kronecker delta (i.e. $\delta_{ij} = 1$, if $i = j$ and $\delta_{ij} = 0$, if $i \neq j$); $\bar{u}$ is the magnitude of mean flow velocity in the subsurface and expressed as $\bar{u} = \sqrt{(u_x^2 + u_y^2 + u_z^2)}^{1/2}$; $\hat{D}$ is the molecular diffusion coefficient and the diffusion term is mostly is assumed zero since the mechanical dispersion is much larger than the diffusion term.

2.3 Recession flow analysis

Recession flow analysis is the well-known tool in hydrology and has several applications to characterize the low flow in a stream provides information concerning the availability of water resource to benefit the planning and management of water related projects such as irrigation, water supply and hydropower plants (*Tallaksen, 1995*). It also used to conceptualize the subsurface storage parameters and estimate aquifer characteristics of a catchment (*Moore, 1992*; *Lamb, 1997).*

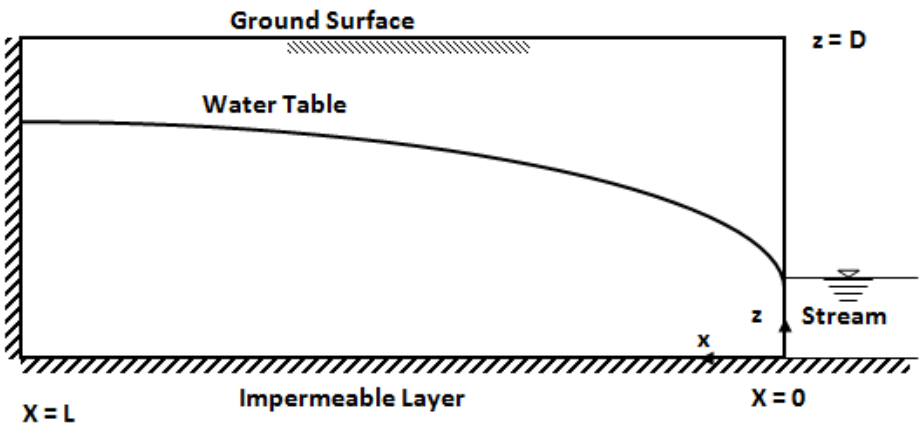

Figure 2.5: Defination sketch for the Dupuit – Boussinesq aquifer model (Brutseart and Nieber, 1977)

On the basis of different approaches, several types of models to describe recession flow have appeared in the literature. In one type of approach, *Horton (1933)* suggested the nonlinear relationship of the outflow discharge as $Q(t) = Q_0 \exp(-at^m)$, where Q_0 is the initial discharge, a and m are constants. Similar relationships have been presented and

discussed based on a simple flow equation by *Werner and Sundquist (1951); Tallaksen (1995)*. Other methods such as modelling recession as reservoir (*Barnes, 1939*; *Fenicia et al., 2006*; *Aksoy and Wittenberg, 2011*; *Chapman, 1997; Harman and Sivapalan, 2009b; Wittenberg, 1999; Wittenberg and Sivapalan, 1999*), using regression equation (*James and Thompson, 1970*; *Vogel and Kroll, 1992*) and empirical relationships (*Radczuk and Szarska, 1989*;*Clausen, 1992*) are among the most widely used approaches.

Boussinesq (1877) introduced non-linear differential equation for unsteady flow from unconfined aquifers to a stream channel by considering the Dupuit assumptions which neglects the vertical flow component and also neglecting the effect of capillarity, groundwater recharge and evapotranspiration (*Brutsaert and Nieber, 1977*). Theoretical equations for groundwater flow derived from the Boussinesq equation have been presented by *Brutsaert and Nieber (1977)*. They have proposed to determine the outflow rate from low flow hydrograph derived from direct measurements of $Q(t)$ and nonlinear Dupuit Boussinseq aquifer model (Figure 2.5) is developed and the parameters for the lumped storage model are determined. This low flow analysis has been extensively applied by various researchers. The storage model they have employed has the form of a power function $dQ/dt = f(Q) = -\alpha Q^{\beta}$ where α and β are constants and can also be obtained from the Dupuit Boussinesq aquifer model by assuming some geometrical similarity of the catchment. Alternatively, the same equation is obtained after combining the non-linear storage–discharge relationship, $Q = aS^{b}$ and with the

continuity equation of a reservoir without inflow, $dS/dt = -Q$. This approach allows developing parameterizations using an inverse procedure, from catchment runoff measurements that already account for the net effects of natural variability of soil and topographic properties. This is based on the relationship between the storage-discharge relationship and the shape of the recession curve extracted from observed streamflow records. It can be shown that the parameters a and b of the storage-discharge relationship are uniquely related to the parameters α and β associated with the recession slope curves which is $\alpha = a^{1/b} b$ and $\beta = 2 - 1/b$.

Part I: Flow Modeling

3 Analysis of the nonlinear storage– discharge relation for hillslopes through 2D numerical modeling[1]

Abstract:

Storage–discharge curves are widely used in several hydrological applications concerning flow and solute transport in small catchments. This article analyzes the relation $Q(S)$ (where Q is the discharge and S is the saturated storage in the hillslope), as a function of some simple structural parameters. The relation $Q(S)$ is evaluated through two-dimensional numerical simulations and makes use of dimensionless quantities. The method lies in between simple analytical approaches, like those based on the Boussinesq formulation, and more complex distributed models. After the numerical solution of the dimensionless Richards equation, simple analytical relations for $Q(S)$ are determined in dimensionless form, as a function of a few relevant physical parameters. It was found that the storage–discharge curve can be well approximated by a power law function $Q/LK_s = a\left[S/L^2(\phi-\theta_r)\right]^b$, where L is the length of the hillslope, K_S the saturated conductivity, $\phi-\theta_r$ the effective porosity, and a, b two coefficients which mainly depend on the slope. The results confirm the validity of the widely used power law

[1] *Adapted from Ali, M., A. Fiori, and G. Bellotti (2012). Analysis of the nonlinear storage--discharge relation for hillslopes through 2D numerical modelling. Hydrol. Process., doi: 10.1002/hyp.9397*

assumption for $Q(S)$. Similar relations can be obtained by performing a standard recession curve analysis. Although simplified, the results obtained in the present work may serve as a preliminary tool for assessing the storage–discharge relation in hillslopes.

3.1 Introduction

The storage-discharge relation is a very important component of catchment hydrology and it is widely used for several engineering applications, such as estimating design floods (*Rahman and Goonetilleke, 2001*), forecasting of low flows for water resource management (*Vogel and Kroll, 1992*), estimating groundwater potential of basins (*Wittenberg and Sivapalan, 1999*) and rainfall runoff models (*Sriwongsitanon et al., 1998*). The matter has been investigated in the framework of base flow recession, hydrograph separation and other related areas of hillslope hydrology (*Brooks et al., 2004; Fiori and Russo, 2007; Graham and McDonnell, 2010; McGuire and McDonnell, 2010; Weiler and McDonnell, 2004*). Based on different principles and approaches, the recession of subsurface flow has been studied by *Brutsaert and Nieber (1977*);*Wittenberg (1994*); *Wittenberg (1999*); *Fenicia et al. (2006*), *Aksoy and Wittenberg (2011*); *Wang (2011*); *Moore (1997*). *Tallaksen (1995*) has discussed various methods and approaches widely used to determine the storage discharge relationship by the recession curve analysis.

One of the widely employed storage-discharge relations is the linear reservoir model, originally defined by *Maillet (1905*), which implies that the aquifer behaves like a single reservoir with storage S, linearly proportional to outflow *Q*, namely $Q = aS$. In this case, the plot of $\log Q_t$ against *S* yields a straight line (*Barnes, 1939*). Moreover *Fenicia et al. (2006*) have also derived actual *S-Q* relation in which the percolated water from the unsaturated reservoir and also the preferential recharge as inflow

to the saturated reservoir are taken into account, for which the S-Q relation was treated as a linear and second order polynomial. However, linear reservoir ($Q = aS$) can very well describe the groundwater behavior for most of the catchments they have studied. In most real cases however, semi-logarithmic plots of flow recessions are still concave (*Aksoy and Wittenberg, 2011*), indicating nonlinear storage discharge relationships.

Recent studies agreed that the outflow of a lumped storage model can be characterized by a general power law function $Q = aS^b$ where *a* and *b* are constants. The constant *b* varies between 0 and 2 or higher for some cases (*Chapman, 1997; Harman and Sivapalan, 2009b; Wittenberg, 1999; Wittenberg and Sivapalan, 1999*) and also it has been proved by physical experiments (*Chapman, 1999; Wittenberg, 1994*). The power law formulation is only occasionally chosen in recession analysis (*Wittenberg, 1994*), and the recession process is commonly formulated in terms of the reservoir inflow and outflow, which can be calculated using the continuity equation.

On the other hand, *Brutsaert and Nieber (1977)* have proposed to determine the outflow rate from low flow hydrograph derived from direct measurements of $Q(t)$. They have developed their models based on the nonlinear Dupuit Boussinseq aquifer model and determined the parameters for the lumped storage model. This low flow analysis has been extensively applied by various researchers. The storage model they have employed has the form of a power function $Q = aS$ $dQ/dt = f(Q) = -\alpha Q^{\beta}$

where α and β are constants and can also be obtained from the Dupuit Boussinesq aquifer model by assuming some geometrical similarity of the catchment. From the solution for the outflow rate they have estimated $\beta_1=3$ and $\beta_2=3/2$ for short time and long time solution respectively.

Recently *Wang (2011)* has used the method proposed by *Brutsaert and Nieber (1977)* at the Panola Mountain Research Watershed, Georgia. The work has elaborated more on the effect of groundwater leakage and return flow on the recession curves. On his work he has studied the recessions for three nested hillslopes and watersheds and estimated recession slope curves (RSC) for different values of a and b based on the observed data for the three watersheds at the Panola mountain.

Parallel to the analytical approximation for computing hillslope subsurface flow, numerical models are increasingly used for computing the recession flow and baseflow analysis, and also for comparison with the analytical approximation (*Lee, 2007; Rocha et al., 2007; Szilagyi et al., 1998*). For example *Lee (2007)* develops a recession model that can provide the theoretical basis of subsurface modeling using dimensionless Richard's equation, treating both saturated and unsaturated flow domains.

The use of the storage-discharge relationship, together with the continuity equation, resembles other similar approaches in hydrological modeling, like e.g. the kinematic model for flood propagation. In essence, the dynamic equation is simplified by a quasi-steady state relation between storage and discharge. The same approach was employed by *Kirchner (2009); Botter et al. (2009)* and *Botter et al. (2010).*

This work aims at the determination of the nonlinear storage-discharge relationship by means of numerical computations carried out using a 2D model. The proposed approach tries to develop simple solutions, with a minimal set of physical parameters, which are as parsimonious and simple as the analytical approaches available in the literature, but relaxing some of the assumptions, like e.g. the boundary conditions and the hydrostatic, Dupuit hypothesis. The relation Q(S) is expressed as function of some simple and dimensionless structural parameters. Although the method embeds some simplifications, it may constitute a preliminary tool for assessing the nonlinear storage-discharge relation to be used in hydrological flow models.

3.2 Mathematical framework and numerical solution

We simplify the hillslope configuration as a sloped parallelogram shape domain. The conceptual model of the hillslope is shown on Figure 3.1. The domain has inflow boundary at the upper face (net precipitation, i.e. subtracted from evapotranspiration), no flow at the left side and lower face, and a mixed boundary condition at the right face of the domain, namely the seepage face. In this study we concentrate on flows driven by groundwater and neglect the possible runoff caused by the emergence of the water table over the ground level. Thus, the thickness of the formation is large enough to accommodate for all the possible storage of water in the system, so that the water table does not intersect the upper face of the domain. The flow domain thus represents a simple unconfined aquifer; it is also assumed that the formation is uniform, i.e the hydraulic properties (e.g. hydraulic conductivity) are constant over the entire domain. The

numerical computations described in the following, have been carried out varying the slope of the catchment.

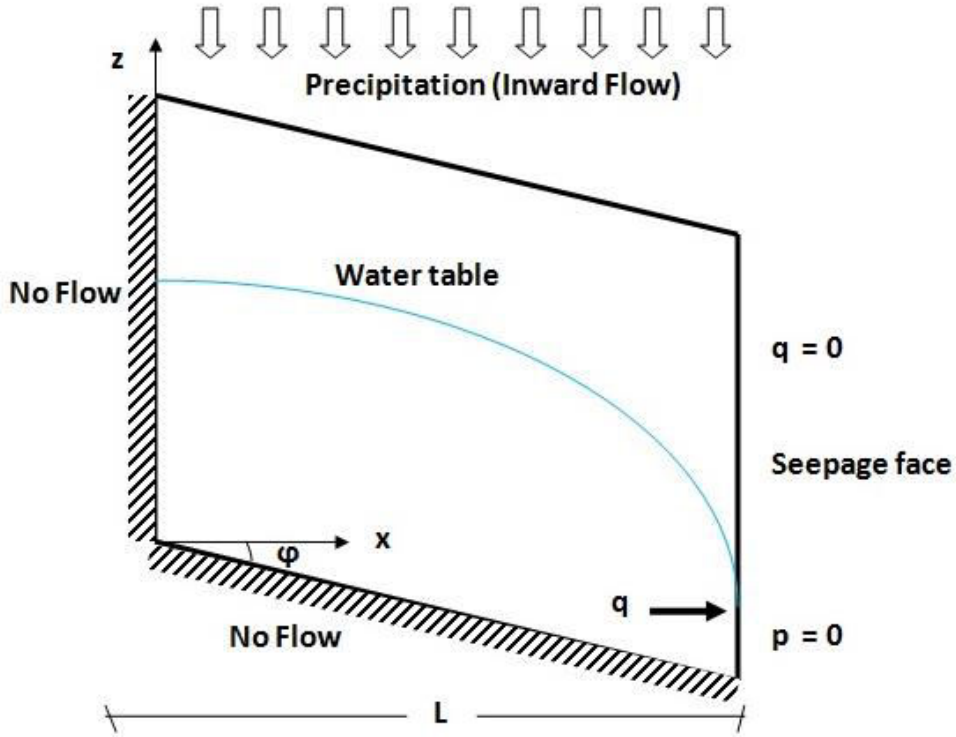

Figure 3.1: Illustration sketch of the conceptual model for the hillslope

We assume that the water flow is described by the Richards equation

$$C(h)\frac{\partial h}{\partial t} = \frac{\partial}{\partial x_i}\left[K(h)\left(\frac{\partial h}{\partial x_i}+1\right)\right]+q \qquad (3.1)$$

with $C(h) = \partial\theta/\partial h$ the specific moisture content, $h(x_i,t)$ the pressure head, *K(h)* the hydraulic conductivity of the material, $\theta(x_i,t)$ the

volumetric water content, q the source/sink term and x_i the spatial coordinate vector.

For this analysis we adopt the Brooks and Corey retention model (Brooks and Corey, 1964) expressed as

$$S_e = \frac{(\theta - \theta_r)}{(\phi - \theta_r)} = \left(\frac{h_b}{h}\right)^{\lambda} \tag{3.2}$$

with S_e the effective saturation, θ_r the residual volumetric water content, ϕ the porosity, h_b the bubbling or air entry pressure head and λ is pore size distribution index. The specific moisture content $C(h)$ therefore becomes

$$C(h) = \frac{\partial \theta}{\partial h} = -(\phi - \theta_r)\lambda \frac{h_b^{\lambda}}{h^{\lambda+1}} \tag{3.3}$$

The hydraulic conductivity of the material can be defined as a function of the saturated hydraulic conductivity (K_s), the bubbling pressure (h_b), the pressure head (h) and the pore size index λ (n=3+2/λ) as follows

$$K(h) = K_s \left(\frac{h_b}{h}\right)^{n\lambda} \tag{3.4}$$

In the following we work with dimensionless variables, as it helps in reducing the number of parameters governing the problem. The dimensionless form of the Richards equation can be derived by normalizing the specific moisture content, the volumetric water content,

the pressure head, the hydraulic conductivity of the material and the sink/source term using the appropriate scaling variables. Thus, we adopt the dimensionless variables

$$x' = \frac{x}{L} \qquad t' = \frac{tK_s}{L(\phi - \theta_r)}$$
$$h' = \frac{h}{L} \qquad q' = \frac{qL}{K_s} \tag{3.5}$$
$$h'_b = \frac{h_b}{L}$$

with L the horizontal size of the hillslope (see Figure 3.1). Substitution of the above into Richards equations yields

$$f_c(h')\frac{\partial h'}{\partial t'} = \frac{\partial}{\partial x'_i}\left[f_k(h)\left(\frac{\partial h'}{\partial x'_i} + 1\right)\right] + q' \tag{3.6}$$

where

$$f_c(h') = \lambda \frac{h_b'^{\lambda}}{h'^{\lambda+1}} \quad ; \; f_k(h') = \left(\frac{h'_b}{h'}\right)^{n\lambda} \tag{3.7}$$

We have employed the above dimensionless Richards equation to formulate the entire problem and perform the simulations. As a consequence of the chosen variables (Equation (3.5)), the water stored in the saturated part of the porous medium (S) and the discharge (Q) can be also written in dimensionless form, as follows

$$S' = \frac{S}{L^2(\phi - \theta_r)}$$
$$Q' = \frac{Q}{LK_s} \tag{3.8}$$

The dimensionless Richards equation is solved by the Earth Science Module of Comsol Multiphysics software (*COMSOL, 2010*). Comsol Multiphysics employs the Finite Element Method to solve partial differential equations. The seepage face develops at the right boundary where water is discharging out from the domain. It is generally not simple to model a seepage face, which needs a switch of the mathematical expression imposed at the boundary, between a constant pressure condition (seepage) and no flow (no seepage). We employ here the mixed (Cauchy) boundary condition algorithm developed by *Chui and Freyberg (2007)*. Adopting the same approach we split the boundary face into a Dirichlet boundary condition for the seepage face (where the prescribed internal pressure $p_0 \geq 0$) and the Neumann condition for the region above the seepage face. The temporal variability of the length of the seepage face is automatically accounted by the method. For details about the algorithm the reader is sent to Chu and Freyberg (2007).

3.3 Result and Discussion

3.3.1 Effect of Soil parameters

Before addressing the storage-discharge relationship we have carried out a set of computations to investigate the sensitivity of the results to changes of the soil parameters. The sensitivity analysis has carried out for

some representative soil types from clay to sand, to cover most of the field soil ranges. Specifically five soil types were chosen (the parameters are shown on Table 3.1) to evaluate their effect on the results of the simulations. To speed up the computations and to reach quickly the stationary conditions (i.e. inflow equals outflow), initial conditions representing full saturation of the formation are imposed. Constant dimensionless inward flux equal to $Q/LK_s = 0.25$ is applied for the entire simulation. The impact of the parameters has been analyzed for different values of the pore size distribution (n) and bubbling pressure (h_b), keeping the other parameters constant.

Table 3-1: Brooks and Corey parameters for different soil types

Soil type	h_b**(cm)**	n	f**(cm^3/cm^3)**	θ_r**(cm^3/cm^3)**
Sand soil	7.26	0.694	0.437	0.02
Loamy sand soil	8.69	0.553	0.437	0.035
Loam soil	11.15	0.252	0.463	0.027
Silt loam	20.76	0.242	0.501	0.015
Clay	37.3	0.165	0.475	0.009

Source: *Rawls et al. (1993)*

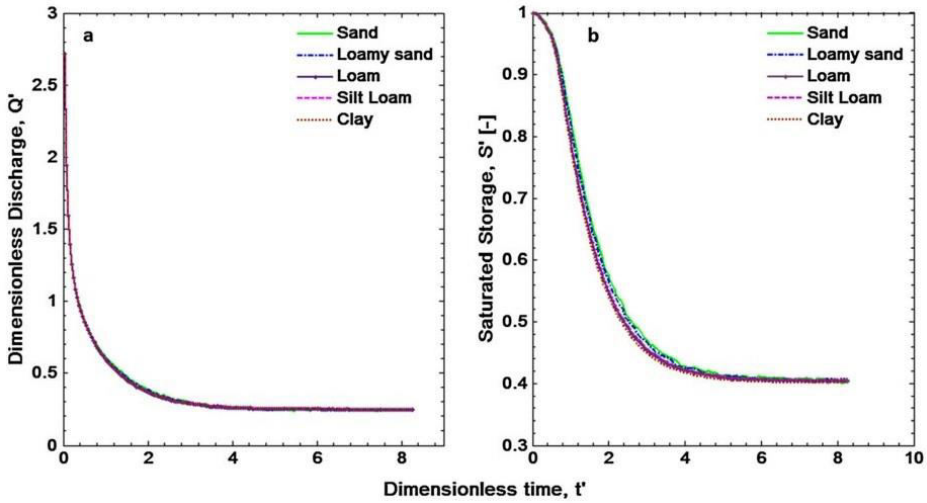

Figure 3.2: Water discharge (a) and saturated storage (b) against time for different soil properties. (Sand, Loamy sand, loam, Silt loam and clay soils)

The dimensionless saturated storage S′ and discharge Q′ has been calculated for the entire simulation. The results (see Figure 3.2) show that changing the unsaturated parameters do not has a relevant impact in terms of non-dimensional variables, on the discharge and the storage, for both the transient and steady-state conditions. The saturated storage calculated from the numerical model for five soil types as shown on Figure 3.2b experiences small variations in the volume of water stored in the system for soils having clay property. This might be due to the capillary fringe, which however seems to have a minor effect on the results. The results were confirmed by other simulations with different configurations. Hence, in the following we shall neglect the impact of the soil parameters in the storage-discharge relation, and we shall make use the parameters of loam soil for all the simulations.

3.3.2 Derivation of Q(S) from steady state analysis

As discussed in the Introduction, the use of storage-discharge relationship implies that the dynamics of the flow is approximated as a sequence of quasi steady-state conditions (e.g. *Sloan, 2000*), following the concept of kinematic modeling. Hence, it is a natural choice to determine the storage-discharge relationship through a series of steady-state numerical simulations. Because of the chosen set of dimensionless variables (equation (3.5)), and the neglect of the influence of the soil parameters (as discussed in the previous Section), the simulation depends only on the slope and the dimensionless discharge Q/LK_s , which at steady conditions equals the inflow from recharge.

Hence, we have performed a set of numerical simulations, with different slopes and dimensionless recharge. Each steady state simulation was carried out, as described in the previous section, by using full saturation initial conditions, imposing a given dimensionless recharge (equal to the desired dimensionless discharge), and performing a transient simulation until steady state is reached (the outflow equals to the infiltration rate). The dimensionless saturated storage $S/L^2(\phi-\theta_r)$ is recorded at the end of the simulations. The same procedure is repeated for several values of the dimensionless recharge and slope. As a final result we have produced a set of six couples of Q and S for each slope. Each computation was carried out using a finite element mesh composed of 1598 triangular nonlinear elements, for a total number of Degrees of Freedom of 3297. The model was run on a standard PC equipped with 4GB of RAM memory and a dual-core CPU (2.90Ghz); each computations required

approximately 3 hours.

The numerical results at stationary conditions are displayed in

Figure 3.3 (dots); each of the six panels refers to a specific slope. The relationship *Q(S)* was derived by best fit of the numerical results. It was found that the results were best represented by a nonlinear, power-law relationship

$$\frac{Q}{LK_s} = a\left[\frac{S}{L^2(\phi - \theta_r)}\right]^b \tag{3.9}$$

where a and b are parameters which depend on the hillslope steepness. The findings seems to confirm the choice for a power-law type of storage-discharge relation usually taken in the literature (e.g., *Kirchner, 2009*; *Botter et al., 2010*), as discussed in the Introduction. The fitted constant b decreases from 1.4 (horizontal slope) to values below unit (b=0.952 for 30^0 and b=0.857 for 45^0).

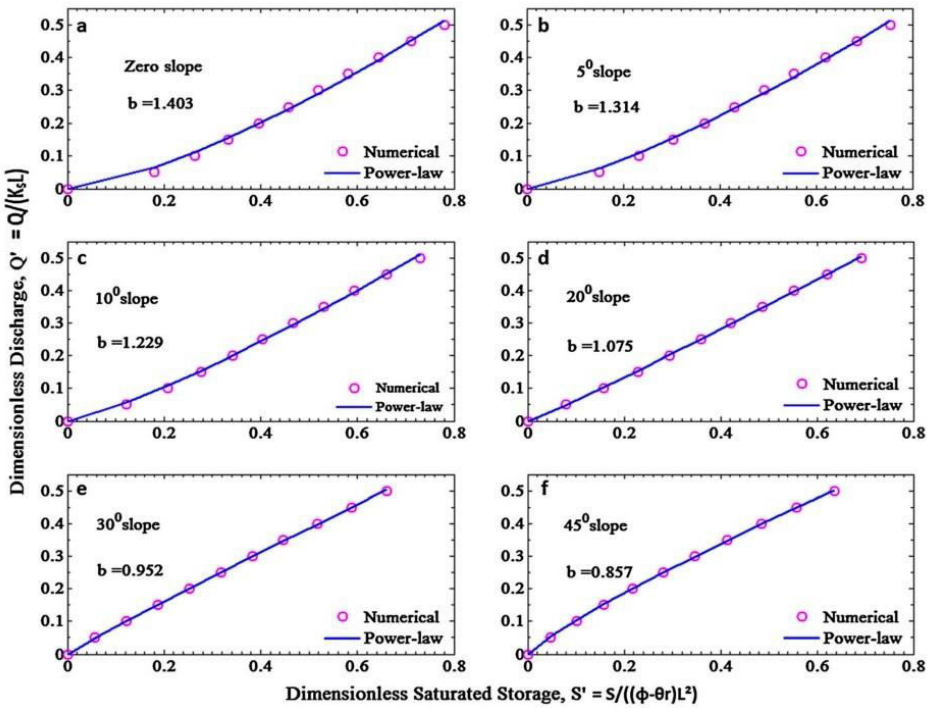

Figure 3.3: The relation between dimensionless saturated storage and discharge from steady state flow simulations. The dots represent the numerical results, while the solid line represents the fitted power-law function. (a) Horizontal slope; (b) 5º slope; (c) 10º (d) 20º (e) 30º and (f) 45º

The exponent b for the horizontal catchment is greater than unity and comparable to the results of *Lee (2007)*, who has obtained that b is 1.24 and 1.35 for flat ground surface and convex - concave topographic catchment respectively. Other studies, (e.g.*Rupp and Selker, 2005*, *2006*) have shown that the analytical solution of the nonlinear Boussinesq equation for sloping aquifers resulted in values of exponent b larger than 1. Field experiments by *Wittenberg (1999)* have shown the same result of

the exponent b with average value of 2. Similarly, *Chapman (1999)* also derived values from 1.62 to 3.24 for 13 catchments in Australia.

In turn, the constant a displays a very small variability, regardless of the slope, in the range 0.72 and 0.74. Hence, we can further simplify the problem and assume a constant $a = 0.73$. Doing so, the parameter b can be easily related to the slope of the catchment by fitting the b-slope relation, obtaining $b=0.5827\phi^2-1.163\phi+1.408$ where ϕ is the slope of the catchment in radian. The curve is displayed in Figure 3.4.

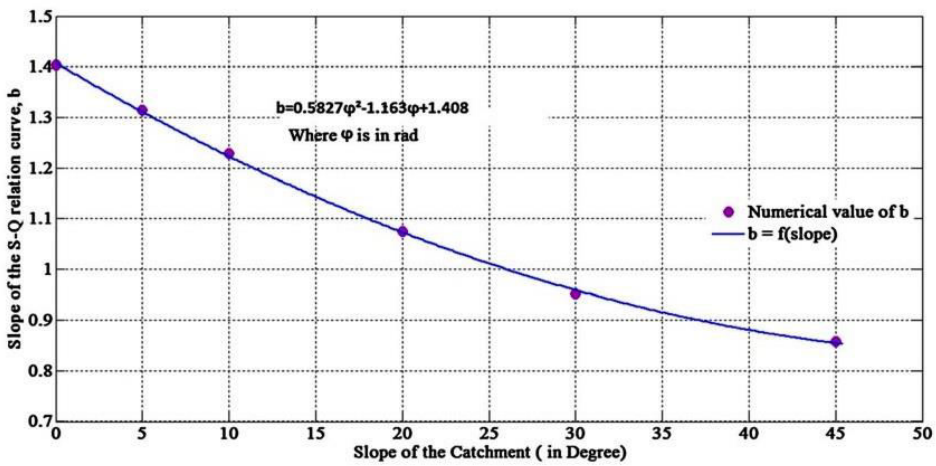

Figure 3.4: Approximated relation between the slope of the catchment and the coefficient b

Summarizing, the steady-state analysis has led to the identification of a power-law storage-discharge relation for the assumed hillslope setup. We found that the power law relation (Equation (3.9)), written in dimensionless variables, can be applied to all the simulated cases with quite good agreement. All the approximations notwithstanding, the curves

may be considered as a first, preliminary approach to estimate the *Q(S)* relation, as function of few relevant physical parameters, like saturated hydraulic conductivity, effective porosity, length and steepness of the hillslope.

3.3.3 Derivation of Q(S) from recession curve analysis

Recession curve is the specific part of the flood hydrograph after a rainfall event, where stream flow reduces. It is dominated by discharge of water from the subsurface during dry conditions and it helps to determine the retention characteristics of the basin and the subsurface storage. The study of the recession curve is also employed to evaluate the volume of the dynamic storage of the subsurface. It is one of the most widely used methods to obtain the storage-outflow relationship curve. It is not our objective here to discuss the modeling approaches of recession analysis, but rather comparing the output relationship curve derived indirectly from recession analysis with the steady state derived one, as outlined in the previous Section. In fact, in the practice it is impossible to measure the water storage S in a hillslope. Conversely, the water discharge is easily measurable, and it is therefore much easier to determine Q(S) from the recession curve analysis. Scope of this Section is to check whether the two approaches (recession curve and steady-state analysis) lead to the same discharge-storage relation. The basic steps for the recession curve analysis are here briefly summarized for the sake of clarity (further details can be found in *Brutsaert and Nieber, 1977*).

In absence of recharge, the continuity equation in dimensionless form

writes as

$$-Q' = \frac{dS'}{dt'} \tag{3.10}$$

Adopting a power law relation for $-Q'(S') = aS'^{b}$, and substituting its inverse relation $S' = (Q'/a)^{1/b}$ in equation (3.9), it yields

$$-\frac{dQ'}{dt'} = a^{1/b} b Q^{2b-1/b} \tag{3.11}$$

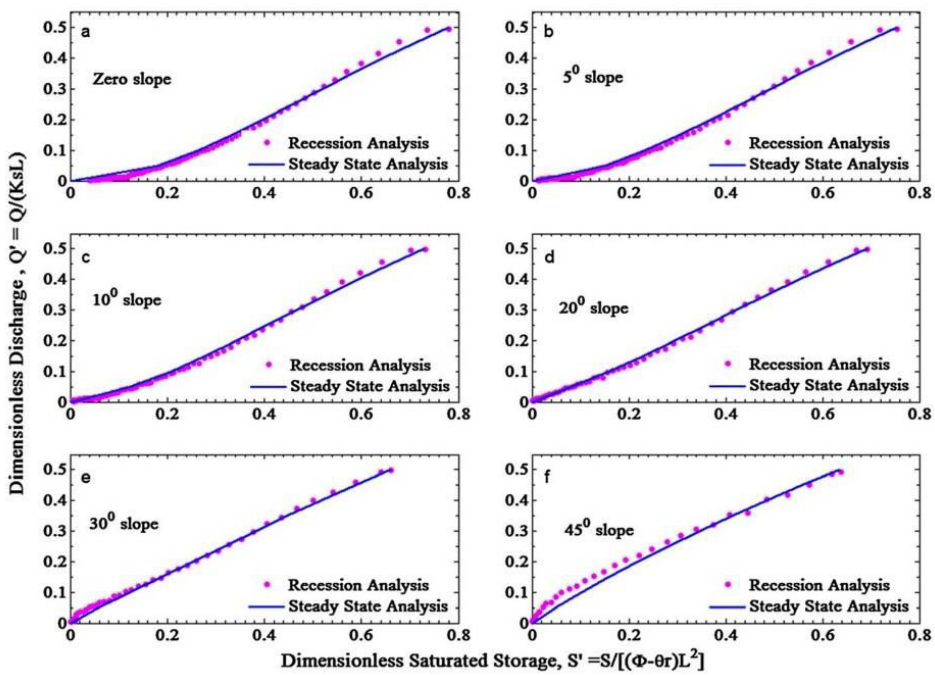

Figure 3.5: Comparison of the storage-discharge relation from steady state simulation with the same obtained by transient simulations. (a) Horizontal slope; (b) 5º slope; (c) 10º slope; (d) 20º slope; (e) 30º slope; (f) 45º slope

Thus, coefficients a and b can be derived from the analysis of the temporal derivative of discharge *Q(t)* as a function of time, by fitting $-dQ/dt$ versus Q to Equation (3.11). The parameters of the conceptual storage model ($Q' = aS'^b$) can be calculated from the recession analysis. However, in the early stages, the slope of the recession curve might be greater than 2, resulting in a negative slope of the storage–discharge curve. Therefore, models for values of $b > 2$ must be recast to provide realistic values of discharge (*Rupp and Woods, 2008*; *Clark et al., 2009*). In our analysis, we never obtained negative values for b as the entire recession curve was fitted, and not only in its early branch. In the following section, we compare a and b coefficients derived from the recession analysis to those presented in the previous section and derived from the steady-state analysis.

A series of numerical simulations were performed for that task. The initial condition is the steady-state configuration analysed in the previous section for the highest recharge rates. Then, recharge is set to zero and free (unsteady) drainage is simulated. For each time step, we calculate the discharge Q and the storage S. First, we checked that the relation Q(S) derived by the unsteady, free drainage analysis was similar to that determined by the steady-state analysis. The comparison is shown in Figure 3.5, in which we plot the numerical results from the unsteady simulation (dots) with the Q –S values obtained through the steady-state analysis (solid lines), performed in the previous section. The comparison suggests that the two types of analysis (steady and unsteady) provide similar results. Perhaps the differences are larger for the steepest case (45º

slope), for which the formation seems to be drained faster than what is predicted by the steady state model. This seems to suggest that for large slopes, dynamic effects may play a more significant role. The previous comparison is based on the assumed availability of the storage S (in our case, it is calculated from the numerical simulations). Thus, we follow the previously outlined recession analysis (which does not require S) and compare dQ/dt as a function of Q with the prediction made in Equation (3.11) with a, b given by the steady-state analysis (Figure 3.3). The results of the procedure are displayed in Figure 3.6, in which the dots represent the numerical results and the solid lines the prediction based on a steady-state analysis. Although dQ/dt exhibits a noisy behaviour, a rather clear trend can be detected. The trend is fairly well predicted by the power law *Q(S)* model elaborated in the steady-state analysis. Consistent with the results from Figure 3.5, the differences are larger for the higher slope. This exercise suggests that the fitting of the a, b parameters through the standard recession analysis may lead to the correct identification of the $Q = aS^b$ structure. This finding is important because, in practice, S is not measurable and the recession analysis is the only way to obtain information regarding the structure of the storage–discharge relation.

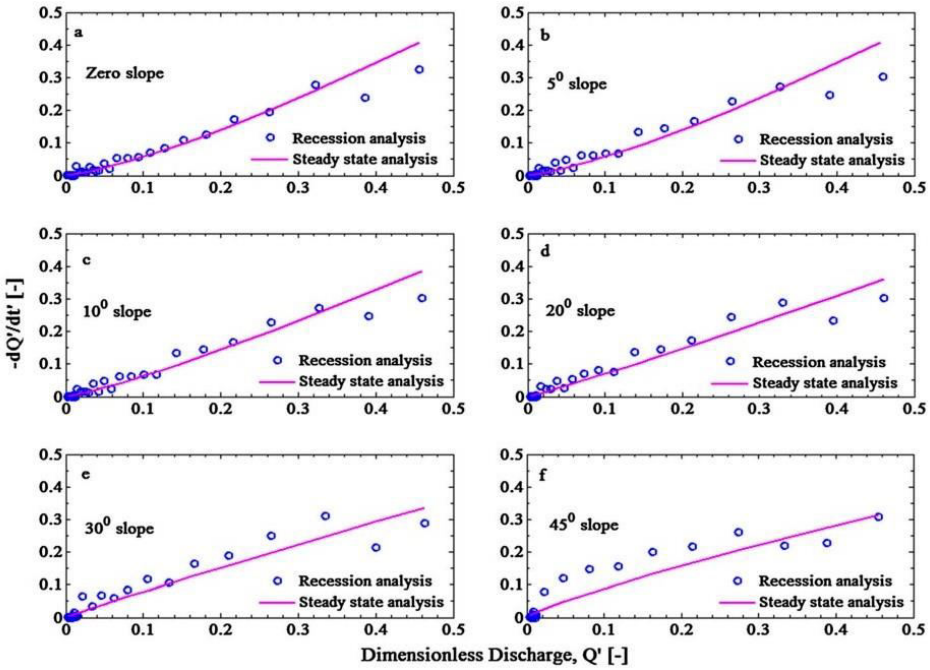

Figure 3.6: Practically, it is hardly possible to measure storage of water in the subsurface; thus it is more convenient to calculate the storage-discharge indirectly from discharge during no-rain conditions (recession curve analysis). The plot displays *-dQ/dt* against *Q* from recession analysis to cross check the possibility of determining the relation curve using the steady state analysis. The rate of discharge *dQ/dt* is calculated from simple finite difference and *Q* is also taken as the average value of the consecutive time steps. (a) Horizontal slope; (b) 5^0 slope; (c) 10^0 slope; (d) 20^0 slope; (e) 30^0 slope; (f) 45^0 slope

3.4 Conclusions

Numerical analysis has been employed to get a better understanding on the formulation of storage-discharge *Q(S)* relationship in hillslopes. The problem has been simplified in order to get a simple expression for *Q(S),*

as function of few physical parameters. Because of the simplifications adopted (like e.g. the shape of the hillslope, *2D* computations, homogeneous soil properties) the derived solution cannot be compared with more complex analyses, e.g. those making use of distributed models. Still, our solution relaxes some of the simplifications usually adopted in the analytical models, like those based on the Boussinesq formulation. Hence, our approach lies in between the simple analytical methods and the more complex distributed models.

By using a steady-state formulation of flow, which is consistent with the "kinematic" nature of models employing the storage-discharge relation, we have found that the dimensionless form of *Q(S)* is approximately a power-law Equation (3.9), which is often used in the hydrologic literature. It was found that the coefficient multiplying the power-law relation is almost constant. Conversely, the exponent depends mainly on the slope of the catchment, and a simple relation was found for it. The value of exponent b obtained for both flat and sloping catchment is comparable to the result of several numerical models and field experiments.

We have also simulated a recession curve analysis, which is the standard tool to infer the storage-discharge relation from measured discharge data. In fact, direct measurements of water storage in the hillslope are practically impossible. It was found that the recession analysis leads to *Q(S)* relation which are very similar to those obtained by the steady-state analysis.

We note again that, because of the (sometimes restrictive) assumptions

adopted, the results of this study may not be universally valid, as real hillslopes are complex and heterogeneous systems; the generalization of the proposed relations to more complex and realistic systems deserves further investigation. Still, the results presented here may serve as a preliminary tool for assessing the storage-discharge relation in a hillslope from physical parameters, like e.g. the length and slope of the hillslope, the saturated conductivity and the effective porosity.

4 Subsurface Stormflow Parameterization, Upscaling from Numerical modeling at Hillslope Scale[2]

Abstract

Subsurface stormflow is an important component of the rainfall-runoff response, especially in steep forested regions. However; its contribution is poorly represented in current generation of land surface hydrological models (LSMs) and catchment-scale rainfall-runoff models. The lack of physical basis of their common parameterizations precludes *a priori* estimation (i.e. without calibration), which is a major drawback for prediction in ungauged basins, or for their use in global models. This paper is aimed at deriving physically based parameterizations of the storage-discharge relationship relating to subsurface flow. These parameterizations are derived through a two-step up-scaling procedure: firstly, through simulations with a physically based (Darcian) subsurface flow model for idealized three dimensional rectangular hillslopes, accounting for within-hillslope random heterogeneity of soil hydraulic properties, and secondly, through subsequent up-scaling to the catchment scale by accounting for between-hillslope and within-catchment heterogeneity of topographic features (e.g., slope). These theoretical simulation results produced parameterizations of the storage-discharge relationship in terms of soil hydraulic properties, topographic slope and

[2] *Adopted from Ali, M., S. Ye, H.-Y Li, M-Y Huang, L.R. Leung, A. Fiori and M. Sivapalan (2014). Subsurface stormflow parameterization for land surface models. Upscaling from Physically Based Numerical Simulations at Hillslope Scale. J. Hydrology(accepted)*

their heterogeneities that were consistent with results of previous studies. Yet, regionalization of the resulting storage-discharge relations across 50 actual catchments in eastern United States, and a comparison of the regionalized results with equivalent empirical results obtained on the basis of analysis of observed streamflow recession curves, revealed a systematic inconsistency. It was found that the difference between the theoretical and empirically derived results could be explained, to first order, by climate in the form of climatic aridity index. This suggests a co-dependence of climate, soils, vegetation and topographic properties, presumably resulting from their co-evolution in the past, and suggests that subsurface flow parameterization needed for ungauged locations must account for both the physics of flow in heterogeneous landscapes, but must also account for the co-dependence of soil and topographic properties with climate, and the mediating role of vegetation.

4.1 Introduction

Due to high infiltration capacities of the soil, steep slopes, and the presence of macropores that enhance downslope water movement, subsurface stormflow is a dominant streamflow generation mechanism in steep forested regions of the world (*Fiori, 2012; McDonnell, 1990; Sidle et al., 2000*). However, its contribution is poorly represented in current generation of land surface hydrological models (LSMs) and catchment-scale rainfall-runoff models. Most LSMs incorporate the role of the subsurface stormflow using various forms of parameterizations (*Huang and Liang, 2006; Huang et al., 2008; Lee et al., 2005; Yeh and Eltahir, 2005*). The lack of physical basis of most common parameterizations precludes *a priori* estimation (i.e. without calibration) has provided the motivation for much research focused on the role of subsurface stormflow and groundwater dynamics on the simulation of land surface water and energy fluxes in climate models.

Recent work by *Hou et al. (2012)* and *Huang et al. (2013)* has shown that water and energy flux predictions at the land surface with the CLM4 model were most sensitive to the subsurface runoff parameterizations (see also *Niu et al., 2005; Niu et al., 2007*). Most current LSMs do not fully account for the contribution of subsurface stormflow to total streamflow and parameters that represent subsurface stormflow are not physically based. For example, the ARNO formulation of subsurface flow (*Todini, 1996*), which is also embedded in the variable infiltration capacity (VIC) model (*Liang et al., 1994*), is empirically based and lacks physical grounds for establishing associated parameters, which limits its extension

to predict in ungauged catchments (e.g., *Huang et al., 2008*). On the other hand, most existing models of subsurface stormflow from hillslopes and small catchments are based on analytical solutions to the Boussinesq equation assuming equivalent representative values of catchment properties (e.g., *Brutsaert and Lopez, 1998; Brutsaert and Nieber, 1977; Rupp and Selker, 2005*, *2006*). This critical review points to limitations of parameterizations of subsurface flow in current LSMs; the intention of the paper is to explore alternative approaches towards the improvement of subsurface flow parameterizations in rainfall-runoff models and LSMs, including how to embed the effects of subsurface heterogeneity in a physically based manner.

This paper is the second of a two-part paper aimed at deriving physically based storage-discharge relations as parameterizations of subsurface stormflow, which can be embedded in land surface models (such as the Variable Infiltration Capacity, or VIC, model (*Liang et al., 1996; Liang et al., 1994*) without the need to resolve the flows at smaller scales explicitly. We are looking for a catchment-scale parameterization of the form:

$$Q = a\,S^b \tag{4.1}$$

with parameters a and b that are meant to capture the net effects of the heterogeneity of soil and topographic properties. Along the way, the paper aims to (1) identify the most important landscape controls on the storage-discharge relationship and (2) use these to develop simple prediction

equation on the basis of measureable landscape characteristics that could be applied to ungauged basins on a regional basis.

One approach to developing such parameterizations is to infer these, using an inverse procedure, from catchment runoff measurements that already account for the net effects of natural variability of soil and topographic properties. We have shown that the parameters *a* and *b* of the storage-discharge relationship can be related to the parameters α and β associated with the recession slope curves (see *Ye et al., 2013*):

$$\alpha = a^{1/b} b \tag{4.2}$$

$$\beta = 2 - 1/b \tag{4.3}$$

where the parameters α and β govern the shape of the recession-slope curve extracted from observed streamflow records. The recession-slope curve, defined by *Brutsaert and Nieber (1977)*, describes the slope of the recession curve after cessation of rainfall, $-dQ/dt$, as a function of discharge *Q*, in terms of a power-function, as follows:

$$\frac{dQ}{dt} = -\alpha\, Q^{\beta} \tag{4.4}$$

In an accompanying paper, *Ye et al. (2013)* proposes an empirical analysis approach that capitalizes on the use of recession curves to derive the storage-discharge relationship. However, runoff measurements are limited to a few locations, and due to the high variability of the factors

that contribute to subsurface stormflow, some of which are not easy to measure, it is not straightforward to extrapolate from gauged locations to ungauged ones. An alternative approach to developing these parameterizations is to use numerical simulation approaches with the use of detailed physically based hydrological models that account for known or assumed forms of spatial variability of soil and topographic properties (*Duffy, 1996; Lee et al., 2005; Robinson and Sivapalan, 1995; Viney and Sivapalan, 2004*). The present study falls in this latter area and builds on considerable prior research activity.

A recent study by *Fiori and Russo (2007)* used a three dimensional numerical model to study flow in heterogeneous hillslopes and found that discharge in the presence of heterogeneous soils is always larger than for homogeneous media with equivalent properties. *Harman and Sivapalan (2009b*) investigated flow through heterogeneous hillslopes and showed that the presence of heterogeneity produce responses fundamentally different from hillslopes with homogeneous soils. The role of topographic variability in controlling subsurface responses at the hillslope scale has also received increased attention in recent times (*Bogaart and Troch, 2006; Freer et al., 1997; Fujimoto et al., 2008; Troch et al., 2003*) since it exerts considerable impact not only on streamflow but also the short term dynamics as well as spatial patterns of soil moisture, and in the long term it also impacts spatial patterns of soil and vegetation properties (*Bachmair and Weiler, 2012*).

The present study is different from previous research in several respects: (i) it aims to derive physically based parameterizations of subsurface

stormflow at the catchment scale, accounting for the effects of heterogeneity of both soil hydraulic properties and topographic slope; (ii) the two-stage up-scaling procedure adopted here (from point to hillslope, and from hillslope to catchment scales) is implemented in a comparative manner in 50 actual catchments; (iii) the parameters of the derived power-law storage-discharge relationships (a and b) are converted to (α and β) and then regionalized through derivation of multiple regression relations with landscape soil and topographic properties, this relationships are then compared against corresponding expressions derived through empirical recession curve analyses on the same 50 catchments (*Ye et al., 2013*). Note that the regression of parameters in the storage-discharge relationships are converted into α and β of the recession curves for the convenience of comparison with the empirically derived relationship. In other words, these two studies approaches the problem of subsurface parameterization from both bottom-up (this study) and top-down (*Ye et al., 2013*) approaches.

4.2 Up-scaling methodology and data resources

The goal of this study is to derive catchment-scale closure relations in the form of storage-discharge relations at steady state that account for the net effects of spatial heterogeneity of landscape characteristics (i.e. soil hydraulic properties and topographic slope). The heterogeneity of landscape properties can be highly complex, multi-scale, and much of it (relating to the soils) unknown. For the purpose of this study we simplify the heterogeneity, without loss of generality, by considering two kinds of spatial heterogeneities: (i) within-hillslope soil heterogeneity (both

random and deterministic), while topographic slope is assumed to remain uniform within the hillslope, and (ii) between-hillslope heterogeneity of topographic slope, whereas the nature of soil heterogeneity is assumed to be the same (and repeated) between hillslopes. In other words, the building blocks of the up-scaling analysis will be the population of hillslopes that constitute a catchment; for simplicity, the hillslopes will be assumed to be planar and rectangular.

Given the nature of spatial heterogeneity assumed above, the proposed work involves a two-step up-scaling procedure: (i) from the point (or local) scale to the hillslope scale, to account for within-hillslope soil heterogeneity, maintaining constancy of hillslope topography, and (ii) from the hillslope to the catchment scale (using parameterized forms of the previous up-scaling to the hillslope scale), now accounting for between-hillslope variability of topography within a catchment. The first step of the up-scaling is carried out with the use of numerical simulations of the Richards' equation at the hillslope scale, which are repeated for several cases by varying the topographic slope and soil hydraulic properties, including different levels of their heterogeneity. Under steady state conditions (i.e., recharge equaling discharge), for all combinations of topographic slope and soil properties, hillslope-scale storage-discharge relations are derived, and expressed in a power-law form. The results of these multiple simulations are pooled together, and regression relationships are derived for the parameters of the storage-discharge relations (i.e., coefficient *a* and exponent *b,* but at the hillslope scale only) in terms of the controlling soil and topographic properties. Together, these

constitute parameterizations of hillslope-scale storage-discharge relations at steady state. The summary results arising from the first up-scaling step to the hillslope-scale are then up-scaled again to the catchment scale, through the application of the "disaggregation-aggregation approach" proposed by *Sivapalan (1993)* and *Viney and Sivapalan (2004)* to account for the effects of between-hillslope heterogeneity of topographic slopes.

The proposed two-step up-scaling procedure is implemented in 50 catchments in eastern United States, which are a subset of the much larger MOPEX dataset (*Duan et al., 2006*), generating power-law form storage-discharge relationships for each catchment (and associated coefficients and exponents). Regional relationships are derived for the coefficient and exponent of these storage-discharge relationships in terms of measured topographic and soil hydraulic properties also at the catchment scale. These are then compared against corresponding regional relationships derived from observed streamflow recession curves for the same 50 catchments, carried out as part of the parallel study by *Ye et al. (2013).* These 50 catchments were chosen under the criteria to minimize the influence from other confounding factors: reasonable number of flow events, minimal impact of regional groundwater and/or snowmelt, minimal human impact and maximum data availability, especially soils data.

4.3 Up-scaling to the hillslope scale: numerical simulations

For the first up-scaling step, we simplify each hillslope as a heterogeneous planar, rectangular hillslope of specified length, width and depth, and specified constant topographic slope. Within each hillslope, we assume an idealized form of the heterogeneity of the surface soil hydraulic conductivity, in the form of a correlated random field in 2-D. In addition to the horizontal, random heterogeneity, the saturated hydraulic conductivity is also assumed to exhibit a further (deterministic) vertical decrease with soil depth.

It is assumed that the 2-D field (i.e., planar, along hillslope surface) of the saturated hydraulic conductivity, K_s, is a stationary and isotropic field following a log-normal probability density function (i.e. $Y = ln(K_s)$ is Gaussian), with assumed known mean $\langle Y \rangle$, variance ($\sigma^2_{\ln K}$) and correlation length (I). We kept other properties such as porosity constant and focus only on the spatial heterogeneity of K_s. We further assume that the random field Y has an exponential auto-covariance (*El-Kadi and Brutsaert, 1985; Fiori and Russo, 2007*) given by

$$C(\xi) = \sigma^2 \exp\left(-\xi / I \right) \tag{4.5}$$

where C is the covariance function; σ^2 is the variance; I is the correlation length and $\xi = x - x'$ is the separation vector. For the characteristic hillslope length scale L, we choose the correlation length such that I/L = 0.04 consistent with the scale of the problem, with the domain being

discretized into equal cells measuring $\Delta x_1/L = \Delta x_2/L = 0.005$ in the horizontal and $\Delta x_3/L = 0.0025$ in the vertical.

The numerical simulations of three-dimensional, saturated/unsaturated flow in heterogeneous porous formations are rather complex and typically require a large computational time. The number of cases to be examined is also large, of the order of 2000. In order to reduce both the computational time and the total number of simulations, we have adopted the single realization approach by *Fiori and Russo (2007)*; the latter consists of employing a flow domain which is large enough to warrant ergodicity, such that the results of the simulations adequately represents the ensemble statistical properties of the flow variables, but not too large, to limit the computational time. Thus, the choice of the domain size results from a trade-off between computational time, number of simulations to be performed and the ergodicity requirement. The single realization of the saturated hydraulic conductivity field used in the simulations was generated using HYDRO_GEN (*Bellin and Rubin, 1996*) and then rescaled in order to respect the constant mean saturated hydraulic conductivity of the surface.

The saturated hydraulic conductivity along the vertical is represented as a deterministic decrease with depth reflecting, amongst other factors, the result of compaction and differential weathering (*Fan et al., 2007*). Following *Beven and Kirkby (1979)*, *Beven (1982)* and *Sivapalan et al. (1987)*, we assume an exponential decrease given by

$$K(z) = Ke^{-fz} \tag{4.6}$$

where $K(z)$ is the saturated hydraulic conductivity at depth z measured from the soil surface, K [LT^{-1}] is the hydraulic conductivity at the soil surface, which has been previously generated by the random field generator, and f [L^{-1}] is an exponential decay parameter. Figure 4.1 shows the saturated hydraulic conductivity field generated corresponding to the above realization.

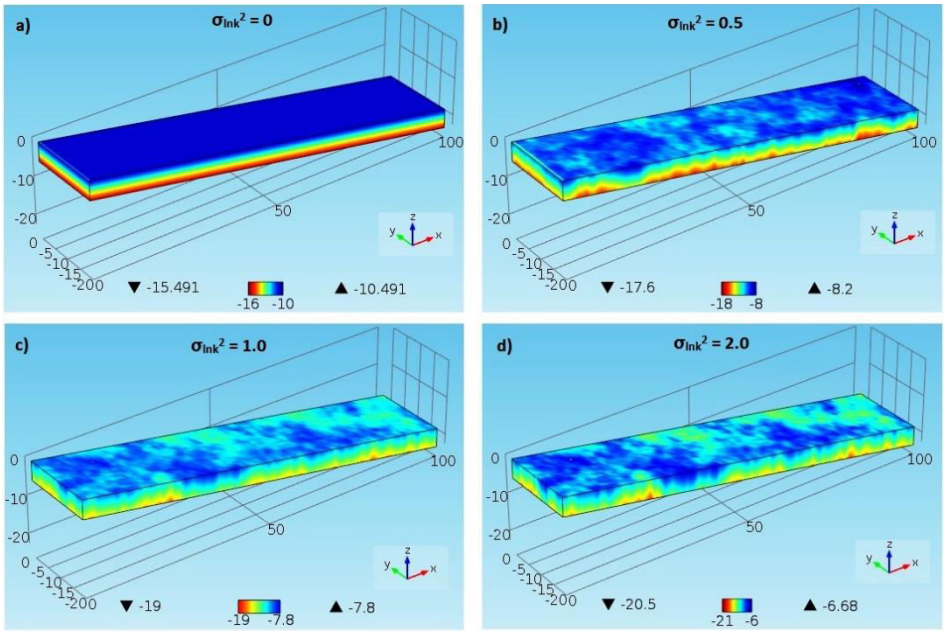

Figure 4.1: Examples of spatial distribution of hydraulic conductivity [*lnK*] are shown for mean surface hydraulic conductivity *Ks* of 28μms^{-1}, topographic slope of 10º and f = 1m^{-1} with different values of spatial variability σ_{lnk}^2 (the color legends are shown in *lnK* where K is in ms^{-1}) The flow domain, which represents a hillslope flow system, is three dimensional (3D) and spans 5m depth, 20m width and 100m length along the Cartesian coordinate system (XYZ) where Z is directed vertically upward.

Subsurface flow within the hillslope is assumed to be governed by the Richards' equation with the focus on saturated flow dynamics only (see Appendix A for the details of the Richards equation formulation). The initial condition is one where the water table is at the surface and the system is fully saturated. The boundary condition at the upper boundary is an assumed net precipitation. The bottom boundary is a no-flow boundary; the same is true for the right, left and upper vertical planes parallel and normal to the flow direction. A seepage face is assumed at the bottom vertical boundary through which water discharges to the stream (Figure 4.2).

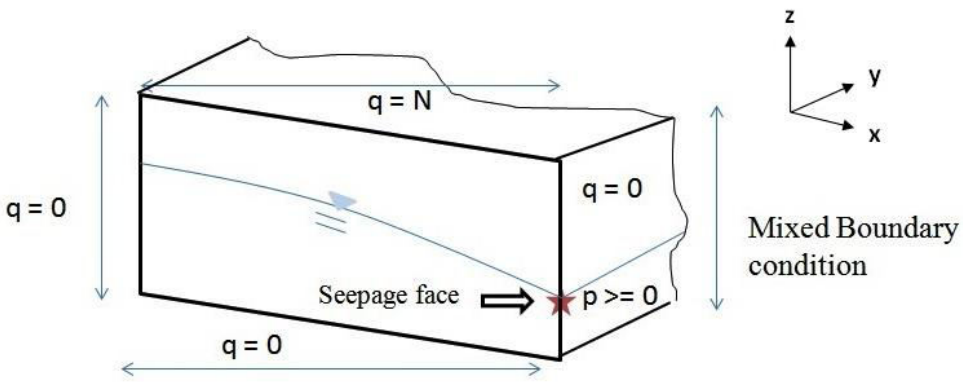

Figure 4.2: Vertical cross section of the 3D flow domain with the boundary conditions

A dimensionless form of Richards' equation is solved by the finite element method using the earth science module of Comsol Multiphysics software that employs numerical methods to solve partial differential equations (*COMSOL, 2010*). The output variables from the model that are of interest are also dimensionless (see *Ali et al., 2013* for details), which are converted back to dimensional forms for the analyses carried out later

in this study. So long as the boundary conditions and the ergodicity assumptions continue to hold, the dimensionless results can be rescaled to obtain results for variable hillslope lengths and depths, as needed for extension to heterogeneous catchments. In order to obtain the S-Q relationship, we have performed a set of numerical simulations with different topographic, soil properties and recharge. Each steady-state simulation was carried out by using full saturation initial conditions, imposing a given recharge (equal to the desired discharge), and performing a transient simulation until steady state is reached. The saturated storage is recorded at the end of the simulations. The same procedure is repeated for several values of the recharge, topographic slope and soil properties in order to produce the required storage discharge curves.

The ultimate result we are looking for at the end of the first-step of the up-scaling procedure is the hillslope-scale storage-discharge relationship, $Q_i(S_i)$, for a given hillslope *i* within a catchment, expressed in the form:

$$Q_i = Q_i(S_i) = a\, S_i^b \qquad (4.7)$$

where Q [L^2/T] is the discharge from the hillslope per unit width of stream and S [L^2] is the saturated zone storage within the hillslope (also per unit width), and the coefficient $\hat{a}$ and the exponent b are constants that reflect the soil and topographic properties of the hillslope. Although the limitations of the assumptions we have made in this modeling

approach and the parameterization of the storage-discharge relationship have been well documented in the literature, it is essential to re-emphasize these here to make sure that our approach can be extended further in the future to enable it to be applied to any ungauged basin, regardless of the specific hydrological characteristics. Some of the limitations and possible remedies for these are: (1) steady-state assumption for the Q-S relation is similar to the widely employed kinematic modeling, in which the continuity equation is coupled with a simplified dynamic formula based on steady-state and it is normally considered an appropriate way of simplifying the model structure and parameterizations. However, the steady state assumption may not be applicable in some cases since recharge rate can be spatially non-uniform and may change over time during a rainstorm and inappropriate for the upslope zone where the saturated depth of the aquifer is large which produces a large deviation of the actual water table from the steady state shape, as shown by *Seibert et al. (2003)* and *Sloan (2000).* (2) The derived storage-discharge relationship is based on the assumption that saturated hydraulic conductivity varies exponentially with depth, which may not be valid for a very shallow soil layer. However, it should be noted that *Beven (1982)* summarized results from a number of field studies on the variation of saturated hydraulic conductivity with depth, which showed that the exponential decay is a reasonable way to describe this dependency. The decrease of K_s with depth may also mimic the presence of discontinuities in the soil-subsoil interface, where the latter is usually less permeable. Hence, it is a convenient and parsimonious way to model vertical contrasts of K_s. A similar procedure is adopted in our model formulation

here, rendering the resulting solutions generally applicable. (3) The assumption that capillarity effects in the unsaturated zone above the phreatic layer can be neglected. In a situation where capillary effects need to be considered, a simple correction term can still be adopted, such as the approach introduced by *Parlange and Brutsaert (1987)* in the context of their kinematic model. However, these extensions are beyond the scope of this paper.

4.4 Derivation of parameterizations of storage-discharge relations

Upon completion of numerical simulations for a large combination of soil and topographic properties, we use variable selection methods to develop empirical relationships between the parameters of the storage-discharge relationship (coefficient a and exponent b) and the landscape (soil and topographic) properties. This is to ensure accurate prediction with a small set of variables that are shown to significantly impact the storage-discharge relationship. The predictor variables include: (1) variables that define the soil hydraulic properties and their spatial variability along the horizontal and vertical soil profiles, and (2) variables that define the hillslope geomorphology, particularly topographic slope.

We first study the influence of each landscape property and their individual effect on subsurface flow and storage, and the storage-discharge relationship. This is done through sensitivity analyses with the simulation model for different combination of predictor variables. Topographic slopes of individual hillslopes were specified as 5, 10, 20,

and 30°; the mean surface hydraulic conductivity (K_s) values used ranged from 3 to 42 μm/s with horizontal heterogeneity ranging from homogeneous to strongly heterogeneous ($\sigma^2_{\ln K}$ = 0.0, 0.5, 1.0 and 2.0); the range of values of the vertical decay parameter, f (m^{-1}), were chosen such that fd = 0.0, 1.25, 2.5 and 5.0. The equilibrium (steady-state) subsurface storage under a range of steady recharge values were computed for these various parameter combinations.

Upon completion of the simulations and the derivation of storage-discharge relations expressed in power-law form, $Q_i = a\, S_i^b$, we used multiple variable regression to develop functional relations relating the parameters a and b (or their logarithmic forms) to the chosen predictor variables. Several regression equations were developed with the combination of the predictor variables involved in the numerical simulation and then the best model was selected based on the Akaike Information Criterion (AIC), which is a measure of the relative goodness of fit used to choose the most suitable model with least information loss (*Akaike, 1974*), with a penalty term included to constrain increase in model size (2k). Since we have a small number of samples in our study, a second order bias correction for AIC was adopted (*Sugiura, 1978*). This criterion is denoted as AICc to make it distinct from AIC and was computed using the following equation,

$$AICc = AIC + \frac{2k(k+1)}{n-k-1} = -2\ln(L) + 2k + \frac{2k(k+1)}{n-k-1} \qquad (4.8)$$

where $\ln(L) = -(n/2)\ln(RSS/n)$ is the maximum log – likelihood, n is the sample size and k is the number of predictors used in each model, RSS denotes the residual sum of squares from the value of the response (i.e. a or b or their logarithm forms) predicted by the fitted model. Furthermore, adjusted R^2 was used to assess the performance of the models compared to the estimated values from the numerical dataset:

$$R_{adj}^{2} = 1 - \frac{SSE}{SST}\frac{n-1}{n-k-1} \tag{4.9}$$

where *SSE* is the sum of squared errors and *SST* is the total sum of squares.

4.5 Up-scaling to catchment scale: disaggregation-aggregation approach

Given the results from the earlier up-scaling, we now need another up-scaling step to extend the hillslope scale parameterization of subsurface stormflow all the way to the catchment scale. For simplicity, especially for computational reasons, we will not undertake numerical simulations of the Richards' equation at the catchment scale to account for both soil and topographic heterogeneity (even though this is technically feasible). Instead, the approach adopted for up-scaling involves dividing a catchment into a large number of representative elementary catchments, each of them being further divided into two or more hillslope building blocks. The parameterizations obtained in the previous step at the hillslope scale are then implemented for the individual hillslopes, and the

results aggregated up to the catchment scale. Figure 4.3 presents a schematic that illustrates the implementation of the modeling.

The proposed up-scaling strategy is subject to a number of simplifying assumptions; 1) natural hillslopes in the catchment are all rectangularly shaped (Figure 4.3) draining to the intermediate stream within each elementary watershed from both sides, and in the case of elementary first order watersheds, a hillslope that drains towards the source node, 2) the effects of natural heterogeneity of soil properties (i.e., saturated hydraulic conductivity) on subsurface flow within hillslopes are fully parameterized, with any between-hillslope heterogeneity of soil properties assumed negligible; and, 3) the only heterogeneity that remains between hillslopes is topographic, and here we assume that only the topographic slope and hillslope length are variable between hillslopes and all other geometric properties remain constant. Clearly, these are strong assumptions but are made to keep the problem tractable. Future work, especially when more information is available on soil properties, can relax these assumptions, and provide more refined and realistic results. It is pertinent to note here that the assumption of rectangular and planar hillslopes is a gross simplification, considering that there is literature pointing to the importance of the shapes of hillslopes in plan and in elevation (convex/concave, converging/diverging) on the dynamics of subsurface stormflow and surface saturation (*O'Loughlin, 1981; Troch et al., 2002; Troch et al., 2003*). It is left to future research to address the issue of corrections that need to be made to the storage-discharge parameterizations.

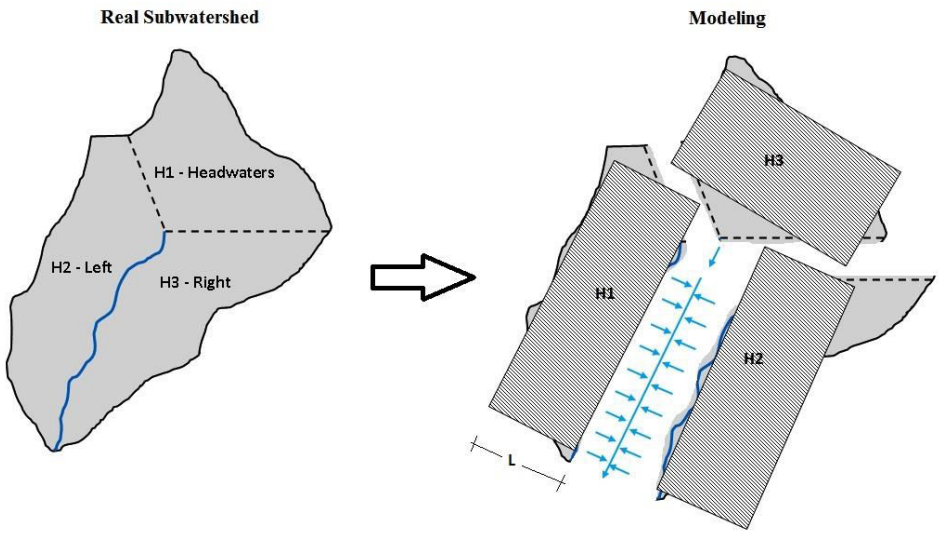

Figure 4.3: Representation of real hillslope with the hypothetical hillslope modelling. The hillslopes are defined as land areas draining either side of the stream reach in each sub-catchment and in the case of headwater sub-catchments (area draining into the source node) an additional hillslope to represent the convergent contributing to a source node. The natural hillslopes are assumed rectangular with hillslope length L along the flow path to the channel.

The up-scaling problem can now be framed as follows: given the storage S at the catchment scale, what is the corresponding discharge, Q? Or, what is the storage-discharge relationship at the catchment scale, $Q = a\,S^b$, and how can we derive this on the basis of the hillslope-scale storage-discharge relationship $Q_i = a\,S_i^b$ derived earlier for individual hillslopes? In this paper the up-scaling is carried out using the disaggregation-aggregation (Figure4.4) approach proposed by *Sivapalan (1993)* and *Viney and Sivapalan (2004).* Assuming quasi-steady state, given the catchment-scale discharge Q, this is disaggregated to recharge (equal to

discharge) per unit area $q = Q/A$, where A is the catchment area. Given this recharge rate per unit area, for a given hillslope i, the steady discharge rate per unit stream width is $Q_i = A_i\, q$, where A_i is the hillslope area per unit stream width. We can then estimate the hillslope scale storage S_i, corresponding to Q_i, through the inversion of the hillslope-scale storage-discharge relationship presented in Eq. 5 above for that hillslope. The catchment-scale water storage can then be obtained through the aggregation (as a weighted average) of all of the hillslope-scale storages, S_i, for all of the hillslopes i constituting the whole catchment, as follows:

$$S = \sum_{i=1}^{n} \frac{A_i}{A} S_i(Q_i) = \sum_{i=1}^{n} \frac{A_i}{A} \left\{ \frac{A_i}{a_i} \frac{Q}{A} \right\}^{1/b_i} \tag{4.10}$$

This estimation procedure is repeated for different values of catchment scale discharge, Q, and in this way the storage-discharge relationship at the catchment scale is derived.

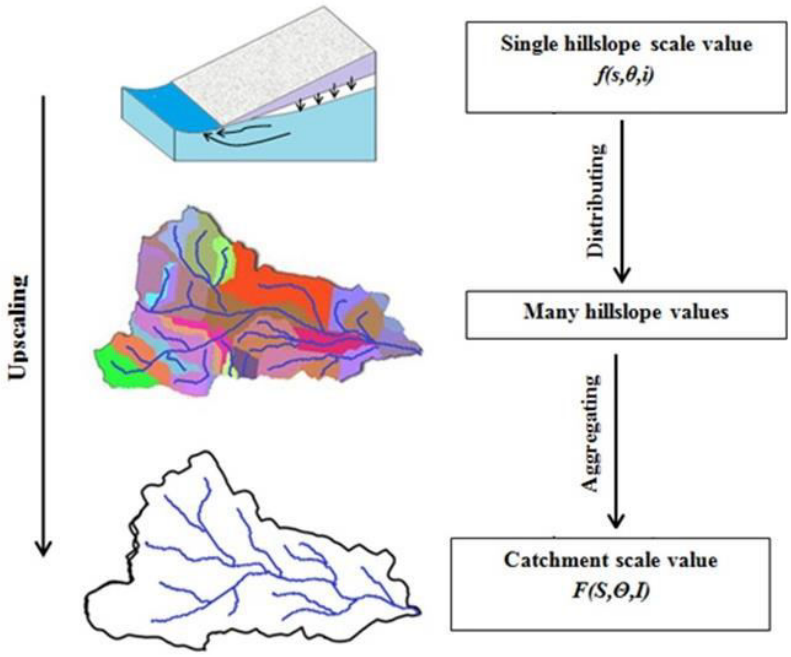

Figure 4.4: schematic that illustrates the implementation of the up-scaling strategy

4.6 Implementation in actual catchments: MOPEX dataset

The up-scaling procedure presented above is implemented in 50 catchments belonging to the Model Parameter Estimation Experiment (MOPEX) dataset, mostly in the East and Midwest of the United States (see Figure 4.5). Topographic slope, aridity index (AI, which is the ratio of mean annual evaporation to mean annual precipitation), drainage density, mean and standard deviation of saturated hydraulic conductivity at the surface, the vertical (exponential) decay parameter of the saturated hydraulic conductivity, soil porosity, soil depth and drainage density were extracted and calculated for these 50 catchments from MOPEX, NHD,

and NRCS SSURGO datasets (*Ye et al., 2013*). These catchment characteristics will later be utilized to develop parameterizations of the storage-discharge relationship (i.e., *a* and *b*) in terms of landscape soil and topographic properties.

The MOPEX dataset provides daily climate and streamflow data from 438 catchments, covering a wide range of climate conditions, landscapes, and ecosystems, ranging from very humid environments in the Northwest to extremely arid conditions in the Southwest of continental United States: http://www.nws.noaa.gov/oh/mopex/index.html. The topographic slope, aridity index and the coefficient and exponent of recession curves were extracted from the MOPEX dataset, while drainage density was extracted from the National Hydrography Dataset (NHD) (http://nhd.usgs.gov/) (see also *Ye et al., 2013*).

Although the MOPEX dataset also provides estimates of saturated hydraulic conductivity, it was a somewhat older qualitative estimate based on soil texture, and the resolution is deemed too coarse for this study. In this study, the soil hydraulic properties are extracted from the USGS SSURGO dataset: http://soils.usda.gov/survey/geography/ssurgo/. The SSURGO dataset is provided by the National Resource Conservation Service (NRCS); it includes both spatial data of the measured map unit, and tabular data of the measurements done within each map unit. The resolution of the SSURGO dataset is 30m, which is about 10 times higher than the STATSGO dataset, and is therefore better suited for the detailed analyses performed in this study. The mean and standard deviation of saturated hydraulic conductivity at the surface, the vertical (exponential)

decay parameter of the saturated hydraulic conductivity and soil porosity were estimated from this dataset. For this study, the soils data at the catchment scale were extracted in a raster format so as to estimate the first two moments and the standard deviation. A procedure was developed to merge the SSURGO data, clip the data by the catchment boundary, retrieve the soil porosity (ϕ), which can be used to describe the soil water storage capacity when combined with soil depth (ϕd), saturated hydraulic conductivity at the top and bottom layer as well as the vertically averaged value for each map unit, and then convert the data to raster data type. These reconstructed raster data with the average porosity or saturated hydraulic conductivity at the surface were then used to compute the spatial average hydraulic conductivity value and its standard deviation

In this paper we will use two of the 50 catchments to demonstrate the up-scaling procedure (as shown in Figure 4.6). These two catchments were selected because of strong differences in climate, topography and soils. Soquel Creek catchment is located along the Central Coast of California, near the southern end of the Santa Cruz Mountains (Figure 2(b) – left panel). The catchment covers a drainage area of 104.1 sq. km with two upstream major tributaries. The elevation decreases from 1036 m above sea level at the highest part to 17 m at the river mouth within a distance of only 16 km along the stream. Its climate is Mediterranean with cool, wet winters and hot, dry summers. Council Creek watershed (Figure 2(b) – right panel) is located in Payne County in north-central Oklahoma. Its drainage area is 80.3 km^2 and total stream length is 68 km. It belongs to the Southern Great Plains and is relatively flat, with topographic elevation

ranging from 333 m at the highest points to 255 m at the river mouth. Table 4.1 summarizes some of the catchment properties of the catchments and their sources.

In order to set up the hillslope building blocks for the up-scaling, we divide each catchment into a population of sub-catchments organized around its stream network. This is done using an appropriate upstream contributing area threshold that generates a drainage network consistent with the observed blue-line stream network from the NHD dataset. The hillslopes are then defined as land areas draining either side of the stream reach in each sub-catchment and in the case of headwater sub-catchments (area draining into the source node) an additional hillslope to represent the convergent contributing to a source node. Digital elevation models (DEM) available for all 50 catchments provide the necessary data to partition the catchments into sub-catchments and then into hillslopes. The up-scaling to catchments scale was performed on the basis of hillslope properties extracted for each constituent hillslope such as topographic slope, mean hydraulic conductivity with its spatial variation within the hillslope and hillslope length, whereas other variables such as soil depth and porosity are assumed to be constant.

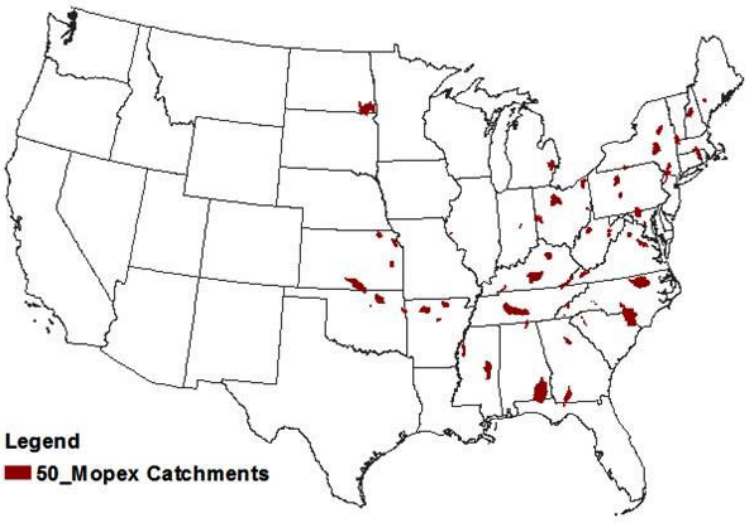

Figure 4.5: Location of MOPEX catchments

Table 4-1: Summary of the available and source of data for the study areas

Data description	Soquel Creek	Council Creek	Data source
Area (km^2)	104.1	80.3	DEM (US geological survey)
Max./min/Elevation (m)	1038/17	362/263	
Mean K_s (cm/day)	15.494	6.23	Soil survey Geographic (SSURGO)
Depth to bed rock (m)	0.89	1.21	Miller and White, 1998
Recession parameter α ($mm^{1-\beta}/day^{2-\beta}$)	1.26	1.97	Ye et al. (2013) and the flow data fromMOPEX dataset
B	2.16	0.99	

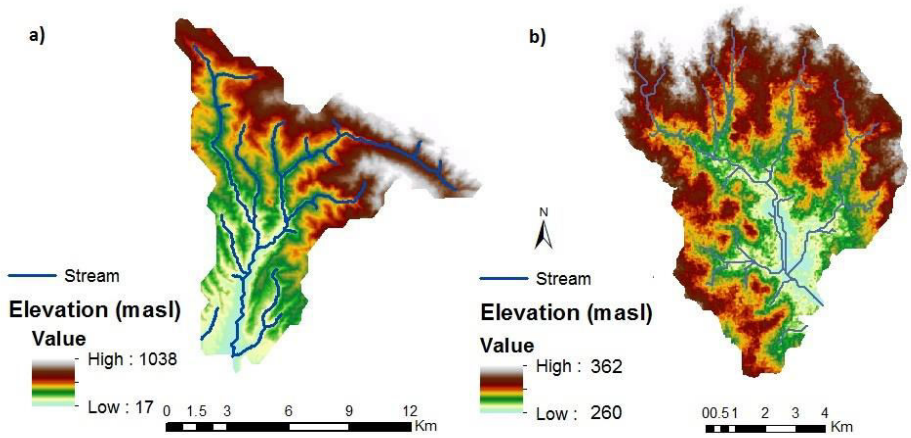

Figure 4.6: Elevation map with river network of a) Soquel Creek watershed, CA b) Council Creek watershed, OK

4.7 Results and discussion

4.7.1 Hillslope-scale simulations

As part of the hillslope-scale simulations, sensitivity analyses were used to investigate the impact of topographic slope and saturated hydraulic conductivity of soils, including both their horizontal and vertical variability on saturated storage, for different recharge rates, under steady state conditions. For this we chose a range of values of the landscape properties in a physically meaningful way, guided by field studies.

Figure 4.7 presents one set of examples of the multiple simulations performed as part of these sensitivity analyses, in each case illustrating the transition from the initial fully saturated condition to the ultimate steady state under the given landscape properties and the assumed recharge rate. Figure 4.7 (a) shows the effect of topographic slope. It can

be seen that for the same soil hydraulic properties, an increase in topographic slope leads to pronounced decreases of the steady state storage value. This result, as well as a similar result in response to changes in the surface hydraulic conductivity, is understandable since increase of slope and/or saturated hydraulic conductivity contributes to an increase of the drainage capacity of the hillslope, and a corresponding decrease of water storage. Figure 4.7 (b) presents the corresponding result in respect of the exponential decrease of saturated hydraulic conductivity with depth. Here, the results are presented in terms of f, the product of the decay parameter f, and soil depth d. The results show that water storage in the hillslope decreases with increase of f. Large f means the hydraulic conductivity at the bottom of the soil is small, and which reduces the drainability of the hillslope, thus helping to retain more water in storage. An opposite result ensues when f is small, and in this way helps to explain the results in Figure 4.7 (b). Figure 4.7 (c) presents the results of sensitivity analyses with respect to the random spatial distribution of hydraulic conductivity. The results show that the impact of the random spatial variability of soil hydraulic conductivity is much less relative to the impacts of the other landscape properties considered in these simulations.

The remainder of the results presented below will utilize the steady state storage values obtained in this way in order to derive the needed storage-discharge relations.

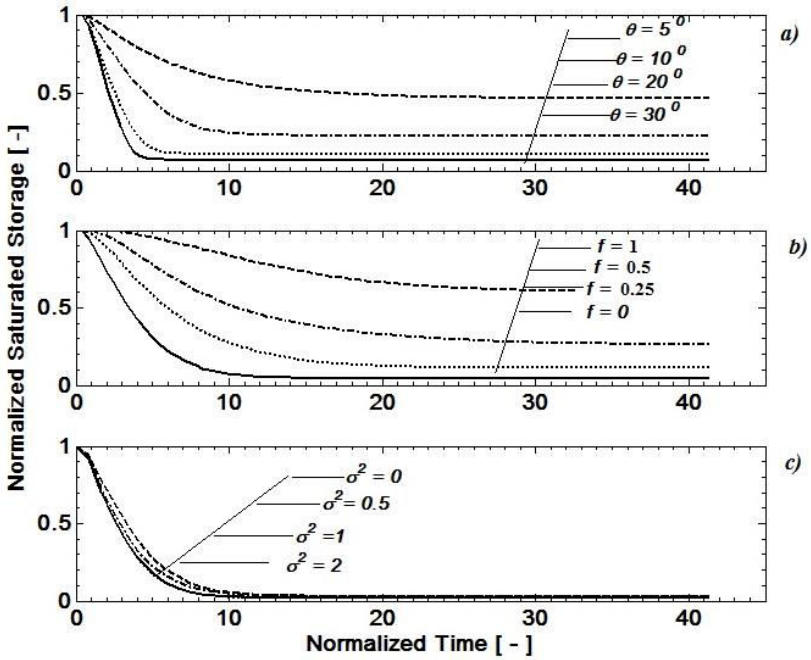

Figure 4.7: Sensitivity analysis of the saturated storage for a) the topographic slope θ, assuming heterogeneous surface soil of $\sigma^2 = 1$, $f = 0$, and constant recharge $q_r = 5mmd^{-1}$ b) exponential decay parameter f assuming heterogeneous surface soil of $\sigma^2 = 1$, topographic slope of $\theta = 10°$, and constant recharge of $q_r = 10mmd^{-1}$ c) the spatial variability of the surface soil hydraulic conductivity, assuming slope θ = 10°, $f = 0$, and constant recharge of $q_r = 10mmd^{-1}$

4.7.2 Developing hillslope scale storage-discharge relations

Multiple hillslope simulations were carried out with the combination of topographic slopes ranging from 5 to 30°, surface hydraulic conductivity K_s ranging from 3 to 42 μm/s, f ranging from 0 to 1m^{-1}, $\sigma^2_{\ln k}$ ranging from 0.0 to 2.0, and uniform recharges at the rates q_r ranging from 0.0 to

10mmd^{-1}. In each simulation the same recharge rate was applied over several days until a steady state was reached. Hillslope scale storage-discharge relationships were then derived from the steady state storage recorded in the system and integrated over the entire domain, and the discharges equal to the applied recharge rates. The exponents and coefficients of storage-discharge relationships were obtained by fitting a power-law equation to results of the numerical simulations (using the MATLAB curve fitting tool box).

Figure 4.8 presents the relationship between landscape properties and the exponent of the storage-discharge relationship curve extracted from the numerical analyses. Figure 4.8(a) shows the impact of hillslope gradient on the exponent of the *S-Q* curve, indicating a significant relationship, which can be fitted with a nonlinear relationship (R_{adj}^2 = 0.56). The scatter in the result suggests that the exponent also depends on other factors and more than one variable is involved in the most appropriate parameterization, in addition to the topographic slope. Figure 4.8(b) indicates a nonlinear relationship between the exponent *b* and surface saturated hydraulic conductivity (R_{adj}^2 = 0.13), whereas the linear relationship with f (R_{adj}^2 = 0.28) shown in Figure 4.8(c) appears to be stronger. Exponent *b* decreases with increase of mean K_s, whereas it increases with increase of the exponential decay parameter, *f*. Clearly, these two relationships, due to their connection to the drainability of the hillslope, are inter-related. On the other hand, as seen in Figure 4.8(d), there appears to be no significant relationship between exponent *b* and $\sigma^2_{\ln K}$ (R_{adj}^2 = 0.006).

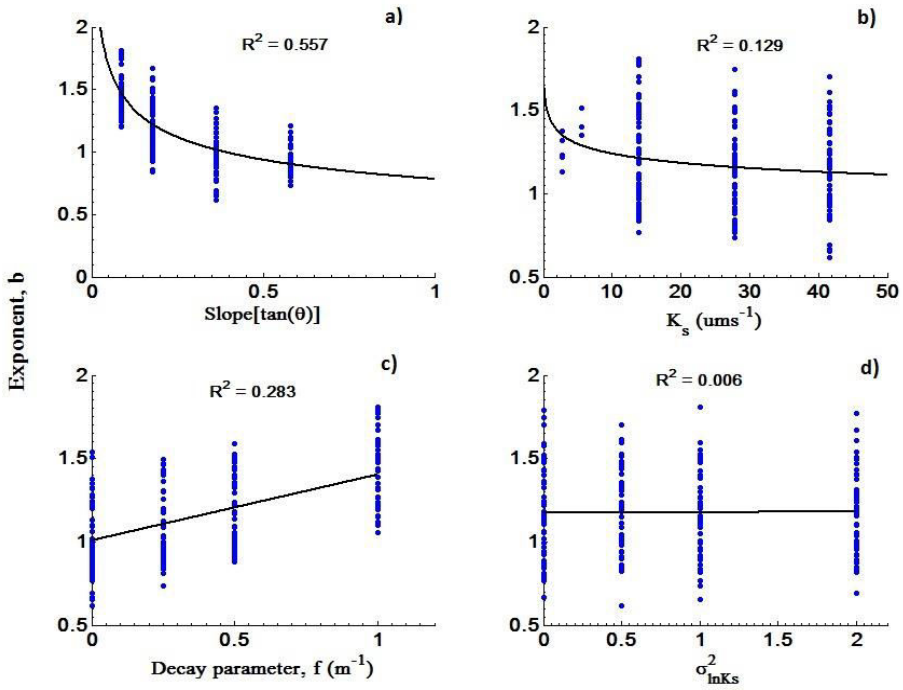

Figure 4.8: The exponent of the power law S – Q relationship curve plotted against a) topographic slope b) Surface hydraulic conductivity c) exponential decay parameter, and d) surface heterogeneity of the hydraulic conductivity

Our analysis next involves the selection of the most influential variables to determine the coefficient and the exponent of the hillslope-scale *S-Q* relationship. The coefficient and exponent must then be expressed in terms of the selected variables in a way that encapsulates the actual processes and accounting for the effects of soil heterogeneity. Stepwise multiple regression analysis yielded the most influential model predictors to form the associated closure relations. The results from possible candidate models from both linear and nonlinear regression analyses shown in Table 4.2 indicate that topographic slope, surface hydraulic

conductivity together with f explain the observed exponents, whereas the impact of random soil heterogeneity, $\sigma^2_{\ln K}$, is found to be negligible. The model predictor based on three selected variables, b ($tan\theta$, K_s, f) has the least *AICc* (i.e. -793.2 for linear and -942.4 for nonlinear models) than the full models developed with a combination of all variables. Interestingly, we found that model fits for the reduced model b ($tan\theta$, K_s, f), i.e., R_{adj}^2 = 0.918, is almost as good as for the full model with all parameters included (R_{adj}^2 = 0.915). Each of the models in Table 4.2 was examined based on their performance to predict the observed exponents and the best model was chosen from the regression analyses ranking their influence on the exponent based on the *AIC* value; the best model turned out to be:

$$b = \frac{\zeta_2 \exp(\varpi_2 fd)}{\tan\theta^{\gamma} K^{\delta_2}} \tag{4.11}$$

where θ is the hillslope gradient, and ζ_b ,γ_b , δ_b and ω_b are constants. Figure 4.9 depicts the good correspondence of the exponent by the proposed model between exponents obtained from numerical simulations and those predicted by the reduced model (Equation (4.11)).

Table 4-2: Model results from some selected subsets of variables estimating the exponent, b, ranked based on their AICc value from the nonlinear regression models

	Linear		Non linear	
Model	**AICc**	**Radj²**	**AICc**	**Radj²**
$b(\tan\theta, K_s, f)$	-793.206	0.86	-942.339	0.9156
$b(\tan\theta, K_s, f, \sigma^2_{\ln k})$	-834.163	0.8616	-938.296	0.9181
$b(\tan\theta, f)$	-752.149	0.7789	-813.021	0.8389
$b(\tan\theta, K_s)$	-605.053	0.5389	-639.537	0.5928
$b(\tan\theta, K_s, \sigma^2_{\ln k})$	-601.628	0.5396	-639.376	0.5947
$b(K_s, f)$	-540.144	0.334	-553.714	0.3523
$b(K_s, \sigma^2_{\ln k})$	-476.018	0.1304	-140.111	0.1353

Using the same approach, the coefficients a of the power-law form of the *S-Q* relationship were also analysed in respect of the influence of the same landscape properties. Figure 4.10 presents how the normalized coefficient $\hat{a} = a(\phi d)^b L^{b-1} / K_S$ changes with topographic slope (Figure 4.10a), hydraulic conductivity, K_s (Figure 4.10b), the normalized exponential decay parameter, f (Figure 4.10c) and the heterogeneity parameter, $\sigma^2_{\ln K}$ (Figure 4.10d).

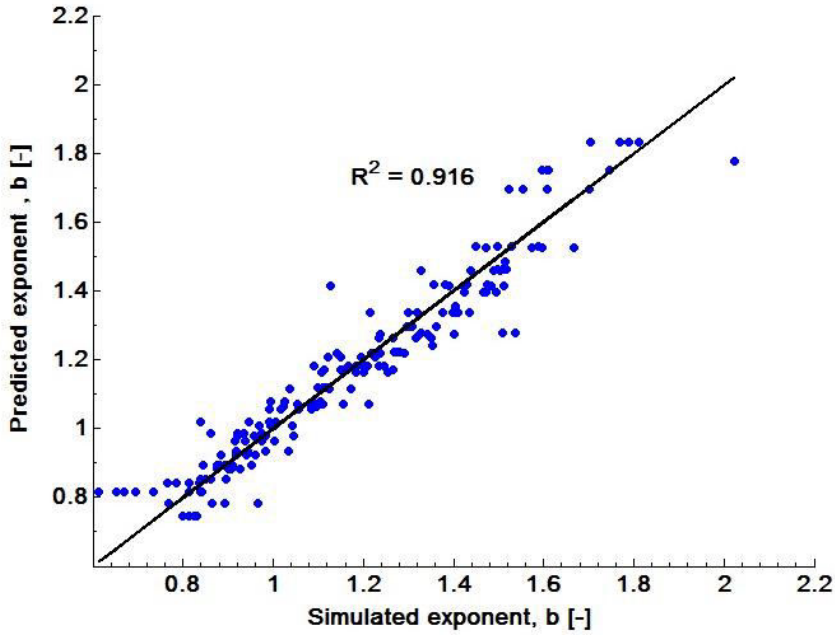

Figure 4.9: The exponent of the power law storage – discharge relationship curve derived from numerical dataset plotted against the predicted value computed from equation (4.11)

The results in Figure 4.10(a) indicate that the topographic slope is a poor predictor of a. The result shows very small variation ($\hat{a}$ ranges from 4.98 – 5.29) for constant K_s = 27.8 μms^{-1}, f = 0.5 and $\sigma^2_{\ln k}$ =1 for a large range of the topographic slopes (5° to 30°). On the other hand, K_s and f in Figure 4.10 (b and c) do explain the coefficient well and the variation is within an acceptable range (R_{adj}^2 = *0.531 and 0.361)*. While heterogeneity did not significantly impact *b*, our result shown in Figure 4.10(d)

indicates that $\sigma^2_{\ln k}$ (R_{adj}^2= *0.165)* has also impact on a. We found that $\hat{a}$ ranged from 3.7 to 4.6 when K_s = 14 μms^{-1} and the heterogeneity, $\sigma^2_{\ln k}$ ranged from 0 to 1 with other variables remaining constant.

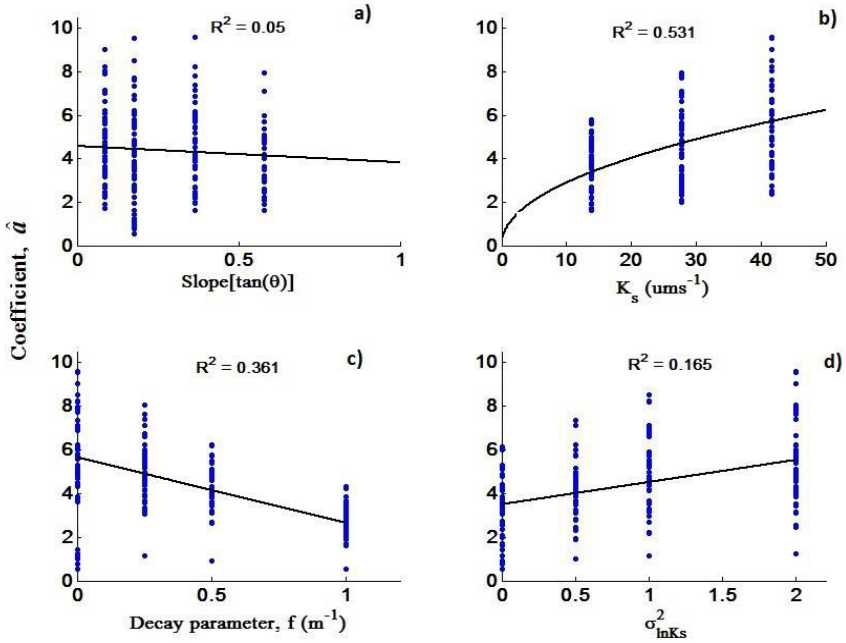

Figure 4.10: The normalized coefficient of the power law storage – discharge relationship curve plotted against a) topographic slope b) Surface hydraulic conductivity c) exponential decay parameter, and d) surface heterogeneity of hydraulic conductivity

Based on the analysis from the multiple-regression, variables K, $\hat{f}$ and $\sigma^2_{\ln k}$ were found to be likely important controls on the coefficient $\hat{a}$. Table 4.3 presents the performance of some selected regression models, sorted according to their *AICc* values. Although the R_{adj}^2 for the full (all variable) model is larger than the other models, it is shown that the three

parameter model, $\hat{a}\,(K, \hat{f}\,, \sigma^2_{\ln k})$ has the least *AICc* (i.e. -211.4 for linear and -464.83 for nonlinear models), indicating that the three variable model can predict the coefficient with minimum inputs. For this reason, chose this model and the resulting closure relation for the dimensional form of the coefficient (i.e denoted as *a*) is as follows:

$$a = \frac{\zeta_a K^{\delta_a+1} \exp(\nu_a \sigma^2_{\ln k} - \varpi_a f d)}{(\varphi d)^b L^{b-1}} \tag{4.12}$$

where ζ_a, δ_a , ν_a and ω_a are constants, d is the soil depth, φ is the porosity and L is the hillslope length. Figure 4.11 shows a very good comparison between the coefficients predicted by the chosen model (Equation (4.12)) and the actual values estimated through numerical simulations.

By combining the expressions for the exponent b and the coefficient a, we can now put together the storage–discharge relationship terms of the total discharge per unit width Q [L^2/T] and total storage per unit width S [L^2] as follows:

$$Q = \frac{\zeta_a K^{\delta_a+1} \exp(\nu_a \sigma_{\ln k}{}^2 - \varpi_a f d)}{(\varphi d)^b L^{b-1}} S^b \tag{4.13}$$

where b is the exponent estimated from Equation (4.12), and φ is drainable porosity, and the other variables and constants are as defined before. The constants shown in the equation are presented in Table 4.4.

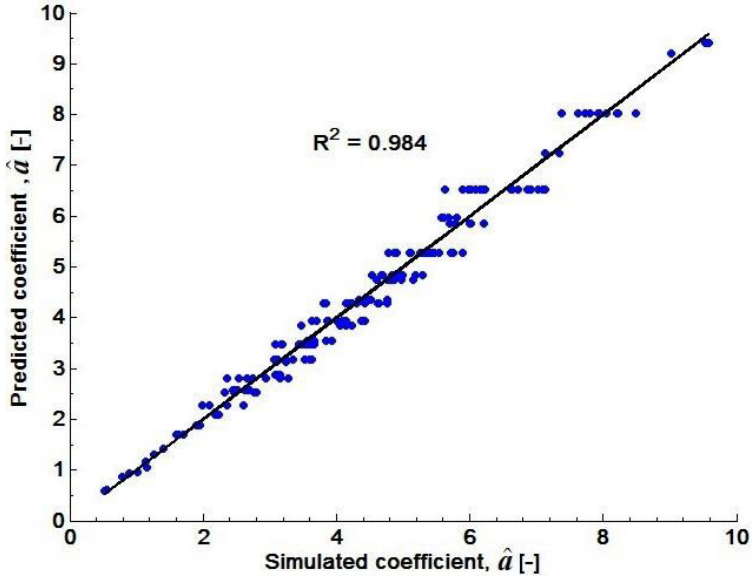

Figure 4.11: The coefficient of the power law storage – discharge relationship curve derived from the numerical dataset plotted against the predicted value computed from equation (4.12)

Examples of the storage-discharge relationship are presented in Figure 4.12, generated with synthetic data of the predictor variables. These represent sensitivity analyses with respect to key predictor variables individually, while keeping other predictor variables constant. For example, Figure 4.12(a) shows that when the topographic slope is increased, with all other variables remaining constant, the exponent of the *S-Q* curve decreases, whereas the coefficient increases, since it also depends on the exponent.

Table 4-3: Model results from some selected subsets of variables estimating the coefficient, a, ranked based on their AICc value from the nonlinear regression models

Model	Linear		Non linear	
	AICc	**Radj^2**	**AICc**	**Radj^2**
$a(K_s, f, \sigma^2_{\ln k})$	-211.412	0.913	-464.837	0.984
$a(\tan\theta, K_s, f, \sigma^2_{\ln k})$	-143.924	0.912	-461.139	0.985
$a(K_s, f)$	-47.1981	0.784	-98.456	0.896
$a(\tan\theta, K_s, f)$	-45.2088	0.782	-97.6005	0.896
$a(K_s, \sigma^2_{\ln k})$	111.5569	0.488	117.0458	0.620
$a(\tan\theta, K_s, \sigma^2_{\ln k})$	113.3526	0.485	118.3311	0.619
$a(\tan\theta, K_s)$	154.0044	0.355	159.4687	0.527

Similarly, Figure 4.12(b) shows that exponent of the storage-discharge relationship decreases with increasing saturated hydraulic conductivity and decreasing exponential decay parameter *f*. On the other hand, the spatial heterogeneity does not have a significant impact on the storage-discharge relationship.

Table 4-4: Regression constants present in the closure equations

Constants	Coefficient	Exponent
ζ	0.65	0.92
δ	0.73	0.11
ω	0.17	0.07
ν	0.21	-
γ	-	0.26

Finally, the disaggregation approach to up-scaling to the catchment scale requires that the storage-discharge relationship given in Equation (4.13)now be expressed in terms of storage and discharge per hillslope area, and not per unit width of stream. Given that $A_i=L$, defining $q=Q/A_i$ and $s=S/A_i$, we then have the corresponding storage-discharge relationship given as follows:

$$q = \frac{\zeta_a K^{\delta_a+1} \exp(\nu_a \sigma_{\ln k}{}^2 - \varpi_a fd)}{(\varphi d)^b} s^b \qquad (4.14)$$

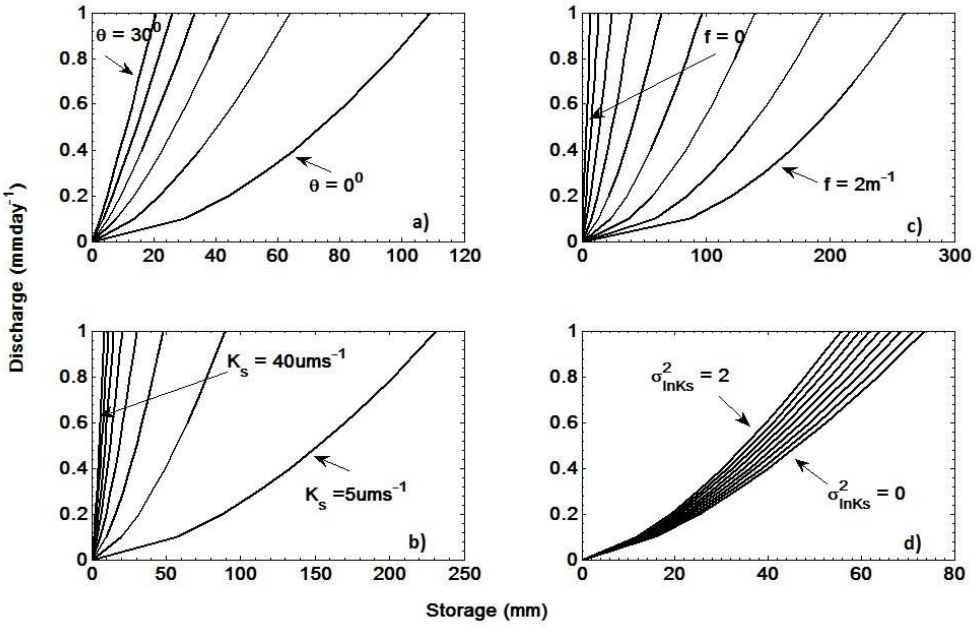

Figure 4.12: Storage – discharge relationship derived from the closure equations for synthetic data with variable a) topographic slope ranges 0 to 30º with 5º interval (other variables are K_s=*14μms*$^{-1}$, f = *1m*$^{-1}$ and σ_{lnks}^2=1) b) Hydraulic conductivity K_s ranging from *5μms*$^{-1}$ to *40μms*$^{-1}$0 with *5μms*$^{-1}$ interval (f = *1m*$^{-1}$, θ = 10º and σ_{lnks}^2=1) c) f ranging from 0 to 2*m*$^{-1}$ with 0.25*m*$^{-1}$ interval (K_s=*14μms*$^{-1}$, θ = 10º and σ_{lnks}^2=1) and d) σ_{lnk}^2 ranging from 0 to 2 with 0.25 interval (K_s=*14μms*$^{-1}$, θ = 10º and f = *1m*$^{-1}$)

4.7.3 Derivation of catchment-scale storage-discharge relationship

The two catchments from the MOPEX dataset were used to demonstrate the up-scaling of the storage-discharge relations from the hillslope to catchment scales. The up-scaling requires sophisticated reprocessing of topographic and soil data. The delineation of sub-catchments and then

hillslopes from digital elevation model (DEM) data is built upon a set of techniques developed over the past few years. Figure 4.13 illustrates the delineated hillslopes in the Soquel Creek (left) and Council Creek (right) with accumulation area thresholds of 300 and 200 pixels, respectively, resulting in 431 and 319 hillslopes, respectively. The up-scaling analyses were performed on the basis of the landscape properties extracted for each hillslope (Figure 4.14 and Figure 4.15), whereas variables such as soil depth and porosity are assumed constant for all hillslopes.

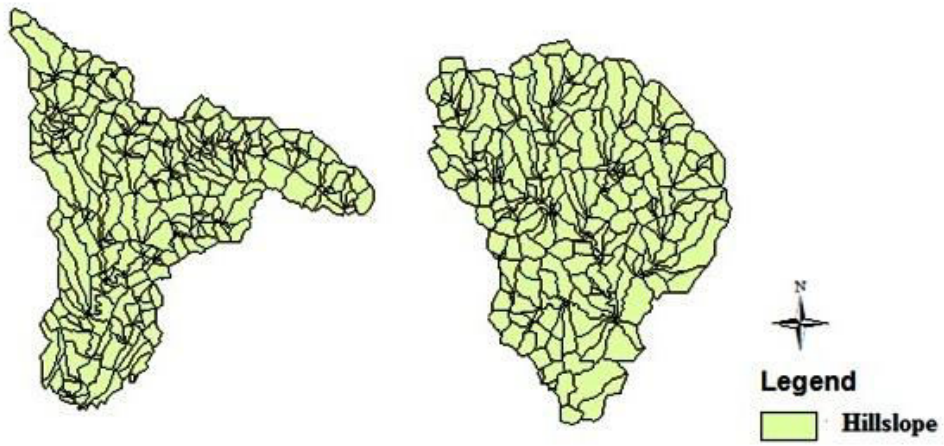

Figure 4.13: Hillslope delineation of Soquel Creek watershed (left: accumulation area threshold of 300) and Council Creek watershed (right: accumulation area threshold of 200)

The up-scaling procedure, i.e., the disaggregation-aggregation approach, outlined in Section 2 is implemented on the two chosen study catchments. We start with representative values of catchment scale discharge, Q, which is converted to uniform recharge $q=Q/A$, assuming steady state

condition. Given the value of q, Equation (4.14) is inverted to generate the magnitudes of the specific storage, $s_i = S_i/A_i$, for all hillslopes within the catchment, using magnitudes of the predictor variables for each component hillslopes and the constants associated with Equations (4.11) and (4.12). Due to the lack of detailed information regarding f, we shall determine the S-Q relationship for a range of values of f, rather than one estimate we have for each catchment obtained from the limited information available. This is done to assess the importance of the f parameter and to provide some insight into the uncertainty of the model predictions.

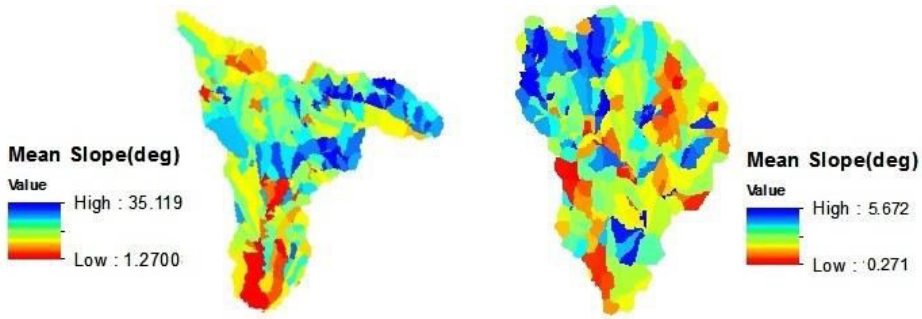

Figure 4.14: Mean topographic slope of the hillslopes in Soquel Creek watershed (left) and Council Creek watershed (right)

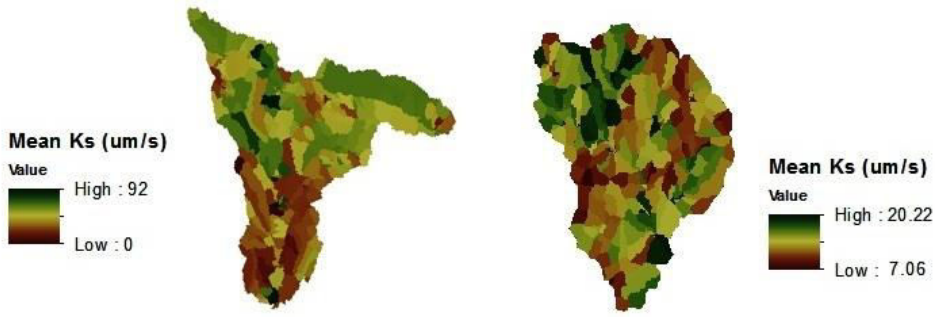

Figure 4.15: Hillslope average surface hydraulic conductivity of Soquel Creek watershed (left) and Council Creek watershed (right)

Result presented in Figure 4.16 shows the storage, s [L] – discharge, q [LT^{-1}] relationships of the Soquel Creek and Council Creek catchments, aggregated from the hillslope scale. It can be seen that the S-Q relationships derived through up-scaling match the results obtained from analysis of recession curves (*Ye et al., 2013*) for $f \approx 0.4m^{-1}$ at the Soquel Creek and $f \approx 0.3m^{-1}$ at Council Creek. The results also indicate considerable sensitivity of the resulting storage-discharge relationships to the magnitude of the f parameter. It can be seen that Soquel Creek exhibits strong nonlinearity in the s-q relationship ($b = 1.35$) whereas Council Creek is more linear ($b = 0.98$). The non-linearity is influenced by topographic slope, also the magnitude of the surface hydraulic conductivity in Soquel Creek. Also, subsurface flow at Soquel Creek originates in the upper catchment, which has a large contribution to the stream, and less water is stored due to the change of relief and high surface hydraulic conductivity (Figure 4.14 and Figure 4.16). Conversely, in Council Creek, topography is relatively flat, and much of the infiltrated

water is stored in the subsurface, and therefore subsurface discharge is relatively low.

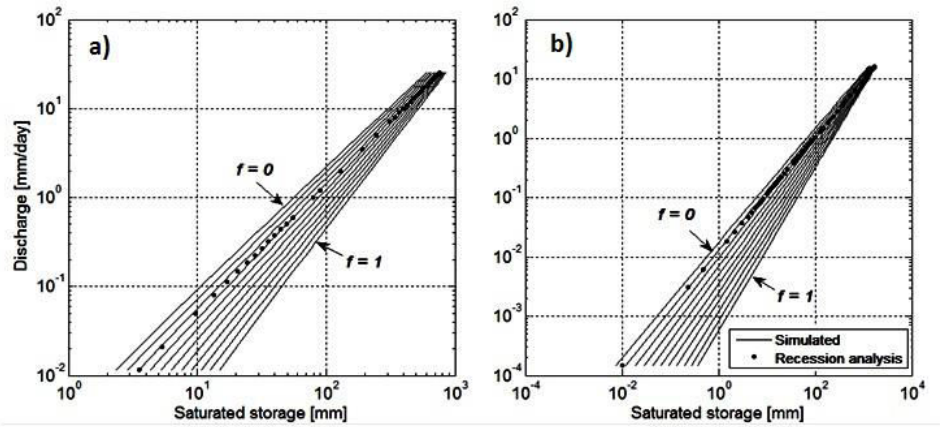

Figure 4.16: Storage discharge curve derived from the hillslope modelling for several values of *f* ranges from 0 to 1 with 0.1 interval (solid lines) and recession analysis of observed stream flow (dot) a) Soquel Creek b) Council Creek

4.7.4 Regionalization of storage-discharge relationship across MOPEX catchments

The up-scaling analyses presented in Section 3.3 above were repeated, and storage-discharge relationships and associated coefficients a and exponents b were derived for all 50 catchments for a range of values of the parameter f. In order to be able to compare these against empirical results obtained through analysis of observed streamflow recession curves, the parameters a and b are converted to parameters α and β associated with the recession slope curves (Equations (4.2)and (4.3)). Multiple regression analyses were next performed against the combination of predictor variables identified as predictors, with the best

models selected with the lowest AIC value. The resulting expressions for α and β are given below:

$$\alpha = \frac{0.0104\theta^{0.67} K_s^{\ 0.92} D_p^{\ 0.01}}{(\phi d)^{0.37}} e^{-(0.85\sigma_{\ln k} + 0.31 f)} \tag{4.15}$$

$$\beta = 1.297(\varphi d)^{0.1} e^{0.15 f - 0.01\theta} \tag{4.16}$$

The result from the theoretical up-scaling approach indicates that the coefficient α of recession curves is a function of topographic slope, surface saturated hydraulic conductivity, porosity, soil depth, and drainage density (i.e. consists of the river network length and the drainage area), which is consistent with the results of previous theoretical studies (*Brutsaert and Lopez, 1998*; *Harman and Sivapalan, 2009a*). Similarly, the result that the exponent depends on soil depth and the exponential decay parameter, *f*, is also consistent with previous theoretical studies (*Rupp and Selker, 2005*, *2006*). The main difference of the present study is that it incorporates the effects of spatial variability of both soil properties and topographic slope, whereas previous results only apply at the hillslope scale with uniform properties.

Now, by fixing the values of the parameter, *f*, to the estimate obtained from the SSURGO soil dataset for each of the 50 MOPEX catchments (*Ye et al., 2013*), regional variations of the magnitudes of α and β can be generated. These are presented in Figure 4.17(a) and (b). It is seen that α is small in the south-eastern part of USA where lowlands are the dominant topographic feature, whereas α values are higher in the

northeast and in catchments in the south-central part. On the other hand, high values of β are found in the east and relatively low values in the center. Figure 4.17 (c) and (d) present the corresponding results derived empirically from the recession curves (taken from *Ye et al., 2013*). They show that there are substantial deviations between the theoretical results and those obtained from the observed recession curves, and that the theoretically derived exponents, α and β show no apparent relationship to the empirical values derived from recession curve analysis. This is a negative outcome of the up-scaling. This could be attributed to: (1) the small scale model, which in this case is based on Richards equation, and its appropriateness in the context of the real world systems, (2) small scale soil parameters, and their representativeness, (3) the upscaling method, including the assumptions made, such as the steady state assumption, and the assumption of complete continuity of the subsurface system all the way to the top of the hillslope. For example, the Richards equation formulation is unable to directly account for the effects of macropore flow and other heterogeneities, and only indirectly through the exponential decay with depth of hydraulic conductivity. Even if we had a model that can account for these effects, there is the added problem of obtaining the corresponding parameter values in actual catchments from standard data. In any case this raises real questions about developing these parameterizations in the short term using the bottom-up approach alone.

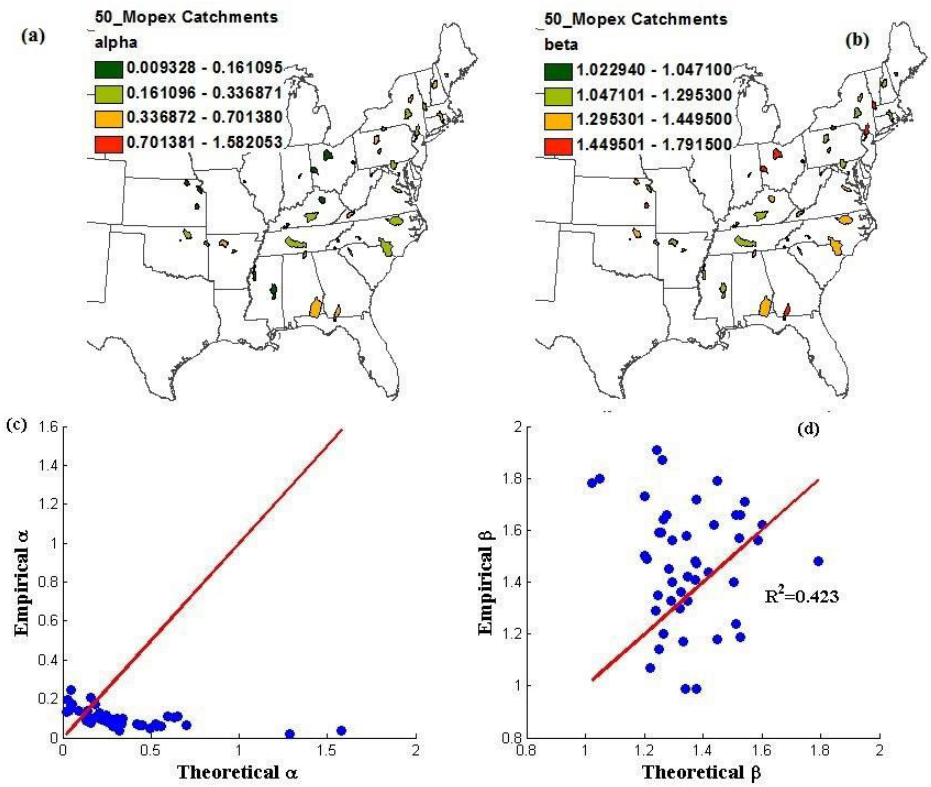

Figure 4.17 Spatial distribution of the recession curve parameters a) α b) β c) the scattered plot of the α values estimated from the bottom-up approach and top-down approach and d) the same as c but for β

In spite of this negative result, further insights into the deviations can be obtained by computing the ratios of the theoretical estimates against the empirical (true) estimates obtained by *Ye et al., 2013*. Again, guided by observations of *Ye et al., 2013*, we look for a dependence of these ratios upon the climatic aridity index (E_p/P, ratio of annual potential evaporation over annual precipitation). Figure 4.18 presents scatter plots of the ratios (theoretical over the empirical/true) of the coefficients, α, and exponents, β. It shows that the ratio of the exponents, β, shows a clear dependence on

E_p/P, providing an interesting insight into the discrepancies between the empirical and theoretical results, whereas the ratio of α values does not show any dependence on E_p/P. The dependence on climate is by far the most important result here. Given that the theoretically derived exponent b has no climate dependence, this is due to the fact that the empirically derived b decreases with increasing aridity E_p/P (from Ye *et al.,* 2014). In view of the direct relationship (both theoretical, see Equation 15, and empirical – see Ye et al., 2014) between b and the exponential decrease parameter f, the climate dependence of b implies a climate dependence of f (for which some evidence exists in Ye et al.). Especially, this further implies that the more arid a catchment is, the smaller f is (which means a deeper hydrologically active layer, deeper root zone, or deep roots): this is a sequence of associations that remains to be explored in an eco-hydrological and hydro-pedological sense.

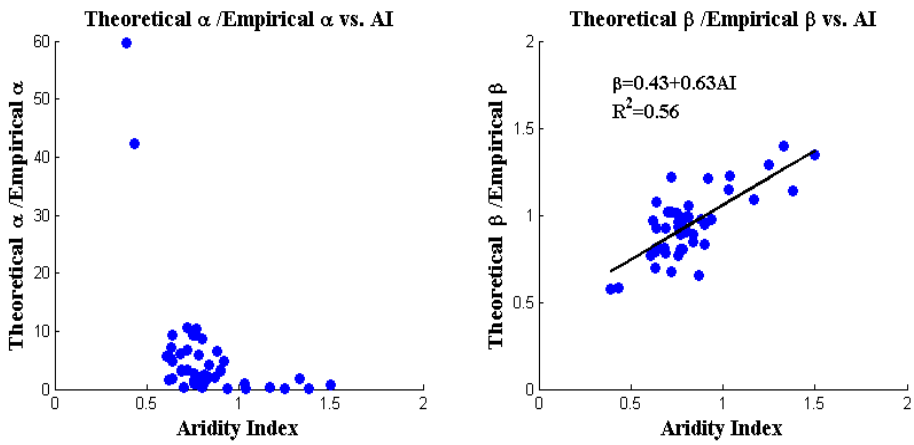

Figure 4.18: Scatter plots of the ratios (theoretical over the empirical/true) of the coefficients, α, and exponents, β

The deviations between the theoretically and empirically derived values of the recession-slope curve parameters can be attributed to several factors: 1) the dependence on climate as discussed above; 2) the inappropriateness of the Darcy's Law-based Richards equation model to account for the structure of heterogeneity present within a catchment; and 3) the uncertainty in the estimates of both topographic and soil hydraulic properties, e.g., estimates of soil heterogeneity and the vertical delay parameter. Improvements to address these weaknesses, including fundamental research to understand the co-dependence of soil and topographic properties, can contribute towards improved estimates of the recession curve parameters (and storage-discharge relationships) in ungauged locations.

4.8 Conclusions

The main aim of this study has been the development of physically based storage-discharge relations governing subsurface stormflow at the catchment scale through parameterization of the effects of within-catchment landscape heterogeneity (i.e., heterogeneity of soil hydraulic properties and key topographic features). The approach involved a two-stage up-scaling. In the first stage, storage-discharge relations were derived at the hillslope scale, accounting for random and systematic heterogeneity of soil hydraulic properties, through recourse to Monte Carlo simulations with a 3-D distributed saturated-unsaturated numerical model of Richards' equation on idealized hillslopes with synthetically generated soil properties. On the basis of the simulation results regression relationships were derived between the parameters of a power-law form

of the storage-discharge relationships (namely the coefficient *a*, and exponent *b*) and measureable soil and topographic properties at hillslope scale. In the second stage, a separate up-scaling procedure was adopted that enabled the effects of the heterogeneity of topographic slopes and hillslope lengths present within actual catchments, leading to new regressions that connected catchment scale parameters *a* and *b* to catchment scale soil and topographic properties. The results obtained are consistent with previous theoretical studies at the hillslope and catchment scales.

The up-scaling procedure was implemented in 50 catchments in eastern United States, and the resulting storage-discharge relations were compared to relationships obtained through regionalization of storage-discharge relations derived from empirical streamflow recession curves. This brought out considerable disparity between the results from these two alternative bottom-up (this study) and top-down (parallel study of *Ye et al., 2013*) approaches. While both approaches led to functional forms for *a* and *b* that were similar, the actual magnitudes of *a* and *b* were quite different.

Comparison with observed exponents showed that in real catchments there is a climate dependence of the storage-discharge relationships, which current physical theory is not able to accommodate. In the short term, for the immediate purpose of developing parameterizations of subsurface flow for LSMs, the way forward to bring about a synthesis of the bottom-up (this paper) and top-down approaches (Ye *et al.,* 2014). This will introduce a physical basis into the empirical parameterizations,

while grounding the theoretical relationships with empirical observations. This will be the next step in this line of research. This raises fundamental questions regarding possible ways forward: (i) how representative are the field measured point-scale soil hydraulic properties, even after accounting for random spatial heterogeneity, of hillslope and catchment scale subsurface flow processes? (ii) how do we account for natural organization of the soil properties over and above the random heterogeneity? and (iii) how do we account for co-evolution of climate, soils, topography and vegetation that gives rise to the self-organization in numerical models of subsurface flow. These are questions that are raised through the work done in this paper, and answers to these questions will require new and fundamental research, which is beyond the scope of this paper.

Part 2: Solute Transport Modeling

5 Travel-time based models for estimating solute transport in hillslopes [3]

Abstract

In this paper we evaluate the performance of four different models for the solute transport prediction in small catchments. All the models employ the concept of travel time distribution (TTD), and the following formulations have been considered: the time-invariant TTD model based on either concentration (TIC) or solute flux (TIF), the Equivalent Steady State approximation (ESS) and the fully time variant model (TV). Detailed numerical simulations were used as a benchmark for the calibration and the assessment of the models' capabilities to simulate transport. We show that the models TIC and TIF, both based on a time invariant formulation of TTD, may either perform not well or do not preserve mass continuity; this is because they were originally developed for steady flow, which is rarely the case in catchments, and their applications to unsteady flows may lead to significant errors. The ESS model performs much better, proving a simple and useful correction to the previous two models. The best predictions are obtained by the TV model, which is also the less parameterized; however, it requires a full description of the input and outflow fluxes and the water storage in the system. The results suggest that a time invariant formulation of the TTD

[3] *Adopted from Ali, M., A. Fiori, D. Russo, A comparison of travel-time based catchment transport models, with application to numerical experiments, Journal of Hydrology, 511, pg. 605-618, http://dx.doi.org/10.1016/j.jhydrol.2014.02.010, 2014.*

is usually inappropriate and not much effective. The performance of all models generally decreases when in presence of evapotranspiration. This depends on the complex and spatially distributed uptake by plants, which is difficult to model through a simple, lumped approach.

Keywords: Solute transport, Tracer, Equivalent steady state, subsurface flow, time variant, time invariant, lumped

5.1 Introduction

Solute transport modeling at the hillslope or catchment scale is a complex hydrological problem due to the complexity of the subsurface physical and geochemical processes, where transient water flow is often the dominant hydrological component (e.g. *Burns et al., 1998; Fiori and Russo, 2007*, *2008; McGuire et al., 2007; Rinaldo et al., 2011*). It is of crucial importance to analyze the physical processes occurring at the hillslope scale in order to explore the fate of solutes coming from different external sources, such as agricultural fertilizers, waste deposits or spill from industrial wastes. The analysis is also important for understanding the tracking of the age of water particles in the subsurface, which may also quantify the contribution of new and old water to the streamflow (*Buttle, 1994; McGlynn et al., 1999; Rodhe et al., 1996; Vitvar et al., 2005*; *McDonnell et al., 2010*; *Fiori, 2012*).

A meaningful and relevant approach to quantitatively estimate the transport of solute into hillslopes or small catchments is through the analysis of the travel time distribution (TTD); the latter is indeed very helpful in predicting the transport and fate of pollutants (*Hrachowitz et al., 2009; McGuire and McDonnell, 2006).* The TTD is typically estimated by examining the release of conservative tracers through the hydrologic forcing (i.e. rainfall) onto a hillslope/catchment (*Beven, 2010; McMillan et al., 2012; Vache and McDonnell, 2006*). Field experiments are undertaken in order to understand the characteristics of the TTD of a solute transport through a catchment system, and thus provide insight into the physical processes ruling the flow and transport mechanisms *Benettin*

et al., 2013; Bertuzzo et al., 2013; Małoszewski et al., 1983; McGuire et al., 2002; Oda et al., 2009; Ozyurt and Bayari, 2005). While those field experiments have been carried out in the past using environmental tracers (*Nyberg et al., 1999*), the range of processes accurately reproduced by the TTD-based approaches is not clear. For instance, most travel-time based, lumped models do not accurately describe the solute transport processes in the subsurface, which is characterized by spatially and temporally variable characteristics and flow processes. In turn, those models are simple and do not employ the complexities usually involved in detailed computational schemes, as well as the requirement of detailed hydrogeological characterization of the physical system; instead, they typically involve travel time distributions that describe integrated transport of solute through the system. In such models, all the processes transferring the inputs to the system into outputs are assumed to be expressed by a simple distribution of travel times which is unique to the system and often valid within the range of flows from which the distribution has be determined (*Niemi, 1990*; *Ozyurt and Bayari, 2005*). Despite the increasing use of the TTD-based models, their performances as function of the system flow condition (e.g. steady or unsteady flow) have not been much explored to date, such that the limitations in practical applications are not totally clear and not much emphasized yet.

A wide range of lumped parameter models (*Hrachowitz et al., 2010; Kirchner et al., 2000*, *2001; Soulsby et al., 2006; Tetzlaff et al., 2007*) and detail physical based numerical models (*Dunn et al., 2007*, 2007; *Fiori and Russo, 2008*) have been developed for estimating the TTD of solutes. Although the numerical models are powerful and in many ways essential

tools for understanding the key flow and transport processes, it is clear that some of the physical parameters cannot be obtained from observation and are usually treated as random (*Dagan, 1989*; *Fiori and Russo, 2007*). Conversely, lumped parameter models are simple and employ TTDs, typically valid under the assumption that the hydrologic system is at steady state (Maloszewski and Zuber, 1996; Kendall and McDonnell, 1998). In real catchments, however, this assumption is not generally valid as flow patterns are ruled by rainfall and evapotranspiration (ET) fluxes, which are by definition time-dependent. In order to overcome the steady flow limitation a few alternative approaches to the time-invariant travel time distribution have been developed in the recent years (see e.g. *Niemi,1977; Zuber,1986; Fiori and Russo,2008; Botter et al.,2010,2011; Rinaldo et al.,2011*) and we will explore some of them in this paper.

The scope of this paper is to evaluate the performance of some categories of solute transport models employing the concept of travel time distribution. The models under consideration involve both time-variant and time-invariant definitions of the TTD, and we shall discuss about the strengths and limitations of each approach, emphasizing the potential ability to predict the solute concentration and the mass recovery at the outlet of the hillslope/catchment system, with and without the presence of evapotranspiration. Finally, we will extend our discussion based on the result and provide guidelines for application of the models regarding their strength and possible drawbacks to estimate the proper TTD.

The model evaluation is performed in two steps. First, the theoretical background for all models is introduced, emphasizing their potentialities, limitations and drawbacks from the sole analysis of their theoretical

framework. We believe that this preliminary comparison is very important in order to summarize and emphasize important features; the latter are found scattered in the existing literature, and have been sometimes overlooked. Then, all the models are tested against the results from detailed and high resolution numerical experiments employing a three dimensional (3D) dynamic model of a conceptual hillslope with real hydrological input (i.e. Rainfall). The simulated concentration in the streamflow was used in order to determine the relevant parameters of the models through a calibration procedure. The model performance is then evaluated after simulation under different validation periods. The choice of numerical experiments is motivated by the possibility to fully control and monitor all the hydrological quantities, within a realistic subsurface setup (unsteady flow, soil/subsoil heterogeneity, uptake by plants, saturated/unsaturated flows etc.). The simulations also provide hydrological data with any spatial and temporal resolution, which is otherwise not easy to obtain in the field, hence allowing us to perform several synthetic transport experiments.

The main scope of the above analysis and test case is to show that, even in the case of a complete knowledge of the system and full data availability (the numerical experiments), there are irreducible and fundamental limitations of some of the models which make their prediction not completely reliable or robust. Thus, this work mainly focuses on basic and fundamental features of some of the existing TTD-based models, while other important problems like data availability, sampling frequency and/or sampling strategies are not considered in this study.

The paper organization is as follows. A description of the numerical experiment (flow and transport modeling, numerical setup, boundary conditions etc.) is presented in Section 2. The four categories of models considered in the study are presented in Section 3, with details on their mathematical framework, their mass recovery capabilities and a discussion on their possible application under unsteady flow conditions. That is followed by the discussion of results, carried out in Section 4; a set of Conclusions, with a summary of the relevant findings and recommendations, closes the work.

5.2 The study case (numerical experiments)

We employ a conceptual hillslope near a surface water stream in which the soil hydraulic properties are spatially distributed. The overall scheme, the details of the numerical modeling and the simulations are presented in *Fiori and Russo (2013),* and we summarize in the following the main points for the sake of completeness.

The system consists of a relatively shallow layer of a high-conductive heterogeneous soil overlying on a thick layer of low-conductive heterogeneous subsoil (bedrock). The flow domain, which represents a part of a large-scale flow system, is three dimensional (3D) and spans 12m depth, 20m width and 20m length along the Cartesian coordinate system (x_1,x_2,x_3) where x_1 is directed vertically downward. The conceptual scheme of the modeling domain and the related boundary conditions are given in Figure 5.1 and further details (including the choice of the domain size) are found in*Fiori and Russo, 2007; Fiori and Russo, 2013*. The system dimensions, which are mainly determined by

computational and ergodicity requirements, cannot account for heterogeneities characterized by scales larger than the domain size.
The subsurface flow is assumed to be locally described by the Richards' equation that governs saturated/unsaturated flow; water uptake by the plant root is proportional to the unsaturated hydraulic conductivity, to the roots' density function, and to the difference between the total pressure head at the root-soil interface, and the reduced water pressure head of the soil, the experiment of *Nimah and Hanks (1973)* was adopted for the macroscopic water sink term in the Richards equation. It is assumed here that the rule for the uptake by plants is the same for both solute and water; the different and opposite rule in which solute is not uptaken was considered in *Fiori and Russo (2007)*. The porous medium is heterogeneous, in which the soil parameters are spatially distributed; they are treated as anisotropic stationary random space functions (RSFs) and characterized by constant mean and depend on scaled separation vector. The solute transport is also described by the classical, one-region, convection-dispersion equation (CDE). *Fiori and Russo (2007)* have shown that the numerical model can lead to preferential owpaths, in both the soil and the subsoil, which are due to the spatial heterogeneity of the hydraulic properties. Also, because of the random distribution of water content and concentration, the uptake of water and solute by plants is spatially distributed and it is nonuniform in the domain.

All the details of the mathematical framework and the numerical solution can be found in *Fiori and Russo (2007)*, and for brevity will not be repeated here. We have also used real meteorological data for the inflow

boundary condition from Denno, northern Italy, which belongs to the Mediterranean humid climate, with warm summers; the major precipitation occurs in fall.

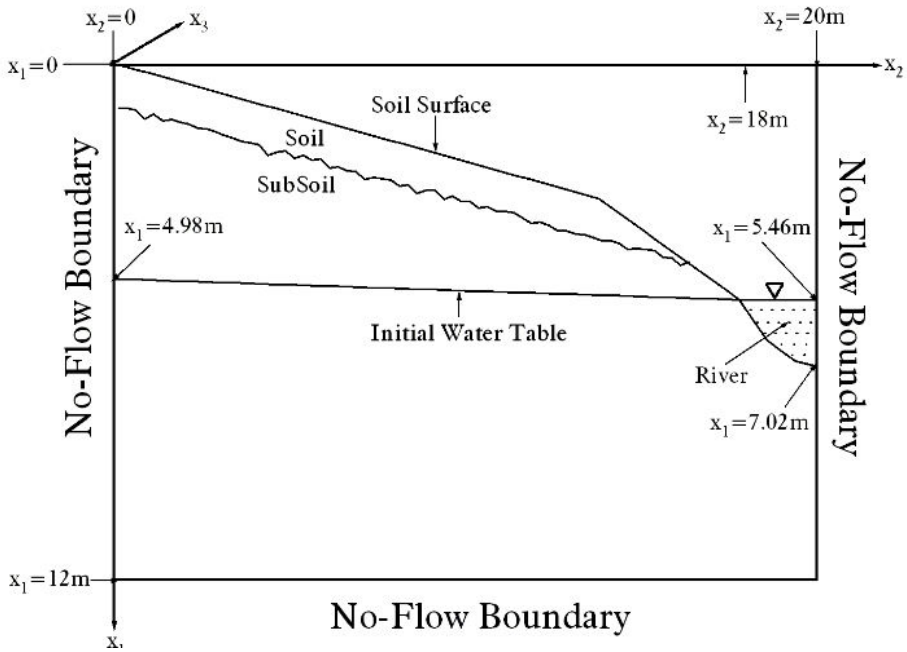

Figure 5.1: Vertical cross section of the 3D flow domain. The vertical x_1x_2 planes located at $x_2 = 0$ and $x_2 = 20$ m are also no-flow boundaries

We study the behaviour of rainfall precipitated in each of the four calendar seasons by marking the rainfall with four different passive tracers, numbered i=1,2,3,4 which correspond to the precipitation occurred in the four seasons of the first year of the simulations, i.e. spring, summer, fall and winter, respectively. The hydrological model was coupled with the transport solver in order to simulate the fate of each solute particle with a unit concentration input. In particular, we calculate

the solute concentration C exiting the system through streamflow when assuming no evapotranspiration, and then again through both streamflow C_Q and evapotranspiration C_{ET}, for each injected mass at season i. This way, we are able to discern the contribution of the rainfall of the i-season to the total water outflow Q, for a period of six consecutive years.

Figure 5.2 displays the cumulated rainfall and outflows derived from the numerical experiment for the rainfall only case (RO), where evapotranspiration is not modelled and similar experiment in the presence of *ET* (RET). Figure 5.3 shows the normalized outflow concentration and the total mass (the inserts) exiting the system through streamflow only (RO, 5.3a) and both streamflow and *ET* (RET, 5.3b), for each of the four periods' injections. Though the injected concentration in all seasons is the same (i.e. unit), the outflow concentration in the streamflow and ET are different because of the spreading taking place in the system and the seasonal variations of rainfall. In the case of rainfall only, the rainfall distribution is the only hydrological forcing to the solute transport and results show that the total solute volume corresponds to the third period (autumn) is higher than the other three seasons; this is due to the stronger precipitation occurring in fall, which typically generates faster water dynamics in the subsurface, with a more rapid mobilization of water. Conversely, the total volume of solute exited through *ET* (Figure 5.3b) is rather similar for the first three seasons, but the minimum solute volume is observed for the fourth period at which there is lower ET (winter). It is seen that the streamflow concentration for the RET case is more intermittent, especially because of the *ET* fluxes near the stream (*Fiori*

and Russo, 2008); this behaviour has a definite impact on the models calibration, as will be shown later. Further discussion on results can be found in *Fiori and Russo (2013)*.

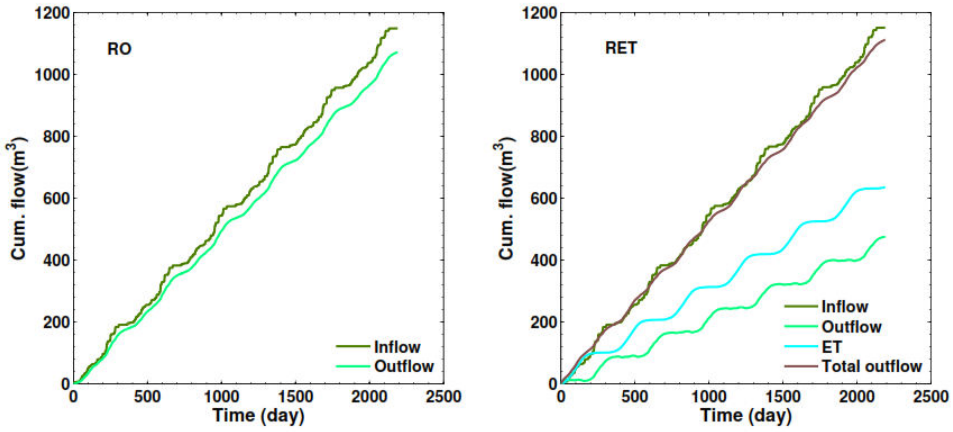

Figure 5.2: Cumulative rainfall and outflow for a) rain only case (in the absence of ET) b) In the presence of ET case. The inserts show the change in the total inflow and outflow volume

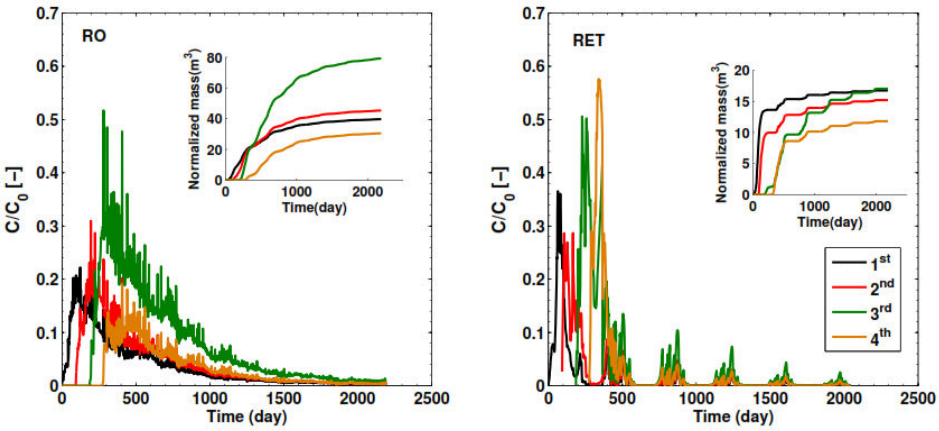

Figure 5.3: Outflow solute concentration obtained from the numerical experiment a) Rain only case b) Rain and ET case. The inserts show the cumulative flux through the streamflow

5.3 Analytical models of catchment transport

We discuss in the following four travel-time based approaches for modeling solute transport in catchments. The approaches are widely employed and mainly differ in a few assumptions regarding the hydrological variable under examination (concentration or solute flux) and the stationarity of flow and/or the travel time distribution. We discuss here the models, some of their properties, their capabilities and limitations based only on their theoretical formulations, while their performance against the numerical experiments shall be analysed later in Section 4.

5.3.1 Time invariant pdf based on concentration (TIC)

A widely employed approach is to model solute transport by assuming a time-invariant travel time distribution, leading to a simple transfer function between input and output concentrations (*Barnes and Bonell,*

1996; Kirchner et al., 2000, *2001; Małoszewski and Zuber, 1982*). The time invariant assumption is strictly valid only when the subsurface flow is stationary, which is unlikely to occur in natural hillslopes where flow patterns are typically unsteady; the limitation of the assumption has been discussed by *Beven (2010)*, *Dunn et al. (2010*) and *Fenicia et al. (2010)* among others. After adopting the time invariant assumption, the input and output concentrations are related through the convolution integral and the catchment properties are characterized by their average values; the temporal variation of flow has generally been ignored so that its response to solute injected in different time instances described by the same travel time distribution(*McGuire and McDonnell, 2006*). Thus, the concentration at the stream outlet *C(t)* after an input concentration C_0 and neglecting evapotranspiration is written as

$$C(t) = C_0(t) * p_s(t) = \int_0^{\infty} C_0(\tau) p_s(t-\tau) d\tau \qquad (5.1)$$

The travel time distribution $p_s(t)$ depends on the "average" flow patterns toward the stream which take place in the hillslope; it has a role similar to the instantaneous unit hydrograph (IUH) which is often used in the rainfall-runoff modeling. However, in general the unit hydrograph is not the same as the travel time distributions of a solute transport (*Fiori and Russo, 2008; Zuber, 1986*), unless flow is at steady-state. An expression similar to equation (5.1) can be written for the concentration C_{ET} and the TTD p_{ET} related to evapotranspiration (ET).

The total injected mass M_{in} and the mass recovered from the system M_{out} in any reference period can be calculated through equation (5.1), as follows

$$M_{in} = \int_0^\infty Q_0(t)C_0(t)dt$$
$$M_{out} = \int_0^\infty Q(t)C_Q(t)dt + \int_0^\infty ET(t)C_{ET}(t)dt \qquad (5.2)$$

where $Q(t)$ is the streamflow discharge and Q_0 the rainfall (L^3/T) applied to the system. It is easy to see that in general $M_{in} \neq M_{out}$ unless steady state conditions apply, i.e. Q_0=Q=const. A similar finding holds when in presence of ET. Thus, the model TIC does not generally fulfill the basic continuity mass requirement for the hillslope system under unsteady flow conditions, which are rather the norm. Though the TIC model has been used in most literatures, the uncertainties from steady state assumption and the neglect of the temporal variability of flow and storage may change the estimated TTD (*Botter, 2012; Rinaldo et al., 2006*); the assumption may be more appropriate for humid catchments where seasonal rainfall variation is less significant (*McGuire et al., 2002*).

For this and the next two models we shall use the gamma distribution to represent the TTDs pertaining to streamflow concentration. The gamma pdf is widely used in the literature and it has a rational background (*Fiori and Russo, 2008; Hrachowitz et al., 2010; Kirchner et al., 2000*), being

both flexible and easy to use. The two parameters gamma distribution is given as

$$p(t) = \frac{t^{\beta-1}}{\beta^{\alpha}\Gamma(\alpha)} e^{\frac{-t}{\beta}} \tag{5.3}$$

where $p_s(t)$ is the TTD, $\Gamma(\alpha)$ is gamma function, α is the shape parameter, and β is the scale parameter. If $\alpha=1$, the gamma distribution degenerates into an exponential distribution. A more general analytical distribution for hydrological transport is the "truncated one-sided stable density", of which gamma and the exponential are special cases (*Cvetkovic, 2011*). Field and theoretical analysis suggest that $\alpha<1$ (*Fiori et al., 2009; Kirchner et al., 2000*). In order to determine the unknown parameters (α and β), which describe the characteristics of the TTD, the system needs to be calibrated against the solute concentration derived from the numerical model that is supposed to be observed.

5.3.2 Time invariant pdf based on solute flux (TIF)

The previous analysis indicates that when rainfall variation are high the TIC model cannot be used (see also *Heidbüchel et al., 2012*) and a more robust approach involving the variation of flow and water storage in the hillslope is needed. Perhaps the simplest approach is the one by *Zuber (1986)* who replaced solute concentration with mass flux (including the variable discharge) in the convolution equation (5.1); the model is denoted in the following as TIF. The convolution expressed in terms of solute fluxes instead of concentration is indeed more meaningful (*Dagan et al., 1992*), especially for flow systems which are not at steady state;

however, the TTD is still time-invariant, i.e. characterized by a unique expression which does not change with time. Despite being more realistic than TIC for unsteady systems, TIF is much less employed in applications. Obviously, when the flow is steady the TIF approach is identical to TIC.

In order to model outflow solute concentration in the presence of evapotranspiration, it is essential here to introduce a partition parameter $\theta(t)$, which denotes the probability that the generic water particle injected at time t is discharged to the stream at $t+\tau$, where the remaining fraction ($1-\theta(t)$) ends up as ET (*Botter et al., 2010; Rinaldo et al., 2011; van der Velde et al., 2010*). Thus, the solute fluxes which exit the system through Q and ET are written as

$$F_Q(t) = \int_0^\infty F_0(\tau)\theta(\tau)p_s(t-\tau)d\tau \tag{5.4}$$

$$F_{ET}(t) = \int_0^\infty F_0(\tau)(1-\theta(\tau))p_{ET}(t-\tau)d\tau \tag{5.5}$$

where $F_0(t) = Q_0(t)C_0(t)$ is the solute injected to the system , $F_Q(t) = Q(t)C_Q(t)$ is the solute flux exiting V through streamflow and $F_{ET}(t) = ET(t)C_{ET}(t)$ is the solute flux exiting through evapotranspiration.

We perform also for the TIF model the mass balance check, as previously done for TIC. The total inflow (M_{in}) and outflow (M_{out}) are given by

$$M_{IN}(t) = \int_0^\infty F_0(t)dt \tag{5.6}$$

$$M_{out} = \int_0^\infty \int_0^t F_0(\tau) p_{tot}(t-\tau) d\tau dt \tag{5.7}$$

with $p_{tot}(t-\tau)$ is the exit time distribution for the entire control volume corresponds to all possible hydrological processes (i.e. *ET* and *Q*) and given by

$$p_{ex}(t-\tau) = \theta(\tau) p_s(t-\tau) + (1-\theta(\tau)) p_{ET}(t-\tau) \tag{5.8}$$

Changing the order of integration in equation (5.8) and recalling that $\int_0^\infty p_{ex}(t)dt = 1$, expression in equation (5.8) can be simplified as

$$M_{out} = \int_0^\infty F_0(\tau) d\tau = M_{IN} \tag{5.9}$$

Thus, contrary to TIC, the model TIF always fulfills the mass continuity principle, and the total mass recovered from the system is always equal to the injected one. However, the above condition is obeyed only for the total mass flux $F_Q + F_{ET}$, and because of the rather uncertain nature of the

partition coefficient θ the mass exiting through either F_Q or F_{ET} may be different from the real one.

5.3.3 Equivalent Steady State approximation (ESS)

An alternative method to account for transient flow regimes is to replace the calendar time in the TTD with the total volumes entered or left the system after a fixed reference time (*Niemi, 1977; Rodhe et al., 1996*); the approach have been recently tested by *Russo and Fiori (2008)* and *Fiori and Russo (2008)* and it was denoted there as Equivalent Steady State (ESS) approximation. As noted by *Rodhe et al. (1996)*, ESS implies that the flow paths are assumed as time invariant. Still, *Niemi (1977)* showed that the approximation may be rather robust and more effective than TIC to analyse transport under unsteady conditions. The solute mass exiting through the evapotranspiration, which was sometimes neglected in the past (see e.g. *Rodhe et al., 1996*), can be also modelled with the ESS approach; it is expected that the TTD parameters are different than those pertaining to streamflow. A rigorous and more general analysis of suitable steady state approximations, for which ESS is a particular case, has been recently carried out by *Cvetkovic et al. (2012)* and *Soltani and Cvetkovic (2013)*.

Following the ESS approach, the injection time (τ) and exit time (t) of the solute flux are expressed by the newly introduced rescaled times τ_R and t_R (see, e.g., *Niemi, 1977*); generalization for $\theta < 1$ leads to

$$\tau_R = \frac{V_0(t)}{\overline{Q}} = \frac{1}{\overline{Q}} \int_0^t \theta(\tau) Q_0(\tau) d\tau \tag{5.10}$$

$$t_R = \frac{V(t)}{\overline{Q}} = \frac{1}{\overline{Q}} \int_0^t Q(\tau) d\tau \tag{5.11}$$

where $V_0(t)$ is the cumulated rainfall volume injected in the control volume and $V(t)$ is the cumulated outflow volume flowing to the stream, while Q is the mean reference discharge over the time interval of interest (e.g. annual mean discharge). Similar rescaled times are also developed for ET in the case of evapotranspiration (i.e. $\theta(t) < 1$) as discussed in the previous section.

Along the ESS approach, the outflow concentration is related to the input concentration through a convolution with the TTD, which is now related to the rescaled times and it is still time-invariant

$$C_Q(t_R) = \int_0^\infty C_0(\tau_R) p_s(t_R - \tau_R) d\tau_R = C_0(t_R) * p(t_R) \tag{5.12}$$

where the TTD p_s is different from the one employed in equation (5.1), unless flow is steady. The concentration $C(t)$ at calendar time t is obtained by converting t_R to t following the same expression in equation (5.10) and (5.11), after performing the convolution. A similar procedure is followed for the ET-related concentration $C_{ET}(t)$, with the obvious change of notation.

Summarizing, the ESS model implies that the same convolution appearing in TIC can be applied by a simple rescaling of calendar times. Recent works (*Fiori and Russo, 2008; Russo and Fiori, 2008; Salvucci*

and Entekhabi, 1994) have shown that the above assumption may be quite effective for unsteady subsurface flow processes. As the other methods, ESS requires that both the inflow and outflow discharges are known in advance, e.g. by hydrological flow modeling or by direct observations. One of the great advantages of ESS as compared to TIC is that it fully preserves mass continuity, i.e. the total mass injected in the system is identical to the total mass exiting the same system; details of the derivations are found in the Appendix. Just like the TIF model, it is not guaranteed that the specific outflow total mass, either for streamflow or ET, is exactly recovered because of the uncertainty related to the partitioning coefficient $\theta(t)$

5.3.4 Time variant pdf approach (TV)

A more consistent and robust approach to model solute transport in catchment would be the one based on a time-variant formulation of TTD. The approach was already envised in *Nauman (1969)* and *Niemi (1977)* for flow in reactors, and the general framework for hydrological transport in catchments was given in a few past contributions (see, e.g., *Bertuzzo et al., 2013; Botter, 2012; Rinaldo et al., 2011*); similar developments were made for the analysis of water age in ocean modeling (*Delhez et al., 1999*). The approach requires the definition of travel time distributions conditioned at both injection and exit times. In order to get simple expressions for the outlet concentration, complete and instantaneous mixing between the injected solute and the water stored in the system is assumed. A similar model was developed by *Duffy (2010)* with a different mathematical approach. Although complete mixing is unlikely in the

subsurface, *Fiori (2012)* has shown that the transport equations pertaining to perfect mixing are, under certain conditions, identical to the transport equation averaged over the catchment thickness, where vertical averaging of concentration is made. Hence, perfect mixing is indeed not strictly required, and one would rather assume "perfect" or "random" sampling (see also *Benettin et al., 2013*). The time-variant approach with random sampling is in the following denoted as TV.

The outflow concentration predicted by the TV model can be derived following the developments of *Rinaldo et al. (2011)*. For the sake of conciseness and simplicity we derive here the same expression by following the simpler (although less general and not directly related to travel time analysis) approach by *Duffy (2010)*. The output concentration is obtained from the global water and mass balance equations, where the hillslope system is considered as a single reservoir. With the usual notation, the water and solute continuity equations are written as

$$\frac{dS(t)}{dt} = Q_0(t) - Q(t) - ET(t) \tag{5.13}$$

$$\frac{dM(t)}{dt} = F_0(t) - F_Q(t) - F_{ET}(t) \tag{5.14}$$

where $S(t)$ is the total water storage and $M(t)$ is the total mass in the system. Following the perfect mixing/random sampling assumption, the solute concentration in the system is $C(t)$, and hence the solute fluxes are equal to $F_0(t) = Q_0(t)C_0(t)$, $F_Q(t) = Q(t)C(t)$ and $F_{ET}(t) = ET(t)C(t)$. Substituting the latter into equation (5.14) and using the water balance

equation (5.15) one gets a first order ordinary differential equation of the outflow concentration

$$\frac{dC(t)}{dt} = \frac{Q_0(t)}{S(t)}\left[C_0(t) - C(t)\right] \tag{5.15}$$

The solute concentration C can be solved analytically from equation (5.15) using the initial concentration $C(0) = 0$, arriving at the simple expression

$$C(t) = \int_0^t C_0(\tau)\frac{Q_0(\tau)}{S(\tau)} e^{-\int_\tau^t \frac{Q_0(x)}{S(x)}dx} d\tau \tag{5.16}$$

In addition, we note that by using equation (5.13), the output concentration can also be written as,

$$C(t) = \int_0^t C_0(\tau)\frac{Q_0(\tau)}{S(t)} e^{-\int_\tau^t \frac{Q(x)+ET(x)}{S(x)}dx} d\tau \tag{5.17}$$

The latter expression is identical to the expression derived by *Botter et al. (2010)* and further developed by *Rinaldo et al. (2011)* and *Botter (2012)*. Equation (5.17) represents the general solution of the TV model which shall be used in the sequel.

We emphasize that the TV model does not have any calibration parameter, but it requires the water storage $S(t)$, besides Q_0 and Q. The change of S can be obtained by a simple mass balance applied to the hillslope system, but the initial storage $S_0 = S(0)$ is anyway not known. Thus, S_0 shall be calibrated in the application example.

5.4 Results

In order to examine the performance of the models and evaluate their parameters, calibration is made in the first period (spring), while validation is performed over the other three periods (summer, fall, winter). We assume that the precipitation input $Q_0(t)$ and the discharge $Q(t)$ to the stream are both known. The models were run on an hourly time scale over a period of six years, for all four seasonal injections. The best set of parameters α and β for the gamma distribution for the first three models (TIC, TIF and ESS) was obtained by minimizing the square root of mean square error (RMSE) between the observed and simulated concentration at the stream. The models performance is also be tested by the coefficient of determination R^2. The objective function employed here typically emphasizes the higher concentrations, and the fitted parameters may depend on the particular objective function employed. As our main purpose is to compare different model formulations, we do not expect that our choice for the calibration strategy may significantly change our conclusions.

In the presence of ET, the additional, partition parameter θ needs to be estimated for the models TIF and ESS, and generally speaking it is temporally variable. The partition parameter θ is calibrated through two step iteration, as follows. As a first step, a constant θ is assumed and the calibration of the three parameters (i.e. α, β and θ) is performed. Assuming that the water flow route is described by the same TTD (*Botter et al., 2008; Rinaldo et al., 2006*), the temporally variable $\theta(t)$ is obtained

from the observed inflow and outflow using the inverse transfer function model (*van der Velde et al., 2010*). Thus, $\theta(t)$ can be obtained through

$$\theta(t) = \frac{1}{Q_0(t)} \int p^{-1}(\tau, t+\tau) Q(t+\tau) d\tau \qquad (5.18)$$

where $p^{-1}(\tau, t)$ is the inverse TTD of discharge to the stream. We have found that the partition coefficient $\theta(t)$ obtained by the above procedure does not depend much on time and the resulting θ oscillates around a constant value, which in turn is equal to the ratio between the total volume flowing to the stream over the total rainfall volume during the six years of the simulation. Hence we have assumed a constant θ in the sequel.

As previously stated, the time variant model TV does not require any calibration. Since the model also requires the evapotranspiration flux $ET(t)$ or the storage $S(t)$ (not explicitly required by the other models), calibration of additional parameters, like e.g. the partition coefficient, may be needed; in the present study we assume that the ET fluxes are known. However, the initial storage ($S_0 = S(0)$) is generally not known in advance and hence it is a parameter requiring calibration.

As introduced in Section 2, two cases shall be examined in the following: (i) rain only (RO) case, in which no ET is present, and (ii) rain and evapotranspiration (RET). Prediction is made of the outflow concentration C, which is compared against the results of the numerical experiments. We also compare the model capabilities to preserve mass continuity within the system, which is not always warranted for unsteady flows, as shown in Section 3.

5.4.1 Rain only scenario

The normalized outflow solute concentration at the stream (left), and the total mass recovered (right) are shown in Figure 5.4, both for the time invariant, concentration-based model TIC. The four figures aligned in the vertical pertain to the four injection periods, which correspond to the four calendar seasons, from top to bottom: spring (calibration), summer, fall and winter. We remind again that all models are calibrated by using data from the first season and verified for the other seasons. The fitted parameters for all models and other quantities of interest (RMSE, R^2, mass balance etc.) are displayed in Table 5.1. Similarly, Table 5.2 shows the model efficiency for the other, validation seasons.

Figure 5.4 shows that C/C_0 is rather well predicted by the TIC model for the first two seasons, while the performance deteriorates for the last two periods. The finding confirms that role played by the seasonal variations of the climatic forcings (e.g. rainfall and evapotranspiration) and the hydrological status of the system, in terms of storage available, groundwater dynamics and outflow discharge. In fact, the rainfall distributions in the first two periods (spring and summer) are characterized by moderate rainfall with similar patterns, whereas the third (fall) and the fourth (winter) seasons are characterized by high and low rainfall distribution, respectively. The results depicted in Figure 5.4e show that the predicted concentration is more diluted than the concentration from the numerical experiment, likely because of the larger precipitations, while the concentration predicted in winter (Figure 5.4g) is a bit larger than the observed value, again reflecting the lower amount of

rainfall to the system (*Fiori and Russo, 2008*). The results suggest that it is generally not possible to adopt a unique (hence time-invariant) TTD to characterize a system characterized by unsteady dynamics, both at small and large temporal scales.

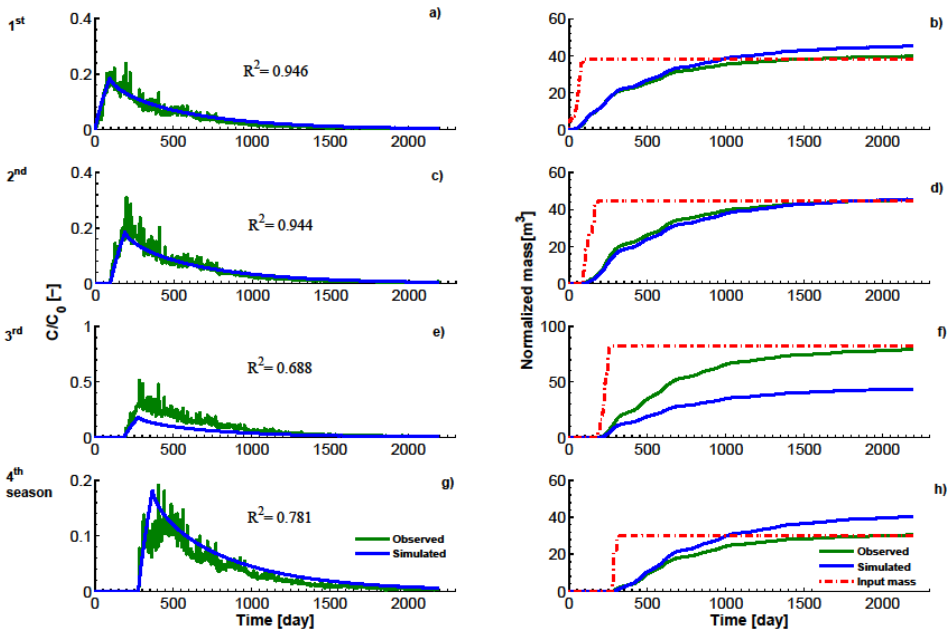

Figure 5.4: Streamflow solute concentration C, observed and predicted by the TIC model (left) and the total outflow mass recovered (right); Period of continuous injection: (a,b) First season (April -June), (c,d) Second season (July — Sep), (e,f) Third season (Oct - Dec), and (g,h) Fourth season (Jan —Mar); Rain only case (RO)

Although the predicted concentration is rather reasonable, the mass injected to the system in each season could not be always recovered at the outlet (see Figure 5.4, right column), which is consistent with the analysis of Section 3. Interestingly, the mass for the second control period is

practically recovered, but we attribute it to causality. Instead, the total mass is severely underestimated in fall and overestimated in winter.

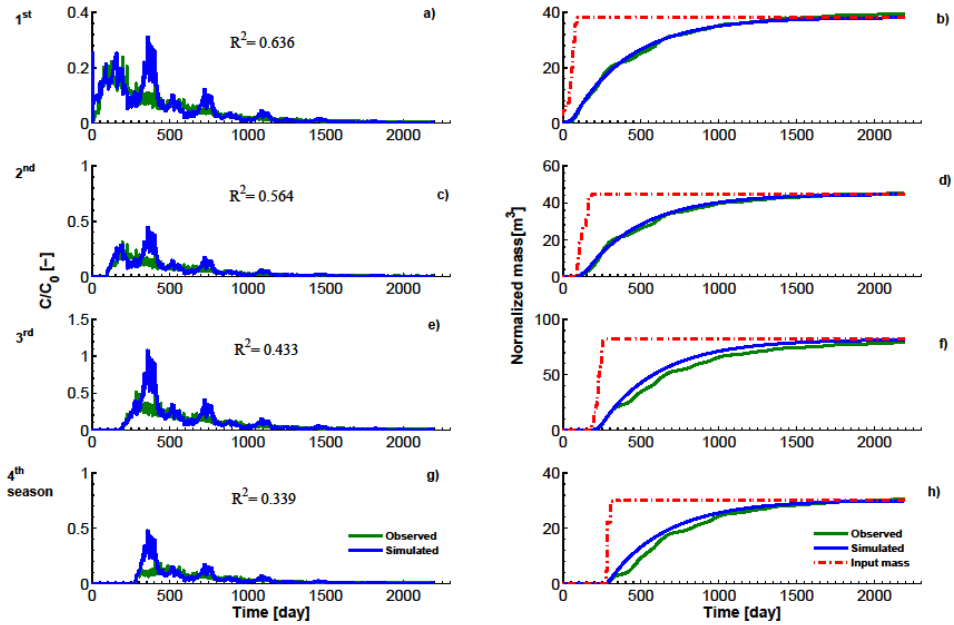

Figure 5.5: Streamflow solute concentration C, observed and predicted by the TIF model (left) and the total outflow mass recovered (right); Period of continuous injection: (a,b) First season (April -June), (c,d) Second season (July — Sep), (e,f) Third season (Oct - Dec), and (g,h) Fourth season (Jan —Mar); Rain only case (RO)

Likewise, Figure 5.5 shows the normalized outflow concentration and the total mass recovery for the TIF model. Unlike TIC, TIF does not seem to accurately predict the concentration. The concentration, which is ratio between the solute flux F_Q and the water discharge Q, is highly influenced by the water discharge, and the resulting concentration

displays a very noisy and oscillatory behaviour. In turn, the mass recovery of the TIF model is perfect, along the discussion of Section 3.2.

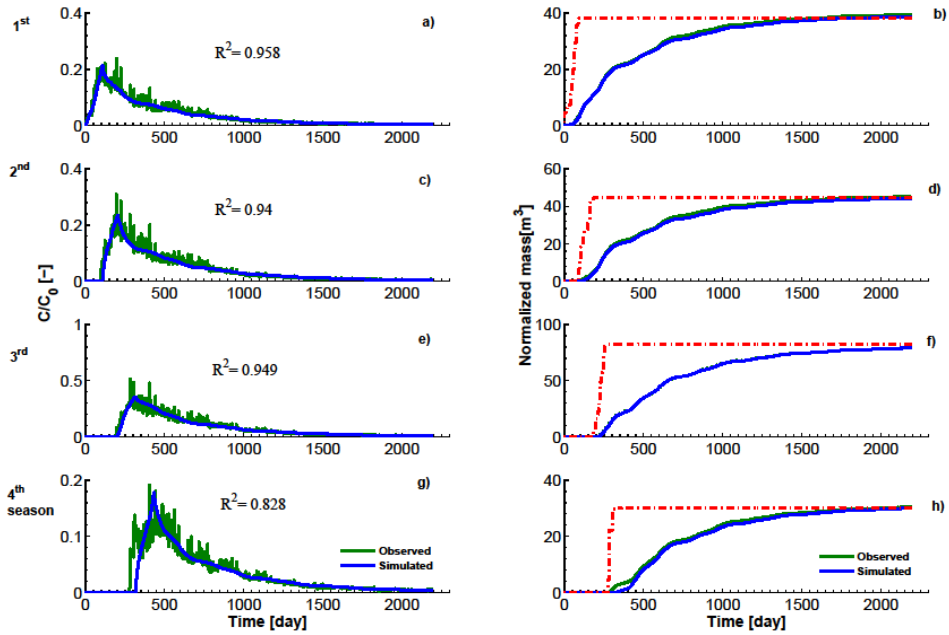

Figure 5.6: Streamflow solute concentration C, observed and predicted by the ESS model (left) and the total outflow mass recovered (right); Period of continuous injection: (a,b) First season (April -June), (c,d) Second season (July — Sep), (e,f) Third season (Oct - Dec), and (g,h) Fourth season (Jan —Mar); Rain only case (RO)

The results pertaining to the ESS model are illustrated in Figure 5.6. The mean travel time obtained by the fitting procedure is equal to 441.24 days (i.e. $\alpha = 0.792$ and $\beta = 561.4$), which is in agreement with the value obtained by *Fiori and Russo (2008)* after analysis of a solute pulse.

Table 5-1: Calibrated model parameters, mean transit time and the mass recovery corresponds to the first season (Rain only case)

Model	R2	RMSE	Model parameters α	β	MTT	M_{obs}	M_{sim}	Relative error (%)
TIC	0.946	0.011	0.885	605.6	535.92	39.6	45.1	13.8
TIF	0.617	0.035	0.954	394.4	376.38	39.6	38.1	3.90
ESS	0.959	0.009	0.792	561.4	441.24	39.6	38.9	1.99
TV	0.966	0.008	-	-	-	39.6	39.2	1.11

Note: M_{obs} and M_{sim} denote the observed and simulated mass recovered

It is seen that the ESS model performs quite well in predicting the streamflow concentration, better than the two previous models (TIC and TIF), with R^2 ranging from 0.83 and 0.96. We remind that, after the change of temporal coordinates, ESS produces a TTD which is different between the four seasons, while TIC and TIF employ the same, time-invariant TTD for all the seasons. Figure 5.6 also shows that the injected mass is completely recovered at the outlet, which is a general property of the ESS model (see Section 3.3).

Figure 5.7 is similar to the previous figures but it refers to the TV model. It is highlighted that the modelled solute concentration is able to reproduce the observed features, that all the fluctuation in the observed

pattern are properly captured by the modelled concentration curves in all seasons with the minimum R^2 = 0.938 for the winter period, which was not predicted so well by the other three models. Figure 5.7 also indicates that the instantaneous total mass injected to the system during the four seasons in the first year of the simulation period is properly recovered throughout the 6 years period. Regarding the only calibration parameter S_0, its calibrated value is equal to $S_{0_{cal}} = 189.75 m^3$ as compared to the "real" initial storage $S_0 = 336.86 m^3$, which was supposed as unknown here. We remark that using the correct S_0 instead of the calibrated one leads to a marked deterioration of the model prediction, with much lower predicted concentrations. The ratio $S_{0_{cal}} / S_o = 0.563$ suggests that only a fraction of the available storage in the system contribute to mixing. In fact, the assumption of perfect mixing may be rather strong when in presence of significant vertical flows, as it happens in our system, especially far from the outlet (see *Fiori and Russo, 2008*); instantaneous mixing cannot occur in such cases. Things might be different in thinner and shallower porous formations, in which the horizontal component of flow is dominant, leading to ratio S_{0cal}/S closer to unit.

Once again, details on the calibrated TTD parameters together with the fitting efficiency R^2 and the mean travel time for all models are found in Table 5.1. Similarly, Table 5.2 shows the model efficiency for the other, validation seasons.

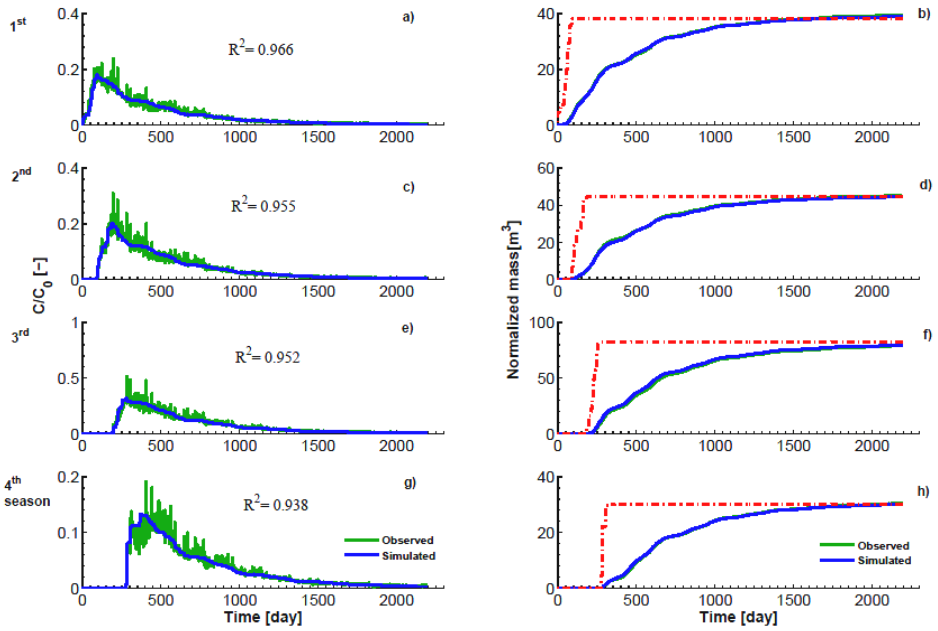

Figure 5.7: Streamflow solute concentration C, observed and predicted by the TV model (left) and the total outflow mass recovered (right); Period of continuous injection: (a,b) First season (April -June), (c,d) Second season (July — Sep), (e,f) Third season (Oct - Dec), and (g,h) Fourth season (Jan —Mar); Rain only case (RO)

Table 5-2: Validated model parameters and the mass recovery at for the second, third and fourth season (Rain only case)

Model	Injection	R^2	RMSE	M_{obs}	M_{sim}	Relative error (%)
TIC	Second	0.9436	0.0121	45.2517	45.5847	0.74
	Third	0.6879	0.0579	79.1481	43.6199	44.89
	Fourth	0.7808	0.0184	30.4331	40.3054	32.44
TIF	Second	0.5482	0.0456	45.252	44.4728	1.72
	Third	0.4178	0.104	79.1489	81.3428	2.77
	Fourth	0.3278	0.0511	30.4335	29.8787	1.82
ESS	Second	0.9585	0.0089	39.6384	38.8531	1.98
	Third	0.9396	0.0122	45.2517	44.3166	2.07
	Fourth	0.9486	0.0205	79.1481	79.0338	0.14
TV	Second	0.9554	0.0104	45.2517	44.7388	1.13
	Third	0.9523	0.0194	79.1481	79.8288	0.86
	Fourth	0.9382	0.0092	30.4331	30.2636	0.56

5.4.2 Rain and ET scenario

In some of the previous studies, the ET-related solute flux has been ignored or taken as proportional to the streamflow concentration (*Benettin et al., 2013; Bertuzzo et al., 2013; Rodhe et al., 1996*). In fact, solute concentration through the plant roots is typically much more difficult to measure than concentration streamflow (*Rodhe et al., 1996*). In the

numerical experiments carried out here we have full knowledge of the solute fluxes, but we shall assume that the ET-related concentration C_{ET} is not available. We shall later model C_{ET} only for checking the total mass balance, as done for the RO case; the calculation of C_{ET} typically requires a fitting of the p_{ET} parameters in the first three models, while the TV model does not require any additional calibration for C_{ET}, which is indeed equal to C.

The relevant parameters of the modelling exercise, along with the fitting efficiency R^2, are shown in Table 5.3 (calibrated) and Table 5.4 (validated). We focus in the following on the additional results driven by the presence of ET, other than those already discussed in the previous Section.

Table 5-3: Calibrated model parameters, mean transit time and the mass recovered through the streamflow at the end of the simulation correspond to the first season (RET case)

Model	**R^2**	**RMSE**	**Model parameters**			**M_{obs}**	**M_{sim}**	**Relative error (%)**
			α	**β**	**MTT**			
TIC	0.599	0.025	1.077	1125.3	1211.95	36.4	37.3	2.40
TIF	0.130	0.0765	1.536	562.79	864.45		35.9	1.35
ESS	0.365	0.0248	1.435	590.45	847.30		37.2	2.37
TV	0.487	0.0293	-	-	-		38.1	4.69

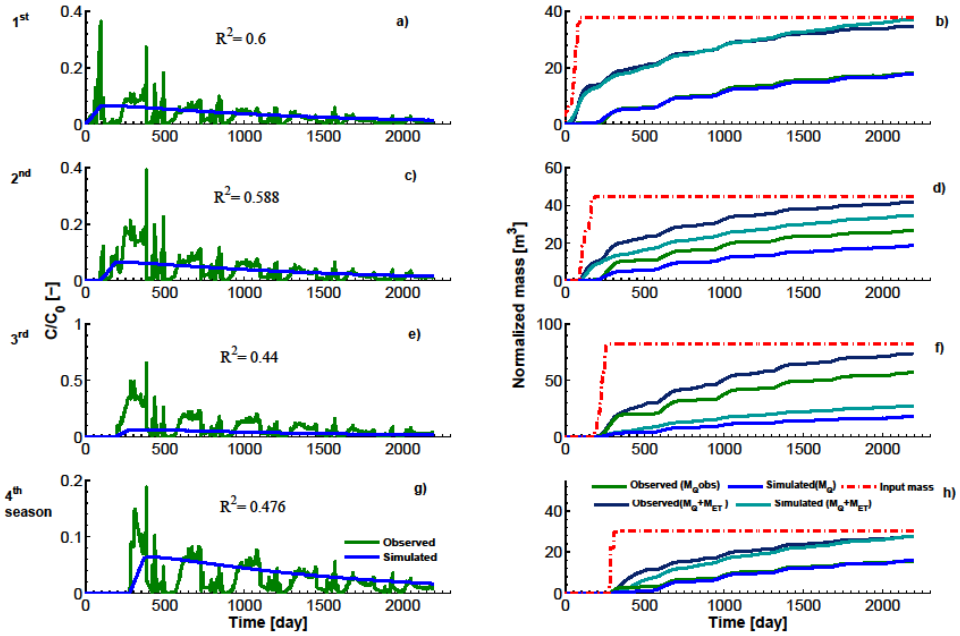

Figure 5.8: Streamflow solute concentration C, observed and predicted by the TIC model (left) and the total outflow mass recovered (right); Period of continuous injection: (a,b) First season (April - June), (c,d) Second season (July - Sep), (e,f) Third season (Oct -Dec), and (g,h) Fourth season (Jan - Mar); Rain and Evapotranspiration case (RET)

Figure 5.8 shows the normalized streamflow concentration and the total mass (streamflow and ET) for the TIC model. As we discussed earlier, the TIC model employs only the inflow solute concentration to predict the solute concentration exiting the outlet; hence, the flow variability cannot be taken into account, and the model does not capture the fluctuations of the outflow concentration due to the unsteady flow and transport. Similar to the RO case, mass balance is not preserved by the model, for the reasons illustrated in Section 3.1. In turn, the TIF model (Figure 5.9)

always fulfils the basic mass continuity requirement, although the recovery is slower because of the presence of ET (this feature depends on the physics of the problem and it is common to all models); however, the streamflow concentration is poorly predicted, for the same reasons explained when discussing the RO case, with high oscillations of C. The intermittent-like behaviour of C described in Section 5.2 has a significant impact on the calibration/validation for all models.

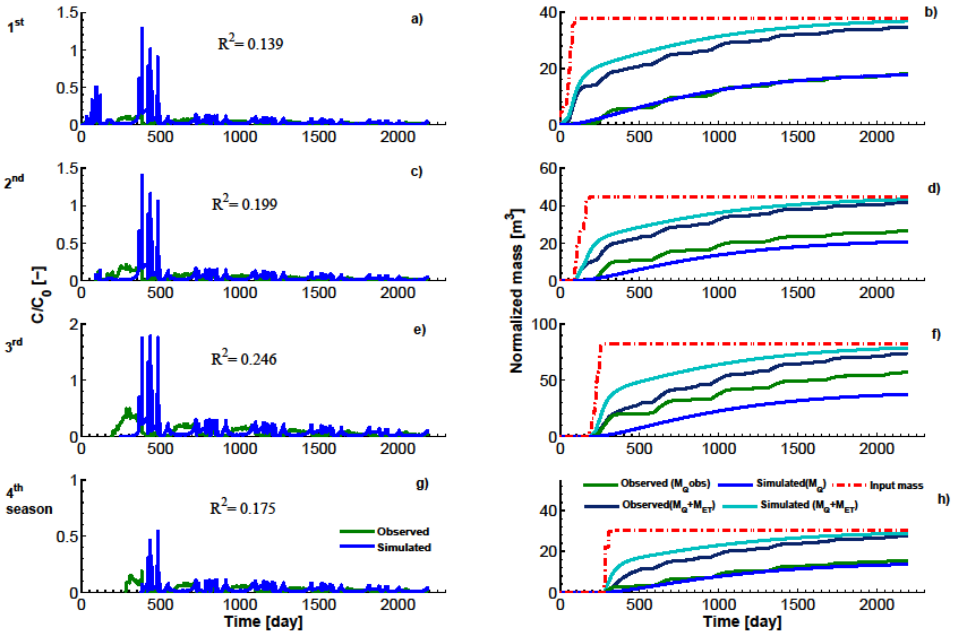

Figure 5.9: Streamflow solute concentration C, observed and predicted by the TIF model (left) and the total outflow mass recovered (right); Period of continuous injection: (a,b) First season (April - June), (c,d) Second season (July - Sep), (e,f) Third season (Oct -Dec), and (g,h) Fourth season (Jan - Mar); Rain and Evapotranspiration case (RET)

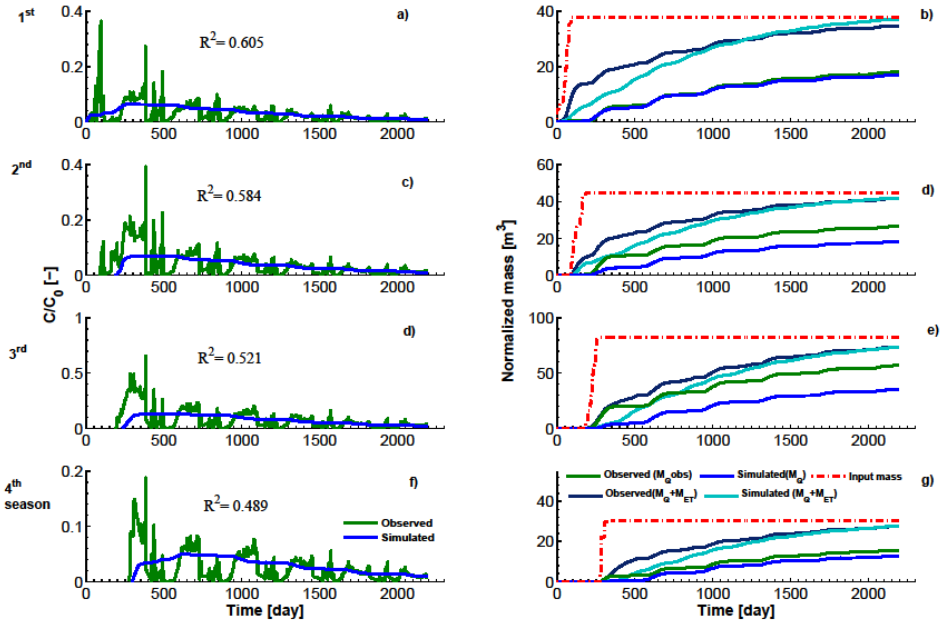

Figure 5.10: Streamflow solute concentration C, observed and predicted by the ESS model (left) and the total outflow mass recovered (right); Period of continuous injection: (a,b) First season (April - June), (c,d) Second season (July - Sep), (e,f) Third season (Oct -Dec), and (g,h) Fourth season (Jan - Mar); Rain and Evapotranspiration case (RET)

The same quantities are reproduced for the ESS model in Figure 5.10. It is seen that the predicted solute concentration does not show a significant improvement over the TIC model, although it somewhat follows more closely the concentration fluctuations. The result, together with the relatively low R^2 and RMSE, highlights the importance of evapotranspiration when studying solute transport in areas in which ET is relevant (*Benettin et al., 2013; Broxton et al., 2009; Rodhe et al., 1996; Stewart and McDonnell, 1991*).Similar to the RO case, the total mass is

fully recovered, again a general property of the ESS model. However, only the total mass $M_Q + M_{ET}$ is preserved, while the separate contributions M_Q and M_{ET} may different from the "real" ones, as shown in the Figure. The result depends on the parameter θ, which is a rather simple approach for capturing the solute partition between streamflow and evapotranspiration. A similar analysis was performed for the time variant approach (TV), with the obvious difference that the streamflow concentration is by definition identical to C_{ET}. The results, depicted in Figure 5.11, indicate that the TIV model does not lead to a significant improvement over the previous model, showing similar inabilities to accurately follow the relatively strong concentration fluctuations. Nevertheless, the earlier peaks seem to be better captured by the TV model, which also shows a general better performance as compared with the other formulations. The total injected mass is perfectly recovered at the outlets, as expected; just like the previous two models, the total outflow masses M_Q, M_{ET} are generally different from the numerical, "true" ones. The results of Figure 5.11 confirm again the importance of evapotranspiration fluxes in the solute transport modelling.

Table 5-4: Validated model parameters and the mass recovered through the streamflow at the end of each simulation corresponds to the second, third and fourth seasons (RET case)

Model	Injection	R^2	RMSE	M_{obs}	M_{sim}	Relative Error (%)
TIC	Second	0.5873	0.0381	41.622	34.681	16.68
	Third	0.4399	0.107	73.8942	27.254	63.12
	Fourth	0.4752	0.0296	27.443	27.6178	0.64
TIF	Second	0.1993	0.0911	41.622	43.3462	4.14
	Third	0.2456	0.1682	73.8942	78.8916	6.76
	Fourth	0.1746	0.0454	27.443	28.9396	5.45
ESS	Second	0.2295	0.0386	41.622	41.8791	0.62
	Third	0.1539	0.0918	73.8942	73.259	0.86
	Fourth	0.1806	0.0284	27.443	27.5552	0.41
TV	Second	0.4846	0.0348	41.622	40.8909	1.76
	Third	0.4577	0.071	73.8942	79.8975	8.12
	Fourth	0.4437	0.0267	27.443	29.2622	6.63

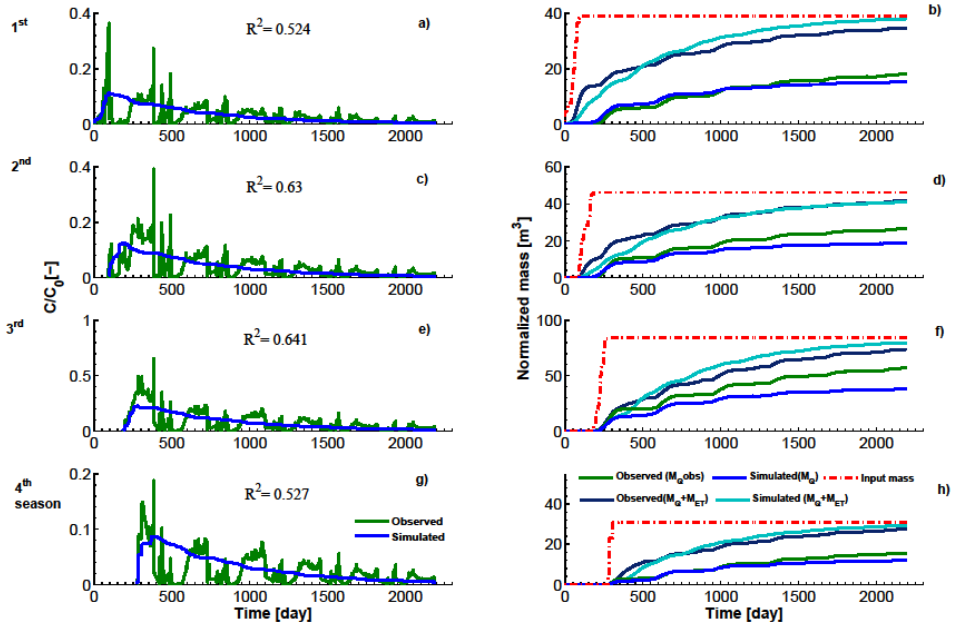

Figure 5.11: Streamflow solute concentration C, observed and predicted by the TV model (left) and the total outflow mass recovered (right); Period of continuous injection: (a,b) First season (April - June), (c,d) Second season (July - Sep), (e,f) Third season (Oct -Dec), and (g,h) Fourth season (Jan - Mar); Rain and Evapotranspiration case (RET)

5.5 Discussion and Conclusions

In this paper, we have evaluated the performance of four different catchment transport models. All the models employ the concept of travel time, and the following formulations have been considered: the time-invariant TTD model based on either concentration (TIC) or solute flux (TIF), the Equivalent Steady State approximation (ESS) and the fully time variant model (TV) based on the assumption of random sampling (also

denoted as full mixing in the literature). The 3D, detailed numerical simulations by *Fiori and Russo (2013*) were used as a benchmark for the calibration and the assessment of the models' capabilities to simulate transport; the numerical simulations allow us to full control the parameters involved in the numerical modelling and have a complete monitoring of the relevant hydrological quantities, like e.g. water fluxes, concentrations and storage, at any spatial and temporal resolution. We have analysed two scenarios: (i) rain only (RO) and (ii) rain and evapotranspiration (RET).

Starting with the most popular TIC model, it was shown by both the theoretical analysis and the application example that it is unable to fulfil the mass continuity requirement, i.e. the total mass exiting the system is generally not equal to the total injected mass. The concentration prediction performed by TIC may be quite reasonable, especially in the RO case, although the model is by definition unable to follow the natural oscillations of C in the stream. In turn, the TIF model always fulfils the mass balance requirement, but the simulated concentrations typically show high fluctuations and the general prediction is far from accurate. The above shortcomings of the TIC and TIF models derive from being based on the steady state flow conditions, while flow in natural hillslopes is typically unsteady. We note that the two models TIC and TIF provide identical results when flow is steady, and thus the differences observed are due only to the unsteady nature of water flow in the system.

The ESS model has the advantages of both TIC and TIF models, i.e. a generally good prediction of C (especially for the RO scenario) and a

perfect agreement between input and output solute masses; also, it is quite able to follow the natural oscillations of streamflow concentration. Hence, ESS is a valid alternative of the commonly employed TIC model, as already emphasized in past work (*Fiori and Russo, 2008; Niemi, 1977; Rodhe et al., 1996*).

The best prediction of streamflow concentration was obtained by the TV model, which is also the less parameterized; also, by definition the TV model always fulfils mass continuity. However, the TV model requires a full description of the input and outflow fluxes and the water storage in the system; in particular, the initial water storage is generally unknown and it needs to be calibrated, and it might differ from the real one.

While the models' performance was generally good for the RO scenario (perhaps with the exception of the TIF model), their behaviour is less satisfactory when ET is included in the analysis. First, the partition coefficient θ needs to be introduced in all models except TV, for which a complete description of the ET fluxes is needed. The coefficient θ is indeed a rather rough measure of the solute partition between streamflow and ET concentrations (C and C_{ET}), which is otherwise much more complex and difficult to represent through a single and global parameter. For example, the solute extraction by plants is not spatially uniform, and it easily increases in the vicinity of the stream. Hence, any global parameters may not be adequate in representing the solute partition within the hillslope. Furthermore, our analysis shows that prediction of total mass in the stream may not be correctly predicted, while the total mass

exiting the system from both the stream and the plants is correctly predicted by models TIF, ESS and TV.

We remark that the "observed data" used in the present study have been obtained from numerical experiments, in which realistic scenarios have been considered. However, real catchments display a higher degree of complexity and some of the assumptions made here (e.g., geometry of the flow domain, validity of Richards's equation, the assumed spatial and statistical structure for the hydraulic parameters, etc.) may limit the general validity of the results obtained in the present study. We tend to believe that one of the major limitations is the lack of spatial heterogeneities characterized by scales similar or larger than the domain size; such heterogeneities may lead to significant changes in the flow paths and hence the associated travel times. Also, the particular rainfall forcings and the plants' sampling strategy adopted for which the solute behaves like water and is fully taken by the plants (while it generally depends on the chemical characteristics of the solute regarding the metabolism process of the plant) may indeed limit the general validity of the conclusions regarding the RET scenario. Although it is difficult to assess the general validity of some of our results, important and general shortcomings of some of the models (like e.g. mass balance issues, wild oscillations of concentration etc) have been emphasized here. In any case, the present results may point at possible problems in the application of transport models built on the steady-state assumption of flow; much work is needed in order to move forward and develop and test alternative formulations of transport models under unsteady flow conditions and with significant evapotranspiration.

6 General Conclusion and perspectives

6.1 Overview

6.1.1 Flow modelling

The soil characteristics of subsurface system are highly heterogeneous with a strong anisotropic character. Therefore, it requires the development of specific methods in order to characterise these systems adequately and to give predictions, e.g. subsurface storage, solute transport from different point sources. This research work advances our understanding of the small scale physical based flow model prediction and the application of the same models at larger scale through up scaling. It deals with the Richards' equation based flow modelling at hillslope scale followed by parameter identification which allows to develop closure equation that can be used for any catchments consist of a population of hillslopes.

The two-stage up-scaling (point to hillslope scale and hillslope to catchment scale) allows the parameterization of the storage-discharge relationship through a physical based numerical model which used to develop similar relationship curves without the need to resolve the flows at smaller scales explicitly. The storage-discharge relations were derived at the hillslope scale in the first stage directly from the simulations, accounting for random and systematic heterogeneity of soil hydraulic properties, through a 3-D distributed saturated-unsaturated numerical model of Richards' equation on idealized hillslopes with synthetically generated soil properties. Then, it has been extended to a catchment scale which employs regression equations derived from the parameters

involved in the simulation and the power law form of the storage discharge relationship.

In the present study it is shown that there is variation between the theoretical and empirical derivations of the recession curve. This can be attributing to several factors such as the uncertainty of the observed data used in the numerical models and involved to develop the empirical derivation, the contribution of the climate factor which is not included in the numerical model and the inappropriateness of the Richards equation. Additional work is needed to address this prediction gap, including fundamental research to understand the co-dependence of soil and topographic properties, can contribute towards improved estimates of the recession curve parameters in ungauged locations.

6.1.2 Solute transport modelling

In this part of the present study, the performance of some categories of solute transport models employing the concept of travel time distribution was evaluated. The models under consideration involved both time-variant and time-invariant definitions of the TTD, and the strengths and limitations of each approach were discussed, emphasizing the potential ability to predict the solute concentration and the mass recovery at the outlet of the hillslope/catchment system. The models employ in the present study are the time-invariant TTD model based on either concentration (TIC) or solute flux (TIF), the Equivalent Steady State approximation (ESS) and the fully time variant model (TV) based on the assumption of random sampling.

Taking in to account all the limitations of the coupled flow and transport model used to obtain observed data, it is shown that all the four models can be used to develop TTD for the steady state system and identical results were found, however, this is not always true for unsteady flow system in which all the models are practically disparate. Thus, for the unsteady flow system, (i) though the flow concentration is practically predicted by TIC model, the mass continuity requirement is not fulfilled, (ii) unlike TIC, the TIF model fulfil the mass recovery but unable to predict the flow concentration (iii) The ESS model is shown a good prediction of the flow concentration and the mass. It can also be used for the solute transport which does not require detail hydrological analysis (iv) the TV models, which is based on random sampling and required full description of the flow system, gives the best prediction of flow concentration and the masses. Therefore, among the four models presented in this study the later can be used to obtain solute transport pattern of the subsurface flow for both flow system (steady or unsteady). In fact, the model requires full description of the subsurface storage which is unlikely possible to obtain in reality.

6.2 Recommendations on future research needs

Beside the above findings of the present study; some limitations has to be considered which needs further research and investigation

Despite the widespread acceptance of the quasi steady state assumption in the literatures (*Beven and Freer, 2001; Beven and Kirkby, 1979; Lamb, 1997; Moore and Thompson, 1996; Watson et al., 2001)* and used in this work to determine the storage-discharge relationship through a series of

steady state simulation, the assumption might not be applicable for some cases as studied by Seibert (2003). The lumped storage discharge curve for a system developed from the assumption that the dynamics of the saturated region of a river basin can be approximated by the successive steady state approximation. This steady state storage – discharge function can then be extended to a recession analysis in conjunction with the continuity equation. However, *Beven (1997)* states that for a variety of different conductivity of the soil in the subsurface profile, or when the depth of the saturated aquifer is large, the derivation of the actual shape of the water table from a steady state shape can be both large enough and last long enough so that the assumption of the quasi steady state dynamics may be invalid. Therefore, it is noted that this assumption works for an aquifer with thin soil over an impermeable bed. *Sloan (2000)* also suggested an alternative discharge function because single-valued storage-discharge functions are often incapable of representing the actual storage-discharge characteristics of a river basin. So there is a need to look the implications of the assumption with a real problem to assess the validity of the steady-state hypothesis.

In section 4, it is also indicated that there is considerable disparity between the results from the two alternative approaches (top-down and bottom-up approaches). This disparity of the results could be due to the climate dependence of the storage-discharge relationships, which the physical theory is not able to account. However, additional fundamental research should be carried out to answer some fundamental questions regarding the representation of the field measured point-scale soil

hydraulic properties, even after accounting for random spatial heterogeneity, of hillslope and catchment scale subsurface flow processes, and physical model which is account for co-evolution of climate, soils, topography and vegetation that gives rise to the self-organization in numerical models of subsurface flow.

As we remark in section 5, "observed data" used to evaluate the performance of the four different models for the solute transport prediction in small catchments have been obtained from numerical experiments, in which realistic scenarios have been considered. However, real catchments display a higher degree of complexity and some of the assumptions made here (e.g., geometry of the flow domain, validity of Richards's equation, the assumed spatial and statistical structure for the hydraulic parameters, etc.) may limit the general validity of the results obtained in the present study. Thus, we suggest that similar analysis shall be carried out based on field observation so that consistent guidelines of TTD approximation can be developed. Also, the particular rainfall forcings and the plants' sampling strategy adopted for which the solute behaves like water and is fully taken by the plants may indeed limit the general validity of the conclusions regarding the RET scenario.

Appendix A: Mathematical framework and numerical Modeling

We simplify the hillslope as a sloped parallelepiped and use a dimensionless formulation of shallow subsurface flow based on a 3-D Richards' equation developed by *Ali et al. (2013).* The hillslope is characterized as a heterogeneous planar, rectangular hillslope of 100 m length, 20 m width and 5 m depth, with a constant topographic slope. In this study we choose the dimensions such that we can neglect runoff caused by the emergence of a water table over the ground level. The form of the Richards' equation used is given by:

$$C(h)\frac{\partial h}{\partial t} = \nabla \cdot \{k(h)\nabla(h+z)\} \qquad \text{(A1)}$$

where C (h) =∂θ/∂h represents the specific moisture content [L^{-1}], t is the time [T], *h* is the pressure head [L], *z* are the elevation head [L], and *K (h)* is the hydraulic conductivity [L T^{-1}]

It is assumed that the local effective degree of saturation and unsaturated hydraulic conductivity are described by the *Brooks and Corey (1964)* functional relationship; i.e. $S_e = (\theta - \theta_r)/(\varphi - \theta_r) = (h_b / h)^{\lambda}$, where S_e is the effective saturation, θ_r is the residual volumetric water content, φ is the porosity, h_b is the bubbling or air entry pressure head, and λ is the pore size distribution index. The specific moisture content $C(h)$ therefore becomes

$$C(h) = \frac{\partial \theta}{\partial h} = -\lambda(\varphi - \theta_r)\left(\frac{h_b^{\lambda}}{h^{\lambda+1}}\right) \qquad \text{(A2)}$$

The hydraulic conductivity is defined as a function of the saturated hydraulic conductivity (K_s), the bubbling pressure (h_b),the pressure head (h) and the pore size index λ (n=3+2/λ) as follows:

$$K(h) = K\left(\frac{h_b}{h}\right)^{n\lambda} \qquad \text{(A3)}$$

A dimensionless form of the Richards equation is derived by normalizing the specific moisture content, the volumetric water content, the pressure head, the hydraulic conductivity of the material and the sink/source term using the appropriate scaling variables. We adopt dimensionless variables by rescaling their dimensional values by the hillslope length L, soil depth d and mean surface hydraulic conductivity Km. The resulting non-dimensional variables are: $\hat{x} = x/L$, $\hat{y} = y/L$, $\hat{z} = z/d$, $\hat{h} = h/d$, $\hat{h}_b = h_b/d$,$\hat{t} = tK\ /L(\varphi - \theta_r)$ and $\hat{K}_s = K/K_m$ where x, y and z are the spatial coordinates.

The dimensionless form of Richards' equation is solved by the finite element method using the earth science module of Comsol Multiphysics software that employs numerical methods to solve partial differential equation (*COMSOL, 2010*). The output variables from the model that are of interest are also dimensionless (interested readers are referred to *Ali et al. (2013)* for details of the dimensional analyses).

In these simulations, the initial condition is one where the water table is at the surface and the system is fully saturated. The boundary condition at the upper boundary is an assumed net precipitation, which is assumed

normal to the hillslope. The bottom boundary is a no-flow boundary; the same is true for the right, left and upper vertical planes parallel and normal to the flow direction. A seepage face is assumed at the right boundary where water discharges from the domain. The boundary face is divided into a Dirichlet boundary condition for the seepage face (along which the prescribed internal pressure $p = 0$) and the Neumann condition for the region above the seepage face (*Chui and Freyberg (2007)).* The temporal variability of the size of the seepage face is automatically accounted for by the method.

Appendix B: Mass recovery of ESS Model

The total mass conveyed to the river (i.e. for t→∞) is equal to

$$M_{Out}(t) = \int_0^\infty \left[F_Q(t) + F_{ET}(t)\right] dt \qquad \text{(B1)}$$

Substitute $F_Q(t) = Q(t)C_Q(t)$ and $F_{ET}(t) = ET(t)C_{ET}(t)$, and switch to the t_R and t_{RE} coordinate system it yields

$$M_{Out}(t) = \overline{Q}\int_0^\infty C_Q(t_R)dt_R + \overline{ET}\int_0^\infty C_{ET}(t_{RE})dt_{RE} \qquad \text{(B2)}$$

and substitution of equation (5.10) and (5.11) for both streamflow and ET yields

$$M_{Out}(t) = \overline{Q}\int_0^\infty\int_0^\infty C_0(\tau_R)\,p_s(t_R - \tau_R)d\tau_R dt_R + \overline{ET}\int_0^\infty\int_0^\infty C_0(\tau_{RE})\,p_{ET}(t_{RE} - \tau_{RE})d\tau_{RE} dt_{RE} \qquad \text{(B3)}$$

Inverting the order of integration and switch to the coordinate system (τ_R, $\varepsilon_s = t_R - \tau_R$) and ($\tau_{RE}$, $\varepsilon_{ET} = t_{RE} - \tau_{RE}$) and the above equation becomes

$$M_{Out}(t) = \overline{Q}\int_0^\infty C_0(\tau_R)d\tau_R + E\overline{T}\int_0^\infty C_0(\tau_{RE})d\tau_{RE} \qquad \text{(B4)}$$

Now we switchback to τ_R (τ_{RE}) to τ, along equation (5.11), for which $d\tau_R = \overline{Q}^{-1}\theta(\tau)Q_0(\tau)d\tau$ and $d\tau_{RE} = \overline{ET}^{-1}\left(1-\theta(\tau)\right)Q_0(\tau)d\tau$ and equation (B4) becomes

$$M_{Out}(t) = \int_0^{\infty} Q_0(\tau) C_0(\tau) d\tau = M_{IN}(t) \tag{B5}$$

This shows the total mass injected in the system is indeed equal to the total outflow mass. However, it is not guaranteed that either of the mass (through streamflow or ET) is recovered due to the uncertainty of the partitioning coefficient $\theta(t)$ only the total one being recovered.

Reference

Akaike H. (1974) A new look at the statistical model identification. *Automatic Control, IEEE Transactions on* 19:716-723. DOI: 10.1109/TAC.1974.1100705.

Aksoy H., Wittenberg H. (2011) Nonlinear baseflow recession analysis in watersheds with intermittent streamflow. *Hydrological Sciences Journal* 56:226-237. DOI: 10.1080/02626667.2011.553614.

Ali M., Fiori A., Bellotti G. (2013) Analysis of the nonlinear storage–discharge relation for hillslopes through 2D numerical modelling. *Hydrological Processes* 27:2683-2690. DOI: 10.1002/hyp.9397.

Allen M.B., Murphy C.L. (1986) A Finite-Element Collocation Method for Variably Saturated Flow in Two Space Dimensions. *Water Resources Research* 22:1537-1542. DOI: 10.1029/WR022i011p01537.

Anderson M.G., Burt T.P. (1990) Subsurface runoff. In Process Studies in Hillslope Hydrology, in: A. M. G. a. B. T.P. (Ed.), *John Wiley & Sons*, New York. pp. 365 - 400.

Azizi M.P., Mahmoodian M.S., Adib A. (2011) Numerical Solution of Richards Equation by Using of Finite Volume Method *World Applied Sciences Journal* 14(12):1838 -1842.

Bachmair S., Weiler M. (2012) Hillslope characteristics as controls of subsurface flow variability. *Hydrol. Earth Syst. Sci.* 16:3699-3715. DOI: 10.5194/hess-16-3699-2012.

Barnes B.S. (1939) The structure of discharge-recession curves. *Transactions, American Geophysical Union* 20:721-725.

Barnes C.J., Bonell M. (1996) Application of unit hydrograph techniques to solute transport in catchments. *Hydrological Processes* 10:793-802. DOI: 10.1002/(sici)1099-1085(199606)10:6<793::aid-hyp372>3.0.co;2-k.

Basha H.A. (2000) Multidimensional linearized nonsteady infiltration toward a shallow water table. *Water Resources Research* 36:2567-2573. DOI: 10.1029/2000WR900150.

Bear J. (1972) Dynamics of Fluids in Porous Media, *Elsevier*, New York.

Bellin A., Rubin Y. (1996) HYDRO_GEN: A spatially distributed random field generator for correlated properties. *Stochastic Hydrology and Hydraulics* 10:253-278. DOI: 10.1007/BF01581869.

Benettin P., van der Velde Y., van der Zee S.E.A.T.M., Rinaldo A., Botter G. (2013) Chloride circulation in a lowland catchment and the formulation of transport by travel time distributions. *Water Resources Research*:n/a-n/a. DOI: 10.1002/wrcr.20309.

Bertuzzo E., Thomet M., Botter G., Rinaldo A. (2013) Catchment-scale herbicides transport: Theory and application. *Advances in Water Resources* 52:232-242. DOI: http://dx.doi.org/10.1016/j.advwatres.2012.11.007.

Beven K. (1982) On subsurface stormflow: an analysis of response times / Sur l'écoulement hypodermique dÛ aux orages: une analyse des temps de réponse. *Hydrological Sciences Journal* 27:505-521. DOI: 10.1080/02626668209491129.

Beven K. (1997) TOPMODEL: A critique. *Hydrological Processes* 11:1069-1085. DOI: 10.1002/(SICI)1099-1085(199707)11:9<1069::AID-HYP545>3.0.CO;2-O.

Beven K. (2002) Towards an alternative blueprint for a physically based digitally simulated hydrologic response modelling system. *Hydrological Processes* 16:189-206. DOI: 10.1002/hyp.343.

Beven K., Freer J. (2001) A dynamic TOPMODEL. *Hydrological Processes* 15:1993-2011. DOI: 10.1002/hyp.252.

Beven K.J. (2010) Preferential flows and travel time distributions: defining adequate hypothesis tests for hydrological process models. *Hydrological Processes* 24:1537-1547. DOI: 10.1002/hyp.7718.

Beven K.J., Clarke R.T. (1986) On the Variation of Infiltration Into a Homogeneous Soil Matrix Containing a Population of Macropores. *Water Resources Research* 22:383-388. DOI: 10.1029/WR022i003p00383.

Beven K.J., Kirkby M.J. (1979) A physically based, variable contributing area model of basin hydrology / Un modèle à base physique de zone d'appel variable de l'hydrologie du bassin versant. *Hydrological Sciences Bulletin* 24:43-69. DOI: 10.1080/02626667909491834.

Blöschl G., Sivapalan M. (1995) Scale issues in hydrological modelling: A review. *Hydrological Processes* 9:251-290. DOI: 10.1002/hyp.3360090305.

Bogaart P.W., Troch P.A. (2006) Curvature distribution within hillslopes and catchments and its effect on the hydrological response.

Hydrol. Earth Syst. Sci. 10:925-936. DOI: 10.5194/hess-10-925-2006.

Botter G. (2012) Catchment mixing processes and travel time distributions. *Water Resources Research* 48:W05545. DOI: 10.1029/2011WR011160.

Botter G., Bertuzzo E., Rinaldo A. (2010) Transport in the hydrologic response: Travel time distributions, soil moisture dynamics, and the old water paradox. *Water Resour. Res.* 46:W03514. DOI: 10.1029/2009wr008371.

Botter G., Milan E., Bertuzzo E., Zanardo S., Marani M., Rinaldo A. (2009) Inferences from catchment-scale tracer circulation experiments. *Journal of Hydrology* 369:368-380. DOI: http://dx.doi.org/10.1016/j.jhydrol.2009.02.012.

Botter G., Peratoner F., Putti M., Zuliani A., Zonta R., Rinaldo A., Marani M. (2008) Observation and modeling of catchment-scale solute transport in the hydrologic response: A tracer study. *Water Resour. Res.* 44:W05409. DOI: 10.1029/2007wr006611.

Boussinesq J. (1877) Essai sur la th6orie des eaux courantes, Du mouvement non permanent des eaux souterraine. *Acad. Sci. Inst. Fr.* 23:252-260.

Broadbridge P., Edwards M.P., Kearton J.E. (1996) Closed-form solutions for unsaturated flow under variable flux boundary conditions. *Advances in Water Resources* 19:207-213. DOI: http://dx.doi.org/10.1016/0309-1708(95)00046-1.

Brooks E.S., Boll J., McDaniel P.A. (2004) A hillslope-scale experiment to measure lateral saturated hydraulic conductivity. *Water Resources Research* 40:W04208. DOI: 10.1029/2003WR002858.

Brooks R.J., Corey A.T. (1964) Hydraulic properties of porous media, in: P. 3 (Ed.), *Colo. State Univ.*, Fort Collins.

Broxton P.D., Troch P.A., Lyon S.W. (2009) On the role of aspect to quantify water transit times in small mountainous catchments. *Water Resources Research* 45:n/a-n/a. DOI: 10.1029/2008WR007438.

Brutsaert W. (1994) The unit response of groundwater outflow from a hillslope. *Water Resources Research* 30:2759-2763. DOI: 10.1029/94WR01396.

Brutsaert W., Lopez J.P. (1998) Basin-scale geohydrologic drought flow features of riparian aquifers in the Southern Great Plains. *Water Resour. Res.* 34:233-240. DOI: 10.1029/97wr03068.

Brutsaert W., Nieber J.L. (1977) Regionalized drought flow hydrographs from a mature glaciated plateau. *Water Resour. Res.* 13:637-643. DOI: 10.1029/WR013i003p00637.

Burns D.A., Hooper R.P., McDonnell J.J., Freer J.E., Kendall C., Beven K. (1998) Base cation concentrations in subsurface flow from a forested hillslope: The role of flushing frequency. *Water Resour. Res.* 34:3535-3544. DOI: 10.1029/98wr02450.

Buttle J.M. (1994) Isotope hydrograph separations and rapid delivery of pre-event water from drainage basins. *Progress in Physical Geography* 18:16-41. DOI: 10.1177/030913339401800102.

Celia M.A., Bouloutas E.T., Zarba R.L. (1990) A general mass-conservative numerical solution for the unsaturated flow equation. *Water Resources Research* 26:1483-1496. DOI: 10.1029/WR026i007p01483.

Chapman T. (1997) A comparison of algorithms for streamflow recession and baseflow separation, in: A. D. McDonald, McAleer, M. (Ed.), International Congress on Modelling and Simulation MODSIM 97, *Hobart*, Tasmania, Australia. pp. 294-299.

Chapman T. (1999) A comparison of algorithms for stream flow recession and baseflow separation. *Hydrological Processes* 13:701-714. DOI: 10.1002/(SICI)1099-1085(19990415)13:5<701::AID-HYP774>3.0.CO;2-2.

Chui T., Freyberg D. (2007) The Use of COMSOL for Integrated Hydrological Modeling, COMSOL Conference, *COMSOL, Inc.*, Boston, MA.

Clark M.P., Rupp D.E., Woods R.A., Tromp-van Meerveld H.J., Peters N.E., Freer J.E. (2009) Consistency between hydrological models and field observations: linking processes at the hillslope scale to hydrological responses at the watershed scale. *Hydrological Processes* 23:311-319. DOI: 10.1002/hyp.7154.

Clausen B. (1992) Modelling streamflow recession in two Danish streams. *Nord. Hydrol.* 23:73-88.

Clement T.P., Wise W.R., Molz F.J. (1994) A physically based, two-dimensional, finite-difference algorithm for modeling variably saturated flow. *Journal of Hydrology* 161:71-90. DOI: http://dx.doi.org/10.1016/0022-1694(94)90121-X.

COMSOL A. (2010) COMSOL Multiphysics Earth Science Module User's Guide

Cooley R.L. (1983) Some new procedures for numerical solution of variably saturated flow problems. *Water Resources Research* 19:1271-1285. DOI: 10.1029/WR019i005p01271.

Cvetkovic V. (2011) The tempered one-sided stable density: a universal model for hydrological transport? . *Environ. Res. Lett.* 6.

Cvetkovic V., Carstens C., Selroos J.-O., Destouni G. (2012) Water and solute transport along hydrological pathways. *Water Resources Research* 48:W06537. DOI: 10.1029/2011WR011367.

Dagan G. (Ed.) (1989) Flow and Transport in Porous Formations, Springer,
New York.

Dagan G., Cvetkovic V., Shapiro A. (1992) A solute flux approach to transport in heterogeneous formations: 1. The general framework. *Water Resources Research* 28:1369-1376. DOI: 10.1029/91WR03086.

Delhez E.J.M., Campin J.-M., Hirst A.C., Deleersnijder E. (1999) Toward a general theory of the age in ocean modelling. *Ocean Modelling* 1:17-27. DOI: http://dx.doi.org/10.1016/S1463-5003(99)00003-7.

Downer C., Ogden F. (2004) GSSHA: Model To Simulate Diverse Stream Flow Producing Processes. *Journal of Hydrologic Engineering* 9:161-174. DOI: doi:10.1061/(ASCE)1084-0699(2004)9:3(161).

Duan Q., Schaake J., Andreassian V., Franks S., Gupta H., Gusev Y., Habets F., Hall A., Hay L., Hogue T., Huang M., Leavesley G., Liang X., Nasonova O., Noilhan J., Oudin L., Sorooshian S., Wagener T., Wood E. (2006) Model Parameter Estimation Experiment (MOPEX): Overview and Summary of the Second and Third Workshop Results. *J. Hydrol.* 320:3-7. DOI: 10.1016/j.jhydrol.2005.07.031.

Duffy C.J. (1996) A Two-State Integral-Balance Model for Soil Moisture and Groundwater Dynamics in Complex Terrain. *Water Resources Research* 32:2421-2434. DOI: 10.1029/96WR01049.

Duffy C.J. (2010) Dynamical modelling of concentration–age–discharge in watersheds. *Hydrological Processes* 24:1711-1718. DOI: 10.1002/hyp.7691.

Dunn S.M., Birkel C., Tetzlaff D., Soulsby C. (2010) Transit time distributions of a conceptual model: their characteristics and sensitivities. *Hydrological Processes* 24:1719-1729. DOI: 10.1002/hyp.7560.

Dunn S.M., McDonnell J.J., Vaché K.B. (2007) Factors influencing the residence time of catchment waters: A virtual experiment approach. *Water Resour. Res.* 43:W06408. DOI: 10.1029/2006wr005393.

El-Kadi A.I., Brutsaert W. (1985) Applicability of Effective Parameters for Unsteady Flow in Nonuniform Aquifers. *Water Resour. Res.* 21:183-198. DOI: 10.1029/WR021i002p00183.

Elnawawy O.A., Azmy Y.Y. (1992) Cell Analytical-Numerical (CAN) method for the solution of the Richards equation., Water Research. pp. 203-209.

Fan Y., Bras R.L. (1995) On the concept of a representative elementary area in catchment runoff. *Hydrological Processes* 9:821-832. DOI: 10.1002/hyp.3360090708.

Fan Y., Bras R.L. (1998) Analytical solutions to hillslope subsurface storm flow and saturation overland flow. *Water Resources Research* 34:921-927. DOI: 10.1029/97wr03516.

Fan Y., Miguez-Macho G., Weaver C.P., Walko R., Robock A. (2007) Incorporating water table dynamics in climate modeling: 1. Water table observations and equilibrium water table simulations. *J. Geophys. Res.* 112:D10125. DOI: 10.1029/2006jd008111.

Fenicia F., Savenije H.H.G., Matgen P., Pfister L. (2006) Is the groundwater reservoir linear? Learning from data in hydrological modelling. *Hydrol. Earth Syst. Sci.* 10:139-150. DOI: 10.5194/hess-10-139-2006.

Fenicia F., Wrede S., Kavetski D., Pfister L., Hoffmann L., Savenije H.H.G., McDonnell J.J. (2010) Assessing the impact of mixing assumptions on the estimation of streamwater mean residence time. *Hydrological Processes* 24:1730-1741. DOI: 10.1002/hyp.7595.

Fiori A. (2012) Old water contribution to streamflow: Insight from a linear Boussinesq model. *Water Resources Research* 48:W06601. DOI: 10.1029/2011WR011606.

Fiori A., Russo D. (2007) Numerical analyses of subsurface flow in a steep hillslope under rainfall: The role of the spatial heterogeneity of the formation hydraulic properties. *Water Resour. Res.* 43:W07445. DOI: 10.1029/2006wr005365.

Fiori A., Russo D. (2008) Travel time distribution in a hillslope: Insight from numerical simulations. *Water Resour. Res.* 44:W12426. DOI: 10.1029/2008wr007135.

Fiori A., Russo D. (2013) Numerical experiments on the age of seasonal rain water in hillslopes, Four Decades of Progress in Monitoring and Modeling of Processes in the Soil-Plant-Atmosphere System: Applications and Challenges *Elsevier*, Naples, Italy.

Fiori A., Russo D., Di Lazzaro M. (2009) Stochastic analysis of transport in hillslopes: Travel time distribution and source zone dispersion. *Water Resources Research* 45:W08435. DOI: 10.1029/2008WR007668.

Fityus S.G., Smith D.W. (2001) Solution of the unsaturated soil moisture equation using repeated transforms. *International Journal for Numerical and Analytical Methods in Geomechanics* 25:1501-1524. DOI: 10.1002/nag.181.

Freer J., McDonnell J.J., Beven K.J., Peters N.E., Burns D.A., Hooper R.P., Aulenbach B., Kendall C. (2002) The role of bedrock topography on subsurface storm flow. *Water Resour. Res.* 38:1269. DOI: 10.1029/2001wr000872.

Freer J.I.M., McDonnell J., Beven K.J., Brammer D., Burns D., Hooper R.P., Kendal C. (1997) Hydrological processes—Letters. Topographic controls on subsurface storm flow at the hillslope scale for two hydrologically distinct small catchmetns. *Hydrological Processes* 11:1347-1352. DOI: 10.1002/(SICI)1099-1085(199707)11:9<1347::AID-HYP592>3.0.CO;2-R.

Fujimoto M., Ohte N., Tani M. (2008) Effects of hillslope topography on hydrological responses in a weathered granite mountain, Japan: comparison of the runoff response between the valley-head and the side slope. *Hydrological Processes* 22:2581-2594. DOI: 10.1002/hyp.6857.

Gillham R.W., Sudicky E.A., Cherry J.A., Frind E.O. (1984) An Advection-Diffusion Concept for Solute Transport in Heterogeneous Unconsolidated Geological Deposits. *Water Resources Research* 20:369-378. DOI: 10.1029/WR020i003p00369.

Graham C.B., McDonnell J.J. (2010) Hillslope threshold response to rainfall: (2) Development and use of a macroscale model. *Journal of Hydrology* 393:77-93. DOI: 10.1016/j.jhydrol.2010.03.008.

Harman C., Sivapalan M. (2009a) Effects of hydraulic conductivity variability on hillslope-scale shallow subsurface flow response and storage-discharge relations. *Water Resour. Res.* 45:W01421. DOI: 10.1029/2008wr007228.

Harman C., Sivapalan M. (2009b) A similarity framework to assess controls on shallow subsurface flow dynamics in hillslopes. *Water Resour. Res.* 45:W01417. DOI: 10.1029/2008wr007067.

Harman C.J., Reeves D.M., Baeumer B., Sivapalan M. (2010) A subordinated kinematic wave equation for heavy-tailed flow responses from heterogeneous hillslopes. *J. Geophys. Res.* 115:F00A08. DOI: 10.1029/2009jf001273.

Healy R.W. (1990) Simulation of solute transport in variable saturated porous media with supplemental information on modification to the US Geological Survey's computer program VS2D, Water-Resourrces Invest., *US Geol. Surv.* .

Heidbüchel I., Troch P.A., Lyon S.W., Weiler M. (2012) The master transit time distribution of variable flow systems. *Water Resour. Res.* 48:W06520. DOI: 10.1029/2011wr011293.

Hogarth W.L., Parlange J.Y. (2000) Application and improvement of a recent approximate analytical solution of Richards' Equation. *Water Resources Research* 36:1965-1968. DOI: 10.1029/2000WR900042.

Hopp L., McDonnell J.J. (2009) Connectivity at the hillslope scale: Identifying interactions between storm size, bedrock permeability, slope angle and soil depth. *Journal of Hydrology* 376:378-391. DOI: 10.1016/j.jhydrol.2009.07.047.

Horton R.E. (1933) The role of infiltration in the hydrologic cycle. *Transactions, American Geophysical Union* 14:446-460.

Hou Z., Huang M., Leung L.R., Lin G., Ricciuto D.M. (2012) Sensitivity of surface flux simulations to hydrologic parameters based on an uncertainty quantification framework applied to the Community Land Model. *J. Geophys. Res.* 117:D15108. DOI: 10.1029/2012jd017521.

Hrachowitz M., Soulsby C., Tetzlaff D., Dawson J.J.C., Malcolm I.A. (2009) Regionalization of transit time estimates in montane catchments by integrating landscape controls. *Water Resour. Res.* 45:W05421. DOI: 10.1029/2008wr007496.

Hrachowitz M., Soulsby C., Tetzlaff D., Malcolm I.A., Schoups G. (2010) Gamma distribution models for transit time estimation in catchments: Physical interpretation of parameters and implications for time-variant transit time assessment. *Water Resour. Res.* 46:W10536. DOI: 10.1029/2010wr009148.

Huang M., Hou Z., Leung L.R., Ke Y., Liu Y., Fang Z., Sun Y. (2013) Uncertainty Analysis of Runoff Simulations and Parameter Identifiability in the Community Land Model – Evidence from MOPEX Basins. *Journal of Hydrometeorology*. DOI: 10.1175/JHM-D-12-0138.1.

Huang M., Liang X. (2006) On the assessment of the impact of reducing parameters and identification of parameter uncertainties for a hydrologic model with applications to ungauged basins. *Journal of Hydrology* 320:37-61. DOI: http://dx.doi.org/10.1016/j.jhydrol.2005.07.010.

Huang M., Liang X., Leung L.R. (2008) A Generalized Subsurface Flow Parameterization Considering Subgrid Spatial Variability of Recharge and Topography. *Journal of Hydrometeorology* 9:1151-1171. DOI: 10.1175/2008JHM936.1.

James L.D., Thompson W.O. (1970) Least Squares Estimation of Constants in a Linear Recession Model. *Water Resources Research* 6:1062-1069. DOI: 10.1029/WR006i004p01062.

Kirchner J.W. (2009) Catchments as simple dynamical systems: Catchment characterization, rainfall-runoff modeling, and doing hydrology backward. *Water Resour. Res.* 45:W02429. DOI: 10.1029/2008wr006912.

Kirchner J.W., Feng X., Neal C. (2000) Fractal stream chemistry and its implications for contaminant transport in catchments. *Nature* 403:524-527. DOI: http://www.nature.com/nature/journal/v403/n6769/suppinfo/403524a0_S1.html.

Kirchner J.W., Feng X., Neal C. (2001) Catchment-scale advection and dispersion as a mechanism for fractal scaling in stream tracer concentrations. *Journal of Hydrology* 254:82-101. DOI: 10.1016/s0022-1694(01)00487-5.

Lamb R.a.B., K. (1997) Using interactive recession curve analysis to specify a general catchment storage model. *Hydrol. Earth Syst. Sci.* 1. DOI: 10.5194/hess-1-101-1997.

Lee D.-H. (2007) Testing a conceptual hillslope recession model based on the storage–discharge relationship with the Richards equation. *Hydrological Processes* 21:3155-3161. DOI: 10.1002/hyp.6537.

Lee H., Sivapalan M., E Z. (2005) Representative Elementary Watershed (REW) approach, a new blueprint for distributed hydrologic modelling at the catchment scale: the development of closure

relations, in: J. W. P. a. A. P. C. Spence (Ed.), PREDICTING UNGAUGED STREAMFLOW IN THE MACKENZIE RIVER BASIN: TODAY'S TECHNIQUES & TOMORROW'S SOLUTIONS, *Canadian Water Resources Association (CWRA)*, Ottawa, Canada.

Lehmann P., Hinz C., McGrath G., Tromp-van Meerveld H.J., McDonnell J.J. (2006) Rainfall threshold for hillslope outflow: an emergent property of flow pathway connectivity. *Hydrol. Earth Syst. Sci. Discuss.* 3:2923-2961. DOI: 10.5194/hessd-3-2923-2006.

Liang X., Lettenmaier D.P., Wood E.F. (1996) One-dimensional statistical dynamic representation of subgrid spatial variability of precipitation in the two-layer variable infiltration capacity model. *Journal of Geophysical Research: Atmospheres* 101:21403-21422. DOI: 10.1029/96JD01448.

Liang X., Lettenmaier D.P., Wood E.F., Burges S.J. (1994) A simple hydrologically based model of land surface water and energy fluxes for general circulation models. *Journal of Geophysical Research: Atmospheres* 99:14415-14428. DOI: 10.1029/94JD00483.

Logan J.D. (1987) Applied Mathematics *John Wiley*, Hoboken, N. J.

Lu Z., Zhang D. (2004) Analytical solutions to steady state unsaturated flow in layered, randomly heterogeneous soils via Kirchhoff transformation. *Advances in Water Resources* 27:775-784. DOI: http://dx.doi.org/10.1016/j.advwatres.2004.05.007.

Maillet E. (1905) Essai d'hydraulique souterraine et fluviale: Librairie scientifique, Hermann, Paris.

Małoszewski P., Rauert W., Stichler W., Herrmann A. (1983) Application of flow models in an alpine catchment area using tritium and deuterium data. *Journal of Hydrology* 66:319-330. DOI: http://dx.doi.org/10.1016/0022-1694(83)90193-2.

Małoszewski P., Zuber A. (1982) Determining the turnover time of groundwater systems with the aid of environmental tracers: 1. Models and their applicability. *Journal of Hydrology* 57:207-231. DOI: http://dx.doi.org/10.1016/0022-1694(82)90147-0.

Marinelli F., Durnford D. (1998) Semianalytical Solution to Richards' Equation for Layered Porous Media. *Journal of Irrigation and Drainage Engineering* 124:290-299. DOI: doi:10.1061/(ASCE)0733-9437(1998)124:6(290).

McDonnell J.J. (1990) A Rationale for Old Water Discharge Through Macropores in a Steep, Humid Catchment. *Water Resources Research* 26:2821-2832. DOI: 10.1029/WR026i011p02821.

McDonnell J.J., McGuire K., Aggarwal P., Beven K.J., Biondi D., Destouni G., Dunn S., James A., Kirchner J., Kraft P., Lyon S., Maloszewski P., Newman B., Pfister L., Rinaldo A., Rodhe A., Sayama T., Seibert J., Solomon K., Soulsby C., Stewart M., Tetzlaff D., Tobin C., Troch P., Weiler M., Western A., Wörman A., Wrede S. (2010) How old is streamwater? Open questions in catchment transit time conceptualization, modelling and analysis. *Hydrological Processes* 24:1745-1754. DOI: 10.1002/hyp.7796.

McGlynn B., McDonnell J., Stewart M., Seibert J. (2003) On the relationships between catchment scale and streamwater mean residence time. *Hydrological Processes* 17:175-181. DOI: 10.1002/hyp.5085.

McGlynn B.L., McDonnel J.J., Brammer D.D. (2002) A review of the evolving perceptual model of hillslope flowpaths at the Maimai catchments, New Zealand. *Journal of Hydrology* 257:1-26. DOI: http://dx.doi.org/10.1016/S0022-1694(01)00559-5.

McGlynn B.L., McDonnell J.J., Hooper R.P., Shanley J.B., Hjerdt K.N. (2001) Hillslope versus riparian zone runoff contributions in headwater catchments: a multi-watershed comparison *EOS, Transactions of the American Geophysical Union*

McGlynn B.L., McDonnell J.J., Shanley J.B., Kendall C. (1999) Riparian zone flowpath dynamics during snowmelt in a small headwater catchment. *Journal of Hydrology* 222:75-92. DOI: http://dx.doi.org/10.1016/S0022-1694(99)00102-X.

McGuire K.J., DeWalle D.R., Gburek W.J. (2002) Evaluation of mean residence time in subsurface waters using oxygen-18 fluctuations during drought conditions in the mid-Appalachians. *Journal of Hydrology* 261:132-149. DOI: 10.1016/s0022-1694(02)00006-9.

McGuire K.J., McDonnell J.J. (2006) A review and evaluation of catchment transit time modeling. *Journal of Hydrology* 330:543-563. DOI: 10.1016/j.jhydrol.2006.04.020.

McGuire K.J., McDonnell J.J. (2010) Hydrological connectivity of hillslopes and streams: Characteristic time scales and nonlinearities. *Water Resources Research* 46:W10543. DOI: 10.1029/2010WR009341.

McGuire K.J., Weiler M., McDonnell J.J. (2007) Integrating tracer experiments with modeling to assess runoff processes and water transit times. *Advances in Water Resources* 30:824-837. DOI: 10.1016/j.advwatres.2006.07.004.

McMillan H., Tetzlaff D., Clark M., Soulsby C. (2012) Do time-variable tracers aid the evaluation of hydrological model structure? A multimodel approach. *Water Resour. Res.* 48:W05501. DOI: 10.1029/2011wr011688.

Menziani M., Pugnaghi S., Vincenzi S. (2007) Analytical solutions of the linearized Richards equation for discrete arbitrary initial and boundary conditions. *Journal of Hydrology* 332:214-225. DOI: http://dx.doi.org/10.1016/j.jhydrol.2006.06.030.

Moore G.K. (1992) Hydrograph Analysis in a Fractured Rock Terrane. *Ground Water* 30:390-395. DOI: 10.1111/j.1745-6584.1992.tb02007.x.

Moore R.D. (1997) Storage-outflow modelling of streamflow recessions, with application to a shallow-soil forested catchment. *Journal of Hydrology* 198:260-270. DOI: http://dx.doi.org/10.1016/S0022-1694(96)03287-8.

Moore R.D., Thompson J.C. (1996) Are Water Table Variations in a Shallow Forest Soil Consistent with the TOPMODEL Concept? *Water Resources Research* 32:663-669. DOI: 10.1029/95WR03487.

Nauman E.B. (1969) Residence time distribution theory for unsteady stirred tank reactors. *Chemical Engineering Science* 24:1461-1470. DOI: http://dx.doi.org/10.1016/0009-2509(69)85074-8.

Neal C., Rosier P.T.W. (1990) Chemical studies of chloride and stable oxygen isotopes in two conifer afforested and moorland sites in the British uplands. *Journal of Hydrology* 115:269-283. DOI: http://dx.doi.org/10.1016/0022-1694(90)90209-G.

Niemi A. (1977) Residence time distributions of variable flow processes. *The International Journal of Applied Radiation and Isotopes* 28:855-860. DOI: 10.1016/0020-708x(77)90026-6.

Niemi A.J. (1990) Tracer Responses and Control of Vessels with Variable Flow and Volume. *Isotopenpraxis Isotopes in Environmental and Health Studies* 26:435-438. DOI: 10.1080/10256019008624351.

Nimah M.N., Hanks R.J. (1973) Model for Estimating Soil Water, Plant, and Atmospheric Interrelations: I. Description and Sensitivity1.

Soil Sci. Soc. Am. J. 37:522-527. DOI: 10.2136/sssaj1973.03615995003700040018x.

Niu G.-Y., Yang Z.-L., Dickinson R.E., Gulden L.E. (2005) A simple TOPMODEL-based runoff parameterization (SIMTOP) for use in global climate models. *Journal of Geophysical Research: Atmospheres* 110:D21106. DOI: 10.1029/2005JD006111.

Niu G.-Y., Yang Z.-L., Dickinson R.E., Gulden L.E., Su H. (2007) Development of a simple groundwater model for use in climate models and evaluation with Gravity Recovery and Climate Experiment data. *Journal of Geophysical Research: Atmospheres* 112:D07103. DOI: 10.1029/2006JD007522.

Noguchi S., Tsuboyama Y., Sidle R.C., Hosoda I. (2001) Subsurface runoff characteristics from a forest hillslope soil profile including macropores, Hitachi Ohta, Japan. *Hydrological Processes* 15:2131-2149. DOI: 10.1002/hyp.278.

Nyberg L., Rodhe A., Bishop K. (1999) Water transit times and flow paths from two line injections of 3H and 36Cl in a microcatchment at Gårdsjön, Sweden. *Hydrological Processes* 13:1557-1575. DOI: 10.1002/(sici)1099-1085(19990815)13:11<1557::aid-hyp835>3.0.co;2-s.

O'Loughlin E.M. (1981) Saturation regions in catchments and their relations to soil and topographic properties. *Journal of Hydrology* 53:229-246. DOI: http://dx.doi.org/10.1016/0022-1694(81)90003-2.

Oda T., Asano Y., Suzuki M. (2009) Transit time evaluation using a chloride concentration input step shift after forest cutting in a Japanese headwater catchment. *Hydrological Processes* 23:2705-2713. DOI: 10.1002/hyp.7361.

Ozyurt N.N., Bayari C.S. (2005) Steady- and unsteady-state lumped parameter modelling of tritium and chlorofluorocarbons transport: hypothetical analyses and application to an alpine karst aquifer. *Hydrological Processes* 19:3269-3284. DOI: 10.1002/hyp.5969.

Panday S., Huyakorn P.S. (2004) A fully coupled physically-based spatially-distributed model for evaluating surface/subsurface flow. *Advances in Water Resources* 27:361-382. DOI: http://dx.doi.org/10.1016/j.advwatres.2004.02.016.

Paniconi C., S. Ferraris, M. Putti, Pini G., Gambolati G. (1994) Three-dimensional numerical codes for simulating groundwater contamination: FLOW3D, flow in saturated and unsaturated

porous media. Pollution modelling, in: P. Zannetti (Ed.), Computer Techniques in Environmental Studies, *Computational Mechanics Publications: Pollution Modeling*, Southampton, UK. pp. 149-156.

Paniconi C., Wood E.F. (1993) A detailed model for simulation of catchment scale subsurface hydrologic processes. *Water Resour. Res.* 29:1601-1620. DOI: 10.1029/92wr02333.

Parlange J.Y., Brutsaert W. (1987) A capillarity correction for free surface flow of groundwater. *Water Resources Research* 23:805-808. DOI: 10.1029/WR023i005p00805.

Pearce A.J., Stewart M.K., Sklash M.G. (1986) Storm Runoff Generation in Humid Headwater Catchments: 1. Where Does the Water Come From? *Water Resources Research* 22:1263-1272. DOI: 10.1029/WR022i008p01263.

Radczuk L., Szarska O. (1989) Use of the flow recession curve for the estimation of conditions of river supply by underground water. *IAHS Publ.* 187:67-74.

Rahman A., Goonetilleke A. (2001) Effects of non-linearity in storage-discharge relationships on design flood estimates MODSIM 2001, International Congress on Modelling and Simulation, Australian National University, Canberra, Australia. pp. 113-117.

Rawls W., Ahuja L., Brakensiek D., Shirmohammadi A. (1993) Infiltration and Soil Water Movement, Handbook of Hydrology, New York, NY.

Richards R. (1931) Capillary conduction of liquid through porous media.

Rinaldo A., Beven K.J., Bertuzzo E., Nicotina L., Davies J., Fiori A., Russo D., Botter G. (2011) Catchment travel time distributions and water flow in soils. *Water Resour. Res.* 47:W07537. DOI: 10.1029/2011wr010478.

Rinaldo A., Botter G., Bertuzzo E., Uccelli A., Settin T., Marani M. (2006) Transport at basin scales: 1. Theoretical framework. *Hydrology and Earth System Sciences* 10:19-29.

Robinson J.S., Sivapalan M. (1995) Catchment-scale runoff generation model by aggregation and similarity analyses. *Hydrological Processes* 9:555-574. DOI: 10.1002/hyp.3360090507.

Rocha D., Feyen J., Dassargues A. (2007) Comparative analysis between analytical approximations and numerical solutions describing recession flow in unconfined hillslope aquifers. *Hydrogeology Journal* 15:1077-1091. DOI: 10.1007/s10040-007-0170-4.

Rodhe A., Nyberg L., Bishop K. (1996) Transit Times for Water in a Small Till Catchment from a Step Shift in the Oxygen 18 Content of the Water Input. *Water Resources Research* 32:3497-3511. DOI: 10.1029/95wr01806.

Rupp D.E., Selker J.S. (2005) Drainage of a horizontal Boussinesq aquifer with a power law hydraulic conductivity profile. *Water Resources Research* 41:W11422. DOI: 10.1029/2005WR004241.

Rupp D.E., Selker J.S. (2006) On the use of the Boussinesq equation for interpreting recession hydrographs from sloping aquifers. *Water Resour. Res.* 42:W12421. DOI: 10.1029/2006wr005080.

Rupp D.E., Woods R.A. (2008) Increased flexibility in base flow modelling using a power law transmissivity profile. *Hydrological Processes* 22:2667-2671. DOI: 10.1002/hyp.6863.

Russo D., Fiori A. (2008) Equivalent vadose zone steady state flow: An assessment of its capability to predict transport in a realistic combined vadose zone–groundwater flow system. *Water Resour. Res.* 44:W09436. DOI: 10.1029/2007wr006170.

Salvucci G.D., Entekhabi D. (1994) Equivalent steady soil moisture profile and the time compression approximation in water balance modeling. *Water Resources Research* 30:2737-2749. DOI: 10.1029/94WR00948.

Seibert J., Bishop K., Rodhe A., McDonnell J.J. (2003) Groundwater dynamics along a hillslope: A test of the steady state hypothesis. *Water Resources Research* 39:1014. DOI: 10.1029/2002WR001404.

Sidle R.C., Kim K., Tsuboyama Y., Hosoda I. (2011) Development and application of a simple hydrogeomorphic model for headwater catchments. *Water Resources Research* 47:W00H13. DOI: 10.1029/2011WR010662.

Sidle R.C., Tsuboyama Y., Noguchi S., Hosoda I., Fujieda M., Shimizu T. (1995) Seasonal hydrologic response at various spatial scales in a small forested catchment, Hitachi Ohta, Japan. *Journal of Hydrology* 168:227-250. DOI: http://dx.doi.org/10.1016/0022-1694(94)02639-S.

Sidle R.C., Tsuboyama Y., Noguchi S., Hosoda I., Fujieda M., Shimizu T. (2000) Stormflow generation in steep forested headwaters: a linked hydrogeomorphic paradigm. *Hydrological Processes* 14:369-385. DOI: 10.1002/(sici)1099-1085(20000228)14:3<369::aid-hyp943>3.0.co;2-p.

Simunek J., Vogel T., Genuchten M.T.v. (1996) HYDRUS-2D code for simulating water flow and solute transport in two-dimensional variably saturated media, *USDA/ARS, U.S. Salinity Lab*, Riverside, CA.

Sivapalan M. (1993) Linking hydrologic parameterisations across a range of scales: hillslope to catchment to region, in: H.-J. Bolle, R. A. Feddes and J. D. Kalma (Ed.), Exchange Processes at the Land Surface for a Range of Space and Time scales, *IAHS Publ*. pp. 115-123.

Sivapalan M. (2003) Process complexity at hillslope scale, process simplicity at the watershed scale: is there a connection? *Hydrological Processes* 17:1037-1041. DOI: 10.1002/hyp.5109.

Sivapalan M., Beven K., Wood E.F. (1987) On hydrologic similarity: 2. A scaled model of storm runoff production. *Water Resour. Res.* 23:2266-2278. DOI: 10.1029/WR023i012p02266.

Sklash M.G. (1990) Environmental isotope studies of storm and snowmelt runoff generation, in: M. G. Anderson, Burt, T. P (Ed.), Process Studies in Hillslope Hydrology. pp. 401–435.

Sloan W.T. (2000) A physics-based function for modeling transient groundwater discharge at the watershed scale. *Water Resources Research* 36:225-241. DOI: 10.1029/1999WR900221.

Soltani S.S., Cvetkovic V. (2013) On the distribution of water age along hydrological pathways with transient flow. *Water Resources Research* 49:5238-5245. DOI: 10.1002/wrcr.20402.

Soulsby C., Tetzlaff D., Dunn S.M., Waldron S. (2006) Scaling up and out in runoff process understanding: insights from nested experimental catchment studies. *Hydrological Processes* 20:2461-2465. DOI: 10.1002/hyp.6338.

Srivastava R., Yeh T.C.J. (1991) Analytical solutions for one-dimensional, transient infiltration toward the water table in homogeneous and layered soils. *Water Resources Research* 27:753-762. DOI: 10.1029/90WR02772.

Sriwongsitanon N., Ball J.E., Cordery I.A.N. (1998) An investigation of the relationship between the flood wave speed and parameters in runoff-routing models. *Hydrological Sciences Journal* 43:197-213. DOI: 10.1080/02626669809492118.

Stewart M.K., McDonnell J.J. (1991) Modeling Base Flow Soil Water Residence Times From Deuterium Concentrations. *Water Resources Research* 27:2681-2693. DOI: 10.1029/91wr01569.

Sugiura N. (1978) Further analysts of the data by akaike' s information criterion and the finite corrections -- Further analysts of the data by akaike' s. *Communications in Statistics - Theory and Methods* 7:13-26. DOI: citeulike-article-id:4666066
doi: 10.1080/03610927808827599.

Szilagyi J., Parlange M.B., Albertson J.D. (1998) Recession flow analysis for aquifer parameter determination. *Water Resour. Res.* 34:1851-1857. DOI: 10.1029/98wr01009.

Tallaksen L.M. (1995) A review of baseflow recession analysis. *Journal of Hydrology* 165:349-370. DOI: http://dx.doi.org/10.1016/0022-1694(94)02540-R.

Tani M. (1997) Runoff generation processes estimated from hydrological observations on a steep forested hillslope with a thin soil layer. *Journal of Hydrology* 200:84-109. DOI: http://dx.doi.org/10.1016/S0022-1694(97)00018-8.

Tetzlaff D., Soulsby C., Waldron S., Malcolm I.A., Bacon P.J., Dunn S.M., Lilly A., Youngson A.F. (2007) Conceptualization of runoff processes using a geographical information system and tracers in a nested mesoscale catchment. *Hydrological Processes* 21:1289-1307. DOI: 10.1002/hyp.6309.

Todini E. (1996) The ARNO rainfall—runoff model. *Journal of Hydrology* 175:339-382. DOI: http://dx.doi.org/10.1016/S0022-1694(96)80016-3.

Tracy F.T. (2006) Clean two- and three-dimensional analytical solutions of Richards' equation for testing numerical solvers. *Water Resources Research* 42:W08503. DOI: 10.1029/2005WR004638.

Troch P., van Loon E., Hilberts A. (2002) Analytical solutions to a hillslope-storage kinematic wave equation for subsurface flow. *Advances in Water Resources* 25:637-649. DOI: http://dx.doi.org/10.1016/S0309-1708(02)00017-9.

Troch P.A., Paniconi C., Emiel van Loon E. (2003) Hillslope-storage Boussinesq model for subsurface flow and variable source areas along complex hillslopes: 1. Formulation and characteristic response. *Water Resour. Res.* 39:1316. DOI: 10.1029/2002wr001728.

Troch P.A., van Loon A.H., Hilberts A.G.J. (2004) Analytical solution of the linearized hillslope-storage Boussinesq equation for exponential hillslope width functions. *Water Resources Research* 40:W08601. DOI: 10.1029/2003WR002850.

Tromp-van Meerveld H.J., James A.L., McDonnell J.J., Peters N.E. (2008) A reference data set of hillslope rainfall-runoff response, Panola Mountain Research Watershed, United States. *Water Resources Research* 44:W06502. DOI: 10.1029/2007WR006299.

Tromp-van Meerveld H.J., McDonnell J.J. (2006a) On the interrelations between topography, soil depth, soil moisture, transpiration rates and species distribution at the hillslope scale. *Advances in Water Resources* 29:293-310. DOI: http://dx.doi.org/10.1016/j.advwatres.2005.02.016.

Tromp-van Meerveld H.J., McDonnell J.J. (2006b) Threshold relations in subsurface stormflow: 1. A 147-storm analysis of the Panola hillslope. *Water Resources Research* 42:W02410. DOI: 10.1029/2004WR003778.

Tsukamoto Y., Ohta T. (1988) Runoff process on a steep forested slope. *Journal of Hydrology* 102:165-178. DOI: http://dx.doi.org/10.1016/0022-1694(88)90096-0.

Tuller M., Or D. (2004) Water retention and characteristic curve, in: D. Hillel (Ed.), Encyclopedia of Soils in the Environment, *Elsevier*, Oxford, UK. pp. 278–289.

Uchida T., Tromp-van Meerveld I., McDonnell J.J. (2005) The role of lateral pipe flow in hillslope runoff response: an intercomparison of non-linear hillslope response. *Journal of Hydrology* 311:117-133. DOI: http://dx.doi.org/10.1016/j.jhydrol.2005.01.012.

Vache K., McDonnell J.J. (2006) A process-based rejectionist framework for evaluating catchment runoff model structure. *Water Resources Research* 42.

van der Velde Y., de Rooij G.H., Rozemeijer J.C., van Geer F.C., Broers H.P. (2010) Nitrate response of a lowland catchment: On the relation between stream concentration and travel time distribution dynamics. *Water Resources Research* 46:W11534. DOI: 10.1029/2010WR009105.

van Genuchten M.T. (1980) A CLOSED-FORM EQUATION FOR PREDICTING THE HYDRAULIC CONDUCTIVITY OF UNSATURATED SOILS. *Soil Science Society of America Journal* 44:892-898. DOI: citeulike-article-id:8827512.

VanderKwaak J.E. (1999) Numerical simulation of flow and chemical transport in integrated surface-subsurface hydrologic systems, *Univ. of Waterloo,* , Waterloo, Ont., Canada.

Viney N.R., Sivapalan M. (2004) A framework for scaling of hydrologic conceptualizations based on a disaggregation–aggregation approach. *Hydrological Processes* 18:1395-1408. DOI: 10.1002/hyp.1419.

Vitvar T., Aggarwal P.K., McDonnell J.J. (2005) A review of isotope applications in catchment hydrology, in Isotopes in the Water Cycle: Past, Present and Future of a Developing Science, edited by: Aggarwal, P. K., Gat, J. R., and Froehlich, K. F. O., 151–169.

Vogel R.M., Kroll C.N. (1992) Regional geohydrologic-geomorphic relationships for the estimation of low-flow statistics. *Water Resour. Res.* 28:2451-2458. DOI: 10.1029/92wr01007.

Wang D. (2011) On the base flow recession at the Panola Mountain Research Watershed, Georgia, United States. *Water Resources Research* 47:W03527. DOI: 10.1029/2010WR009910.

Wang X.S., Ma M.G., Li X., Zhao J., Dong P., Zhou J. (2010) Groundwater response to leakage of surface water through a thick vadose zone in the middle reaches area of Heihe River Basin, in China. *Hydrol. Earth Syst. Sci.* 14:639-650. DOI: 10.5194/hess-14-639-2010.

Watson F.G.R., Grayson R.B., Vertessy R.A., Peel M.C., Pierce L.L. (2001) Evolution of a hillslope model, International Conference on Modelling and Simulation, MODSIM 2001, Canberra, Australia. pp. 461 – 467.

Weiler M., McDonnell J. (2004) Virtual experiments: a new approach for improving process conceptualization in hillslope hydrology. *Journal of Hydrology* 285:3-18. DOI: http://dx.doi.org/10.1016/S0022-1694(03)00271-3.

Weiler M., McDonnell J.J. (2006) Testing nutrient flushing hypotheses at the hillslope scale: A virtual experiment approach. *Journal of Hydrology* 319:339-356. DOI: http://dx.doi.org/10.1016/j.jhydrol.2005.06.040.

Wenninger J., Uhlenbrook S., Tilch N., Leibundgut C. (2004) Experimental evidence of fast groundwater responses in a hillslope/floodplain area in the Black Forest Mountains, Germany. *Hydrological Processes* 18:3305-3322. DOI: 10.1002/hyp.5686.

Werner P.W., Sundquist K.J. (1951) On the groundwater recession curve for large watersheds. *IAHS* 33:202-212.

Wittenberg H. (1994) Nonlinear analysis of flow recession curves, *IAHS Publication*. pp. 61-67.

Wittenberg H. (1999) Baseflow recession and recharge as nonlinear storage processes. *Hydrological Processes* 13:715-726. DOI: 10.1002/(sici)1099-1085(19990415)13:5<715::aid-hyp775>3.0.co;2-n.

Wittenberg H., Sivapalan M. (1999) Watershed groundwater balance estimation using streamflow recession analysis and baseflow separation. *Journal of Hydrology* 219:20-33. DOI: 10.1016/s0022-1694(99)00040-2.

Woods R., Rowe L. (1996) The changing spatial variability of subsurface runoff across a hillside. *Journal of Hydrology (NZ)* 35(1):51–86.

Ye S., H.-Y Li, Huang M.-Y., Ali M., Leung L.-Y.R., Wang S.-W., Sivapalan M. (2013) Subsurface stormflow parameterization for land surface models, 1. Derivation from regional analysis of streamflow recession curves. *Submitted to Journal of Hydrology*.

Yeh G.T. (1981) FEMWATER: a finite element model of water flow through saturated-unsaturated porous media, *Rep. ORNL-5601, Oak Ridge National Laboratory*, Oak Ridge, TN.

Yeh G.T. (1992) User Manual: A finite Element Model of Water Flow through saturated- Unsaturated porous media, *Department of Civil Engineering* The Pennsylvania State University.

Yeh G.T., Cheng H.P., Huang G.B., Zhang F., Lin H.C., Edris E., Richards D. (2004) A numerical model of flow, heat transfer, and salinity, sediment, and water quality transport in watershed systems of 1-D stream-river network, 2-D overland regime, and 3D subsurface media (WASH123D: version 2.0), technical report, *CHL Waterw. Exp. Stn., U.S. Army Corps of Eng*, Vicksburg, Miss.

Yeh G.T., Huang G.B., Cheng H.P., Zhang F., Lin H.C., Edris E., Richards D. (2006) A first-principle, physics-based watershed model : WASH123D, in: a. D. K. F. V. P. Singh (Ed.), Watershed Models, *CRC Press*, Boca Raton, Fla. pp. 211-244.

Yeh P.J.F., Eltahir E.A.B. (2005) Representation of Water Table Dynamics in a Land Surface Scheme. Part I: Model Development. *Journal of Climate* 18:1861-1880. DOI: 10.1175/JCLI3330.1.

Zaidel J., Russo D. (1992) Estimation of finite difference interblock conductivities for simulation of infiltration into initially dry soils. *Water Resources Research* 28:2285-2295. DOI: 10.1029/92WR00914.

Zuber A. (1986) On the interpretation of tracer data in variable flow systems. *Journal of Hydrology* 86:45-57. DOI: http://dx.doi.org/10.1016/0022-1694(86)90005-3.

Short Biography of the Author

Melkamu Alebachew Ali was born at a small town Tenta in Northern part of Ethiopia, on March 18, 1984. After finishing high school in 2000, he studied Bachelor of Science in Hydraulic Engineering at Arba Minch University, which he graduated with distinction in 2006. Up on his graduation, he joined Arba Minch University as Graduate assistant in 2006 at the Department of Hydraulic and Water Resource Engineering. During his one year career, he has taught courses like Hydraulics, Open channel Hydraulics and Road Drainage design.

In the period 2007-2009, he studied a Master of Science in Hydro-informatics and Water management (Jointed Master of Science in Hydro informatics and Water management from University of Nice Sophia- Antipolis, University of Newcastle (United Kingdom), Brandenburg University of Technology (Germany), Budapest University of Technology and Economics (Hungary), Technical University of Catalonia (Spain)). His M.Sc. thesis was entitled "Application and validation of 2D Hydrodynamic flood Modeling, Case study of Tous Dam break". He has also worked his internship for 6 months at the Danish Hydraulic Institute and allows him to advance his experience on the DHI software such as MIKE11, MIKE21, MIKESHE and MIKEFLOOD. After graduation he went back to Ethiopia and worked for two years as Lecturer at the ArbaMinch Institute of Technology.

In January 2011, Melkamu received a full scholarship for his Ph.D. study from Italian government. He joined the University of RomaTre, civil engineering department with a research interest including: integration of subsurface – subsurface flow, hillslope flow modeling, and solute transport modeling.

As part of his PhD research activity, Melkamu travelled to University of Illinois Urbana-Champaign, USA as a visiting researcher for duration of one year. He engaged with a research project of Newtonian-Darwinian synthesis to predict storage discharge relationship in ungauged basins - Regional patterns in storage discharge relationship across continental United States, and links to climate, soil, vegetation and topography with research teams from UIUC and Pacific Northwest National Laboratory (PNNL). In March 2013, Melkamu returned back to RomaTre University and continued his research activity where he finalized his PhD thesis with some scientific publications.

Publications

- **Ali, M.**, A. Fiori, D. Russo, A comparison of travel-time based catchment transport models, with application to numerical experiments, Journal of Hydrology, 511, pg. 605-618, http://dx.doi.org/10.1016/j.jhydrol.2014.02.010, 2014.

- **Ali, M.**, S. Ye, H. -Yi Li, M. Huang, L. R. Leung, A. Fiori and M. Sivapalan (2013). Subsurface Stormflow Parameterization for Land Surface Models: Up-scaling from Physically Based Numerical Simulations at Hillslope Scale. Journal of Hydrology (accepted).

- Ye, Sheng, H.-Yi Li, M. Huang, **M. Ali**, L. R. Leung, S. Wang and M. Sivapalan (2013). Subsurface stormflow parameterization for land surface models, 1. Derivation from regional analysis of streamflow recession curves. Journal of Hydrology (accepted)

- **Ali, M**., Fiori, A. and Bellotti, G. (2013), Analysis of the nonlinear storage–discharge relation for hillslopes through 2D numerical modelling. *Hydrol. Process*., 27: 2683–2690. doi: 10.1002/hyp.9397

Conferences

- Ye, Sheng ; Li, Hong-yi; Huang, Maoyi; **Ali, Melkamu**; Leung, Lai-yung; Wang, Shao-wen; Sivapalan, Murugesu. Derivation of Subsurface Stormflow Parameterization from Regional Analysis of Streamflow Recession Curves: A Possible Climate Dependence? AGU Chapman Conference, October 2013, Tucson, AZ, USA.
- Sheng Ye, **Melkamu Ali,** and Murugesu Sivapalan. Parameterization of the Effects of Landscape Heterogeneity on Integrated Subsurface Runoff Response: A Reconciliation of Newtonian and Darwinian Approaches. *SESE research review*, Urbana-Champaign, 2013

- Sheng Ye, Hongyi Li, **Melkamu Ali,** Maoyi Huang, Lai-Yung Leung, Murugesu Sivapalan. Regional patterns of recession curves and their relationships with climate, soil, vegetation and topography across the continental United States. *AGU Fall meeting*, San Francisco, 2012.

- **Ali, M**., A. Fiori, G. Bellotti. Determination of discharge storage relation using numerical models for homogeneous 2D hillslopes. Computational Model for Water Resources CMWR 2012, Urbana-Champaign, 2012